Development of an Interference Probe for the Simultaneous Measurement of Turbulent Concentration and Velocity Fields

Alaïs Hewes

Master of Engineering

Department of Mechanical Engineering

McGill University

Montréal,Québec

August 8, 2016

A thesis submitted to the Faculty of Graduate Studies and Research in partial fulfillment of the requirements for the degree of Master of Engineering

ACKNOWLEDGEMENTS

First, I would like to express my sincere gratitude to my supervisor, Professor Mydlarski, for his guidance and support throughout the course of my work. I am grateful for the knowledge he has taught me, for his patience and encouragement every time I struggled to build my probes, and for his generous help with my thesis.

I am also grateful to the National Science and Engineering Research Council of Canada (NSERC) for funding my research.

I would additionally like to thank my colleagues for their assistance, especially Jordan Stoker, who taught me to build my first hot-wire probe.

Finally, I would like to thank my parents, along with all my family and friends, for their continuous encouragement and support. A special thanks is extended to my sister Sélène, for always being willing to step in when I needed a second set of hands in the lab.

ABSTRACT

The present work focuses on the design and optimization of a thermal-anemometry-based interference probe used to simultaneously measure concentration and velocity fields in turbulent flows. Although a small number of previous investigations have successfully performed such measurements, little work has been done to investigate or explain the necessary components in creating such a specialized probe, which necessitates that one hot-wire-anemometry sensor be operated downstream of, and micrometers from, a second one. The effects of different overheat ratios, wire separation distances, wire diameters, and wire materials, are studied as part of this investigation. Experiments performed in the non-buoyant region of a helium-air jet revealed that successful concentration and velocity measurements required an interference probe containing (i) two wires of differing diameters and (ii) a small separation distance, of about 10 μm, between the wires. Furthermore, the upstream wire should be operated at a high overheat ratio and the downstream wire should operated at a low overheat ratio. From six interference probes of varying designs constructed within this thesis, an optimal interference probe, consisting of a 5 μm tungsten wire, 10 μm upstream of a 2.5 μm platinum-rhodium wire, was identified. The accuracy and precision of this probe was validated against flows of known conditions, previous studies, and measurements from a single-normal hot-wire probe, for which the accuracy and precision have been well established.

RÉSUMÉ

Ce travail se concentre sur la conception et l'optimization d'une sonde d'interférence à base d'anémométrie thermique utilisée pour simultanément mesurer les champs de concentration et de vitesse dans des écoulements turbulents. Bien qu'un petit nombre d'investigations précédentes aient réussi à effectuer ces mesures avec succès, peu de travail a été fait pour examiner et expliquer les composants nécessaires d'une telle sonde spécialisée, qui nécessite qu'un capteur d'anémométrie thermique soit opéré en aval, et à quelques micromètres, d'un deuxième. Les effets des rapports de surchauffe, la séparation entre les fils, les diamètres des fils, et les matériaux des fils, sont étudiés dans le cadre de cette investigation. Des expériences, effectuées dans la région non-flottable d'un jet turbulent, révèlent que des mesures de concentration et de vitesse bien réussies exigent une sonde d'interférence contenant (i) deux fils de diamètres différents et (ii) une petite distance de séparation, d'environ 10 μm, entre les fils. De plus, le fil en amont devrait être opéré à un rapport de surchauffe élevé et le fil en aval devrait être opéré à un rapport de surchauffe assez faible. En comparant les six sondes d'interférence de conceptions variées construite dans cette thèse, une sonde d'interférence optimale, consistant d'un fil de tungstène de 5 μm, en amont d'un fil de platine-rhodium de 2.5 μm, a été identifiée. La précision de cette sonde a été validée contre des écoulements de conditions connues, des études précédentes, et les mesures d'une sonde à fil-chaud, dont la précision a déjà été établie.

TABLE OF CONTENTS

ACKNOWLEDGEMENTS iii

ABSTRACT iv

RÉSUMÉ v

LIST OF TABLES viii

LIST OF FIGURES ix

NOMENCLATURE xi

1 Introduction 1

1.1 Background, Motivation and Overall Objectives 1
1.2 Specific Objectives 3
1.3 Literature Review 4
1.3.1 Overview of Thermal Anemometry 4
1.3.2 Characteristics of a Hot-Wire Probe's Performance 7
1.3.3 Review of Concentration and Velocity Measurements Using Thermal Anemometry 8
1.3.4 Concentration and Velocity Measurements Using Methods Other than Thermal Anemometry 21
1.4 Organization of the Thesis 24

2 Experimental Apparatus 25

2.1 Description of the Experimental Apparatus 25
2.2 The Helium/Air Mixing System 28
2.3 The Mass Flow Meter and Mass Flow Controller 30
2.4 Automation of He/Air Mixing System 32
2.5 The Calibration System 34

3 Instrumentation 36

3.1 Single-Normal Hot-Wire Probe 36
3.2 Interference Probe 36

3.2.1 Design 38
3.2.2 Construction 46
3.2.3 Calibration 59
3.2.4 Data Acquisition 65

4 Effects of Design Characteristics on the Performance of an Interference Probe 67

4.1 Characteristics of an Ideal Interference Probe 67
4.2 Effect of the Overheat Ratio 69
4.3 Effect of the Wire Separation Distance 82
4.4 Effect of the Wire Diameter 86
4.5 Effect of the Wire Material 90
4.6 Optimal Probe Design 90

5 Validation of the Interference Probe of Optimal Design 92

5.1 Results in a Laminar Jet 92
5.2 Results in a turbulent jet 97
5.2.1 Concentration Results 97
5.2.2 Velocity Measurements in a Turbulent Jet 103
5.3 Assessment of the Accuracy and Precision of the W-Pt/R-10 Probe and Realization of Design Goals 105

6 Conclusion 108

6.1 Review of the Thesis 108
6.2 Extensions of the Present Work 110

REFERENCES 111

Appendix A - Calculations of Fluid Properties in Helium/Air Mixtures 119

Appendix B - Characterization of the Buoyancy Effects in the Jet 120

LIST OF TABLES

Table		page
1.1	Summary of thermal anemometry probes developed for concentration and velocity measurements	20
3.1	Physical properties of common hot-wire materials	41
3.2	Summary of interference probes developed in this thesis	44
4.1	Concentration statistics for experiments performed on the W-Pt-35, W-W-55, and W-W-25 probes at $x/D = 10$	74
4.2	Velocity statistics for experiments performed on the W-Pt-35, W-W-55, and W-W-25 probes at $x/D = 10$	77
4.3	Accuracy of measurements using the W-W-55 and W-W-25 probes in a laminar jet	81
5.1	Comparison of measurements using the W-Pt/R-10 probe in a laminar jet with known flow conditions	93
5.2	Concentration statistics measured by interference probes in turbulent flows of pure air	98
5.3	Velocity statistics measured by the W-Pt/R-10 probe and a single-normal hot-wire probe in a turbulent flow of pure air at x/D=10	106
B.1	Characterization of buoyancy effects in various flow conditions	121

LIST OF FIGURES

Figure		page
2.1	Experimental apparatus	26
2.2	Schematic of the experimental apparatus	27
2.3	Data acquisition system for the helium/air mixing system	33
3.1	Steps for construction of a single-wire probe	48
3.2	Wire transfer block	51
3.3	Micromanipulator	51
3.4	Steps to remove primary wire holder	52
3.5	TS1-1240 X-Wire probe	55
3.6	W-Pt-35 probe constructed using Method 1	57
3.7	King' Law calibration for a platinum-rhodium single-normal hot-wire	61
3.8	King's Law calibration for the upstream wire of the interference probe in flows of different concentrations	63
3.9	Variation of coefficients A and B from King's Law with concentration	64
4.1	Comparison of the effects of the overheat ratio on the calibration map of the W-Pt-35 Probe	70
4.2	Comparison of the effects of the overheat ratios on the PDFs of concentration measured by the W-Pt-35, W-W-55 and W-W-25 probes at $x/D = 10$	73
4.3	Comparison of the effects of the overheat ratios on the PDFs of velocity measured by the W-Pt-35, W-W-55 and W-W-25 probes at $x/D = 10$	76
4.4	Comparison of the effects of the overheat ratios on the calibration map for the W-Pt-35, W-W-55, and W-W-25 probes	79

4.5 Comparison of the effect of separation distance on the concentration spectra measured by the W-W-55, W-W-25, W-W-20, and W-W-10 probes at $x/D = 10$ 83

4.6 Comparison of the effect of separation distance on the velocity spectra measured by the W-W-55, W-W-25, W-W-20, and W-W-10 probes at $x/D = 10$ 84

4.7 Comparison of the effect of diameter ratio on the spectra measured by the W-W-10 and W-Pt/R-10 probes at $x/D = 10$ 87

5.1 Concentration and velocity PDFs measured by the W-Pt/R-10 probe at $x/D = 0$ 93

5.2 Calibration map of the interference probe with mean values from experiments at $x/D = 0$ 95

5.3 Calibration map for the W-Pt/R-10 probe with the mean value from experiment in air at $x/D = 10$ 98

5.4 Comparison of the concentration spectra measured by the W-Pt/R-10 probe with the concentration spectra measured by Sirivat and Warhaft (1982) 101

5.5 Concentration PDFs measured by the W-Pt/R-10 probe at $x/D = 10$ 102

5.6 Comparison of the velocity spectrum measured by the W-Pt/R-10 probe with the velocity spectrum measured by a single-normal hot-wire probe at x/D=10. 104

5.7 Comparison of the velocity PDF measured by the W-Pt/R-10 probe with the velocity PDF measured by a single-normal hot-wire probe at $x/D = 10$ 106

NOMENCLATURE

Roman Symbols

A	Calibration constant in King's Law
A_f	Hot-film calibration constant in King's Law
A_w	Hot-wire calibration constant in King's Law
B	Calibration constant in King's Law
B_f	Hot-film calibration constant in King's Law
$\overline{B_m}$	Mean calibration constant in the air/gas mixture (McQuaid and Wright 1973)
B_w	Hot-wire calibration constant in King's Law
C	Concentration (in terms of the helium mass fraction)
$\overline{C}$	Mean concentration
c	Fluctuating concentration
C_j	Concentration at the jet exit
c_{rms}	Standard deviation of the concentration
d	Diameter of the wire
D	Diameter at the jet exit
E	Anemometer output voltage
e	Fluctuating anemometer voltage
$\overline{E_a}$	Mean voltage in air (McQuaid and Wright 1973)
E_d	Downstream wire anemometer output voltage
$\overline{E_g}$	Mean voltage in the gas of interest (McQuaid and Wright 1973)
$\overline{E_m}$	Mean voltage in the air/gas mixture (McQuaid and Wright 1973)

E_u Upstream wire anemometer output voltage

F Froude number

g gravitational constant

h Heat-transfer coefficient

I Current through the wire

k Thermal conductivity of fluid

M_{air} Molecular weight of air

M_{He} Molecular weight of helium

n Calibration exponent in King's Law

n_{av} Averaged calibration exponent for King's Law in different flows

Nu Nusselt Number

OH Overheat ratio

ΔP Pressure drop

Pr Prandtl Number

Q Volumetric flow rate

Q_{air} Volumetric flow rate of air

Q_{He} Volumetric flow rate of helium

Q_{tot} Total volumetric flow rate

R_0 Resistance of the wire at 0°C

Re_λ Taylor scale Reynolds number

R_w Resistance of the wire

Re Reynolds Number

Re_D Jet Reynolds number

Re_M Grid Reynolds number (Sirivat and Warhaft 1982)

S_c Concentration sensitivity

S_θ Temperature sensitivity

S_u Velocity sensitivity

T_0 0°C Reference temperature

T_a Ambient temperature

T_f Film temperature $(T_w + T_a)/2$

T_w Temperature of the wire

U Velocity

u Fluctuating velocity

U_j Velocity at the jet exit

u_{rms} Standard deviation of velocity

V_{MFC} Voltage from the mass flow controller

V_{MFM} Voltage from the mass flow meter

w_{He} mass fraction of helium (Appendix B)

X Desired mass fraction of helium

x Distance from jet exit

x_1 Non-dimensional buoyancy length scale

x_{air} mole fraction of air

x_{He} mole fraction of helium

Y Volumetric fraction of helium

Greek Symbols

α Thermal accommodation constant (1.3.2.2); thermal diffusivity (1.3.2.3)

α_0 Temperature Coefficient of Resistivity at 0°C

α_{20} Temperature coefficient of resistivity at 20°C

α_a Temperature coefficient of resistivity at ambient temperature

η Kolmogorov length scale

θ	Fluctuating temperature
μ	Viscosity of the fluid
μ_{air}	Viscosity of air
μ_{He}	Viscosity of helium
μ_{mix}	Viscosity of a helium/air mixture
ξ	Distance that the thermal field of the wire extends in the upstream direction
ρ	Density of the fluid
ρ_{air}	Density of air
ρ_{He}	Density of helium
ρ_{mix}	Density of a helium/air mixture
ρ_j	Density at the jet exit
χ	Resistivity
χ_{20}	Resistivity at 20°C

CHAPTER 1
Introduction

1.1 Background, Motivation and Overall Objectives

Fluid flow is a ubiquitous aspect of engineering practice – essential to the understanding and analysis of numerous engineering and environmental applications, such as the flow of air over an aircraft wing, oil through a piping system, or water in a river or canal. Fluid flows can be divided into two distinct regimes: laminar flow and turbulent flow. Laminar flows are characterized by fluid particles that move in parallel layers or "laminae," and in which mass, momentum, and energy transfers primarily take place through diffusion processes at the molecular level. The simplest of these flows can be solved analytically from the Navier-Stokes equations, and more complicated laminar flows can be solved using computational methods.

The vast majority of fluid flows however, are turbulent and far more complex than laminar flows. There is no precise definition of turbulence, but turbulent flows all share the characteristics that follow (Tennekes and Lumley 1972). Such flows arise due to instabilities in laminar flows and occur at large Reynolds numbers, where the latter is defined as the ratio of inertial to viscous forces and is a useful tool in determining whether a flow can be classified as laminar or turbulent. Once a flow has become turbulent it becomes random, or irregular, and exhibits three-dimensional velocity and vorticity fluctuations. Advection by the fluctuating velocity fields leads to enhanced mixing of mass, momentum, and energy. In other words, turbulent flows are highly diffusive. This is one of the most important features of turbulence

and essential in numerous engineering and scientific fields such as aerodynamics, combustion, meteorology, and oceanic sciences, as well as many aspects of everyday life. The diffusivity of turbulence is what allows a room to be heated efficiently or for milk to be rapidly mixed into a cup of coffee. A final salient characteristic of turbulent flows is that they are dissipative. Without a continuous source of energy, turbulent flows decay rapidly as energy from the mean flow is converted into internal energy by the viscous shear stresses. For further details on the physics that underpin turbulent flows, the reader is referred to the textbooks by Tennekes and Lumley (1972) or Pope (2000).

As turbulent flows are nonlinear and chaotic, the equations that govern them are extremely difficult to solve. Even the simplest turbulent flows have no analytical solutions, and computational methods require vast resources given the large range of length and time scales that occur in turbulence. Engineers frequently turn to models that simplify or approximate the Navier-Stokes equations to solutions. Numerous models with varying amounts of accuracy, level of description, computational cost, and range of applicability have been developed. Use of these models requires both a fundamental understanding of turbulence as well as rigorous experimental data to validate them.

The mixing of scalars, such as temperature, pollutants, or any other chemical species, within turbulent flows is an important sub-field in the study of turbulence and is relevant to the fields of convective heat transfer, environmental pollutant dispersion, and combustion. Accordingly, turbulent scalar mixing has been the subject of a number of studies. Most of these studies have focused on the simplest case of scalar mixing – the mixing of a single passive scalar in turbulence. However many turbulent flows contain more than one scalar – the mixing of temperature and salinity

in an oceanic mixed layer being one example. When it comes to the mixing of multiple scalars, many turbulent models make erroneous or questionable assumptions by either assuming equal molecular diffusivities for all scalars or neglecting the effects of molecular diffusivity at high Reynolds numbers (Lavertu *et al.* 2008). Experimental methods can be used to assess the validity of the above assumptions, or to come up with new models for turbulent scalar mixing. To do so, it is necessary to be able to accurately measure the evolution of these scalars.

Thermal anemometry has proven to be an effective tool for measuring turbulence in gas flows, and has typically been used to measure both velocity and temperature. Its use has also been extended to measure concentration in certain cases. However, simultaneous measurement of both concentration and velocity fluctuations, which is essential for studying the evolution of concentration in a turbulent flow, remains a difficult task. Although such probes have successfully been built, many of these modified hot-wire probes are applicable only under certain conditions, and the documentation on their design is scarce. Attempts to recreate such probes can prove to be challenging and a more thorough investigation of their design is merited.

1.2 Specific Objectives

The aim of this work is to (i) develop a hot-wire probe to simultaneously measure the instantaneous concentration and velocity within turbulent flows with high temporal and spatial resolution and (ii) identify the essential characteristics in the design of such a probe. To this end, the effects of overheat ratio, wire diameter, wire material and wire separation distance are studied to determine the optimal design of

the probe and preliminary results are presented. Preliminary measurements in a turbulent helium-air jet are furthermore used to benchmark the accuracy and precision of the probe.

1.3 Literature Review

The development and investigation of thermal-anemometry-based probes used to simultaneously measure concentration and velocity requires a thorough understanding of thermal anemometry and its potential for making such measurements. In the current section, an overview of the theory behind thermal anemometry, as well as some of the characteristics of a hot-wire probe's performance are presented. Following that, a detailed discussion of the use of thermal anemometry in making concentration, velocity, and simultaneous concentration and velocity measurements in flows of variable concentration is given. Finally, concentration and velocity measurements using methods other than thermal anemometry are briefly discussed to motivate the present work.

1.3.1 Overview of Thermal Anemometry

Thermal anemometry remains one of the principal research tools for turbulent research due to its (i) extensive historical use, (ii) high temporal and spatial resolution, and (iii) relatively low cost compared to other experimental tools. A brief overview of the technique will be provided as it essential to an understanding of this thesis. Comprehensive reviews of the subject can be found in Hinze (1959, 1975), Corrsin (1963), and Comte-Bellot (1976), and detailed descriptions of the basic principles of hot-wire anemometry can be found in the books by Perry (1982) and Bruun (1995).

Thermal anemometry is based on the principles of convective heat transfer. A fine metal wire or a thin film is heated by running an electric current through it. Applying

conservation of energy to a section of length l of an infinite wire, one observes that a balance between the conversion of electrical energy into internal energy and the convective heat transfer rate exists at steady state. Radiation effects are not included as they are typically negligible (Comte-Bellot 1976; Wasan and Baid 1971). As the wire can be approximated as infinite, conductive end losses are neglected and one obtains the following equation:

$$I^2 R_w = \pi dlh(T_w - T_a) = \pi lk(T_w - T_a)Nu, \tag{1.1}$$

where I is the current through the wire, R_w is the resistance of the wire, d is the diameter of the wire, h is the heat transfer coefficient of the wire segment, T_w is the temperature of the wire, T_a is the ambient temperature and k is the thermal conductivity of the fluid.

Based on Kramers (1946) experiments on wires in air, water, and oil, the Nusselt number ($Nu = hd/k$) can be related to the Reynolds number ($Re = \rho dU/\mu$) and the Prandtl number (Pr) in the form below:

$$Nu = 0.42Pr^{0.2} + 0.57Pr^{0.33}Re^{0.5}. \tag{1.2}$$

An alternative, and popular (though not used in the present work), heat transfer correlation was developed by Collis and Williams (1959) and includes a dependence on the film temperature (T_f):

$$Nu(T_f/T_a)^{-0.17} = 0.24 + 0.56Re^{0.5}. \tag{1.3}$$

Furthermore, the electrical resistance can be related to the temperature difference as follows (Bruun 1995):

$$R_w = R_0[1 + \alpha_0(T_w - T_0) + \dots]. \tag{1.4}$$

In the equation above, T_0 ($T = 0°\text{C}$) is the reference temperature for the resistance (R_0) and the temperature coefficient of resistivity (α_0), but other reference temperatures can be used. Using equations 1.2 and 1.4, the energy balance can be expressed as

$$\frac{I^2 R_w}{R_w - R_a} = 0.42\frac{\pi k l}{\alpha_0 R_0} Pr^{0.2} + 0.57\frac{\pi k l}{\alpha_0 R_0} Pr^{0.33}\left[\frac{\rho d}{\mu}\right]^{0.5} U^{0.5}, \tag{1.5}$$

where ρ is the density of the fluid, μ is the viscosity of the fluid, and U is the velocity. This can be simplified to have the form:

$$E^2 = A + BU^{0.5}(T_w - T_a), \tag{1.6}$$

where E is the anemometer output voltage as opposed to the wire voltage. In isothermal flow the temperature difference is constant and can be absorbed into the constants A and B. The resulting equation is typically known as King's Law:

$$E^2 = A + BU^{0.5}. \tag{1.7}$$

To account for the conduction to the prongs and other slight deviations from the idealized case, King's Law can be written in a more generalized form:

$$E^2 = A + BU^n, \tag{1.8}$$

where the exponent on the velocity is not fixed to being 0.5. The constants A, B and n and can be found by calibrating the hot-wire probe in a known flow. It should

be noted that although A and B are constants, they are also functions of the flow conditions and dependent on both the temperature and the composition of the fluid in which they are calibrated. For this reason hot-wires are typically calibrated before each use.

1.3.2 Characteristics of a Hot-Wire Probe's Performance

In the previous subsection, a general overview of the theory behind hot-wire anemometry was presented. In the current subsection, some of the common characteristics related to the performance of a hot-wire probe are listed. A typical hot-wire probe has both high temporal and spatial resolution. In most conditions, a hot-wire probe operated in the constant-temperature mode,[1] will have a flat frequency response up to 50 kHz, making measurements up to several hundred kHz possible (Bruun 1995). The spatial resolution, which is dictated by the length of the wire, can be made to be about 0.5 mm. This is not much larger than the Kolmogorov length scale (known to be on the order of 0.1 mm in most flows), and is sufficient for making measurements with high spatial resolution. Though the spatial resolution can be improved by decreasing the length of the wire, if the length-to-diameter ratio is too small (< 200), conductive end losses will be increased, resulting in a degradation of the frequency response and a less uniform temperature profile along the wire (Bruun 1995). Consequently, dimensions for a hot-wire probe are often

[1] Hot-wire probes can be operated in either the constant-temperature or constant-current modes. In the constant-temperature mode, the probe resistance, and therefore the temperature, is kept constant. In the constant-current mode, the current is kept constant, and the probe temperature varies. The constant-temperature mode is typically used due to its better frequency response. See Bruun (1995) for a more detailed discussion.

chosen as a compromise between minimizing the adverse effects of conductive end losses and improving the spatial resolution. Besides having high temporal and spatial resolution, hot-wire probes are known to be very accurate and have very high signal-to-noise ratios. In carefully controlled experiments, the accuracy of a hot-wire probe may be as small as 0.1-0.2%, though in most applications, it is around 1%. Additionally, the high signal-to-noise ratio makes it relatively easy to obtain a resolution of one part in 10000 (Bruun 1995).

The characteristics listed above make hot-wire probes ideal instruments for measuring various turbulent fields, such as the velocity, temperature, or concentration fields. A single wire allows measurement of one component of the velocity field, two sensors can be used to measured two components, and three sensors are used to measure all three components. Temperature measurements can be made using very fine wires (known as cold-wires) operated in the constant current mode. These cold wires can be combined with other hot-wires to make simultaneous temperature and velocity measurements. The literature on velocity, temperature, and simultaneous temperature and velocity measurements is already extensive, and can be reviewed in the references listed at the beginning of section 1.3.1. Although concentration and simultaneous concentration and velocity measurements are possible, the techniques for doing so are far more complex, and will be discussed in the following subsection.

1.3.3 Review of Concentration and Velocity Measurements Using Thermal Anemometry

Although the vast majority of hot-wire measurements have been made in air, given that the coefficients A and B from the King's Law equation (equation 1.8) are found to vary with flow composition, it is expected that a hot-wire's response will

vary with the concentration of one gas within a multi-gas mixture. Early theoretical work from Corrsin (1949) suggested that it was possible to solve for the mean concentration of the flow given knowledge of the fluid properties, and that the fluctuating concentration and velocity could be inferred from the voltages of two hot-wire probes of differing diameters. Such work is based on the fact that in a heterogeneous isothermal mixture, the fluctuating voltage signal (e) is found to be:

$$e = S_u u + S_c c, \tag{1.9}$$

where the velocity and concentration sensitivities, S_u and S_c respectively, are found to be:

$$S_u = \frac{\partial E}{\partial U} = \frac{nB(C)U^{n-1}}{2[A(C) + B(C)U^n]^{0.5}}, \tag{1.10a}$$

$$S_c = \frac{\partial E}{\partial C} = \frac{A'(C) + B'(C)U^n}{2[A(C) + B(C)U^n]^{0.5}}, \tag{1.10b}$$

such that their ratio is given by:

$$\frac{S_u}{S_c} = \frac{nB(C)U^{n-1}}{A'(C) + B'(C)U^n}, \tag{1.11}$$

where $A'(C)$ and $B'(C)$ are the derivatives of the calibration constants in King's Law, A and B respectively, with respect to concentration (C).

The fluctuating velocity (u) and concentration (c) can be found from two linearly independent forms of the equation for the fluctuating voltage signal. This is possible by using two-hot-wires with differing S_u/S_c ratios at the same point. Per Corrsin's (1949) suggestion, this can be achieved by using two wires of different diameters, as the coefficient B is dependent on the diameter of the wire. He additionally noted that ordinary differences in A and B between two different wires of the same nominal

diameter, may also prove to be sufficient in obtaining differing S_u/S_c ratios. Following Corrsin's (1949) work, different techniques for measuring concentration, velocity, or both in flows of varying concentration were developed.

1.3.2.1 Concentration Measurements in Variable Concentration Flows

Aspirating probes, first referenced by Blackshear and Fingerson (1962) were recognized to be capable of measuring concentration in binary mixtures. Choked-nozzle aspirating probes were subsequently developed by D'Souza *et al.* (1968) and elaborated on by Brown and Rebollo (1972), Adler (1972), Perry (1977), Wilson and Netterville (1981), Birch *et al.* (1986), and Cabannes *et al.* (2004), among others. These probes consist of a hot-wire or hot-film placed within a sample tube and upstream or downstream of a nozzle. The tube is exposed to a gas mixture, and during operation a vacuum is applied such that a choked-nozzle condition is achieved. It can be shown that since the velocity is a function of the sonic speed, the probe's response is sensitive only to the concentration (or density) of the gas mixture. A number of works have made successful use of aspirating probes such as those of Ng and Epstein (1983), Ahmed and So (1986), White (1987), Ninnemann and Ng (1992), and Guibert and Dicocco (2002). These probes are however limited in their use. Due to the spatial requirements between the probes, it is not possible to combine a hot-wire with an aspirating probe to simultaneously measure concentration and velocity (Harion *et al.* 1996).

1.3.2.2 Velocity Measurements in Variable Concentration flows

Other researchers have focused on investigating the response of a hot-wire or hot-film to different gases or different concentrations. Kassoy (1967) and Aihara *et al.* (1967) were among the first to do so. They studied the response of a hot-wire in

helium-nitrogen mixtures with the aim of eventually simultaneously measuring concentration and velocity. They observed significant deviations from King's Law with increasing helium concentration. This was attributed to temperature slip[2] effects due to the low thermal accommodation coefficient[3] of helium on tungsten and other common hot-wire materials. In response to this, Kassoy (1967) developed a theoretical relationship for the Nusselt number that accounted for variable flow properties and temperature-slip effects, and Aihara *et al.* (1967) conducted experiments to validate Kassoy's (1967) work. Although their results showed good agreement between experiment and theory in pure gases, they are not directly applicable to hot-wire anemometry studies because Kassoy's (1967) theoretical work was derived for (i) $Re \ll 1$, a range that is lower than that typically found in hot-wire anemometry studies, and (ii) infinite cylinders, while the experiments of Aihara *et al.* (1967) were done on hot-wires of l/d ratios of 1000, a ratio far greater than that of a typical hot-wire.

Baccaglini *et al.* (1969) extended the above investigation for nitrogen-neon mixtures, which, similarly to helium, also have a low thermal accommodation coefficient on tungsten. Unlike helium, the molecular weight of neon is close to nitrogen. It

[2] Temperature slip (similar to velocity slip) at a surface, is a temperature jump that occurs if the gas and surface are not at thermal equilibrium.

[3] The thermal accommodation constant α "can be thought of as the ratio of the average increase of the gas molecules after striking the surface to the increase in energy they would have if they remained near the surface long enough to come into equilibrium at the surface temperature. $\alpha = 0$ if the gas 'accomodates' no energy from the surface, and $\alpha = 1$ if gas molecules striking the surface come into thermal equilibrium at the surface temperature." (Pitts and McCaffrey 1986)

was shown that a calculation of the effective slip parameter in mixtures (necessary to apply Kassoy's (1967) theoretical work to mixtures) agreed well in the nitrogen-neon mixtures but not in the nitrogen-helium mixtures. This was hypothesized to be due to the differences in molecular weights and the physical phenomena that occur in such mixtures. As the experiments performed by Aihara *et al.* (1967) were done for $Re < 0.1$, Wu and Libby (1971) measured the Reynolds number dependence of the Nusselt number in air, helium, and helium-air mixtures over a more reasonable range of Reynolds numbers, finding that differences between experiments and theory could be again be attributed to thermal slip. Later studies, such as those of Simpson and Wyatt (1973) and Pitts and McCaffrey (1986), have gone on to find similar results. Simpson and Wyatt (1973) concluded that even for hot-films, which are weakly influenced by thermal slip effects, thermal diffusion effects in helium-air mixtures could increase thermal slip, and cause calibration results to fall below their predicted values. As no theory exists to account for these effects, direct calibration of hot-wire or hot-film probes is necessary for precise use in helium-air mixtures. Pitts and McCaffrey (1986) offered a comprehensive study of the corrections needed to correlate Nu as a function of Re in a wide variety of gases, including helium. These corrections include conduction losses, temperature dependence of molecular properties, non-continuum effects, and accommodation effects. They noted that the accommodation effects in helium were particularly significant, while for other gases the temperature dependency of gas molecular properties was the most important correction to be made.

Additional studies of the effects of gas composition variations on hot-wire response include the works of Wasan *et al.* (1968), Wasan and Baid (1971), Andrews *et al.* (1972), and Banerjee and Andrews (2007). Wasan *et al.* (1968) and Wasan and

Baid (1971) developed an expression for the velocity in terms of fluid properties that enabled them to make measurements of the mean velocity in flows of variable composition and to extrapolate velocity data in binary mixtures from calibrations performed at two composite concentrations. This approach is limited in its use; for binary mixtures including gases of significantly differing molecular weights, the viscosity and thermal conductivity cannot be approximated by linear interpolation (Banerjee and Andrews 2007). Andrews *et al.* (1972) noted difficulties in obtaining accurate values for the thermal accommodation coefficient. This can be problematic since the thermal accommodation can have a significant effect on heat transfer correlations used to predict the hot-wire response.

1.3.2.3 Simultaneous Concentration and Velocity Measurements in Variable Concentration Flows

Simultaneous measurements of concentration and velocity fluctuations using hot-wire anemometry appear to have been first been developed by Way and Libby (1970). Following Corrsin's (1949) suggestion, they used a probe composed of hot-film and a hot-wire. Initially, they assumed that both wires were spaced with sufficient distance such that they both followed a King's law equation of the form:

$$E_w^2 = A_w(C) + B_w(C)U^{0.5}, \tag{1.12a}$$

$$E_f^2 = A_f(C) + B_f(C)U^{0.5}, \tag{1.12b}$$

where the subscript w refers to the wire and the subscript f refers to the hot-film. Since both the wire and film were assumed to have the same exponent, the equations could be re-expressed in the form

$$E_w^2 = A_w\left[1 - \left(\frac{B_w}{B_f}\right)\left(\frac{A_f}{A_w}\right)\right] + \left(\frac{B_w}{B_f}\right)E_f^2 = a(C) + b(C)E_f^2. \tag{1.13}$$

If the coefficients A_w, B_w, A_f, B_f were known from calibration, the concentration could be found using the above equation and the velocity could be calculated using one of the King's Laws equations (equation 1.12). Use of this method required $a(C)$ or $b(C)$ to vary with concentration. It was found that when the wires were placed sufficiently far apart that they did not interfere with each other, $a(C)$ and $b(C)$ were sufficiently weak functions of concentration that it was impossible to distinguish voltages resulting from high concentrations and low velocities from those resulting from low concentrations and high velocities. This is believed to be due to the low thermal accommodation of helium, thus requiring an alternate method of measurement in helium-air mixtures. When the wire and film were placed close enough that their thermal fields interfered, the sensitivity to concentration was greatly enhanced, and it was possible to solve for concentration and velocity. From testing various configurations, they determined that the optimal configuration was one in which the wire was operated at a low overheat ratio, the film was operated at a high overheat ratio, and the wire was upstream of the film. In this case, the wire was located in the thermal field of the film and no longer followed King's Law. However, since the film was unaffected by the wire's presence, it still followed King's Law. This type of probe is known as an interference or Way-Libby probe, and the specific details of its design are given in table 1.1.

Way and Libby (1971) developed a calibration and data reduction scheme for the interference probe described above, and assessed its accuracy in a variety of ways. They found reasonable agreement in their results with flows of known, constant concentration, as well as with previously published data in similar flows in concentration and velocity ranges of interest. Although they noted degraded accuracy in regions

of high concentration and low velocity, these conditions were rarely encountered in the flows they studied, so they concluded that it did not affect their results. They also concluded that a high degree of care during the calibration process was required for accurate results, as even small drifts in voltages could have significant effects on calculated velocity and concentration data.

A handful of further studies have based their measurement techniques on the interference probe. Riva *et al.* (1994) made use of a Way-Libby probe with slight modifications to study turbulent boundary layers with large density gradients. Given that the Way-Libby probe is limited in its range of concentration and velocity measurements, Harion *et al.* (1996) developed an improved method for measuring concentration and velocity using hot-wire anemometry. In the process of doing so they analyzed the hot-wire/hot-film interference probe for various configurations of overheat ratios. The probe Harion *et al.* (1996) studied is similar in design to the one developed by Way and Libby (1970). The interference effect of the probe can be expressed in terms of the distance (ξ) that the thermal field of the film extends in the upstream direction. This length can be approximated from a balance between the longitudinal advection and molecular diffusion so that:

$$\frac{U(T_f - T_\infty)}{\xi} = \frac{\alpha(C)(T_f - T_\infty)}{\xi^2}, \tag{1.14}$$

and

$$\xi \approx \frac{\alpha(C)}{U}, \tag{1.15}$$

where $\alpha(C)$ is the thermal diffusivity and dependent on concentration. From the above equation, it is expected that, in helium-air mixtures, ξ will be (i) small in low concentration, high speed flows, leading to a small interference effect, and (ii)

large in high concentration, low-speed flows, leading to a much stronger interference effect. This is consistent with the results of Way and Libby (1970), where they noted that for very low speed and high concentration flows, no electrical input would be required to maintain the wire at a constant temperature. Harion *et al.* (1996) observed that the choice in overheat ratio was very delicate. If the difference in temperature between the wire and film was too large, the wire voltage would tend to zero in low concentration, low-speed flows. But if the difference in temperature was too low, the calibration map would tend towards the result of a single hot-wire, making it impossible to accurately solve for u and c. In order to minimize the interference effects, which were deemed impractical,[4] it was decided to operate the wire at a high overheat ratio and the film at a low overheat ratio. This had the added advantage of producing linear iso-concentration curves in the calibration map, and simplifying the data reduction scheme. With minimal thermal interference effects, Harion *et al.* (1996) found that the measurement of concentration and velocity was due to differences in diameter. Increasing the diameter ratio of the wires/films had the effect of increasing the voltage shift between the iso-concentration curves. Although satisfactory measurements were obtained up to 300 Hz, the large diameter of the film lead to a deterioration in accuracy at higher frequencies. Harion *et al.* (1997) and Soudani and Bessaïh (2006) both made use of this probe to make density and velocity measurements in turbulent helium/air boundary layers, and Harion

[4] When interference effects are present, the probe's response is extremely sensitive to the separation distance. As this distance was difficult to set and control, Harion *et al.* (1996) deemed it more practical to minimize interference effects so the separation distance would not be so crucial to the operation of the probe.

et al. (1997) developed an additional probe based on similar principles to make simultaneous density and shear stress measurements at a wall. Furthermore, a brief investigation by Jonáš *et al.* (2003) revealed that the assumption of the equality of exponents used by Way and Libby (1970) was incorrect, and that equation 1.13 is not accurate enough for use with a probe operating in a weak-interference regime.

Stanford and Libby (1974) extended the use of the Way-Libby probe to make simultaneous measurements of concentration, c, and two velocity components, u and v. This was done by adding a swept film to the interference probe to measure the v-component of velocity. The interference probe was modified slightly so that the wake effects of the wire on the swept film could be eliminated. Instead of being orthogonal to the film, the wire was positioned at a 30° angle to the film. This had the added effect of increasing the interference between the wire and the film, which increased the operating range of the probe. A similar probe was used by LaRue and Libby (1977, 1980) to make measurements in the turbulent boundary layer using helium slot injection. They noted that the frequency response of the wire in the interference probe was lower than that of the film – a result likely attributed to its low overheat ratio. Aihara *et al.* (1974) and Panchapakesan and Lumley (1993) were also able to measure concentration and two velocity components. The former achieved this using two parallel hot-wires as an interference probe, with a third wire to measure the lateral velocity fluctuations, while the latter used an interference probe and an X-wire hot-wire probe. The interference probe was composed of two nearly parallel tungsten wires separated by a distance on the order of 5 μm, and was mounted on an X-wire probe such that distance between the interference probe and the X-wire was roughly 1 mm. Panchapakesan and Lumley (1993) achieved a frequency response of 6 kHz by keeping the overheat ratios of the wires in the interference probe high.

Sirivat and Warhaft (1982) used the principles of the interference probe to make measurements of the concentration, velocity, and temperature fluctuations in air-helium mixtures. The 3-wire probe they developed was composed of a modified Way-Libby or interference probe sensitive to concentration and velocity fluctuations, with a third wire to measure the temperature fluctuations. The interference probe consisted of a 3 μm tungsten wire operated at an overheat ratio of 1.2, positioned 5 μm in front[5] of a 5 μm platinum-rhodium wire operated at an overheat ratio of 1.6. The third wire was a 3 μm tungsten wire operated at an overheat ratio of 1.05 and sensitive to concentration, velocity, and temperature fluctuations due to its low overheat ratio. The probe was found to have an adequate frequency response to the velocity and temperature fluctuations, and it was believed that the frequency response of the system to helium fluctuations should be comparable to those of the velocity and temperature fluctuations.

In addition to interference probes, whose designs are summarized in table 1.1, a few other methods involving hot-wire anemometry have been developed to make concurrent concentration and velocity measurements. McQuaid and Wright (1973) developed a method for measuring concentration fluctuations in air/gas mixtures, which was dependent on knowledge of the mean concentration. They defined the

[5] The language used by Sirivat and Warhaft (1982) is rather ambiguous. They refer to a front and back wire, but it is unclear which of these is the downstream or the upstream wire.

velocity and concentration sensitivity, S_u and S_c, respectively, to be:

$$S_u = n\overline{B_m}\frac{\overline{U}^{n-1}}{2\overline{E_m}}, \tag{1.16a}$$

$$S_c = \phi(\overline{C}, c)\frac{\overline{E_g}^2 - \overline{E_a}^2}{2\overline{E_m}}, \tag{1.16b}$$

where $\overline{E_g}$ was the mean voltage of the wire in the gas of interest, $\overline{E_a}$ was the mean voltage in air, $\overline{E_m}$ was the mean voltage in the air/gas mixture, $\overline{B_m}$ was the mean calibration constant of the mixture, and $\phi(\overline{C}, c)$ was a function of the mean concentration ($\overline{C}$) and the fluctuating concentration (c), and specific to each gas of interest. In agreement with Corrsin's (1949) work, they determined that two wires with differing S_u/S_c ratios were required to simultaneously measure concentration and velocity fluctuations. They, however, disagreed with Corrsin's conclusion that the sensitivity ratio was independent of wire temperature. By comparing results in different gases, they found that larger S_u/S_c ratios lead to more accurate results. They identified hydrogen, helium, and methane as favorable gases for such studies, but ultimately performed their experiments in argon due to cost and issues with flammability. They also determined that the optimal combination of hot-wires involved a small-diameter wire at a high overheat ratio and a large diameter-wire at low overheat ratio. McQuaid and Wright (1974) applied the techniques described above in a turbulent round jet, and validated those results against studies in the literature.

Chassaing (1979) also proposed an alternate method capable of making concentration and velocity measurements in CO_2-air mixtures. He used two parallel hot-wire probes operated with different overheat ratios, one of which had an overheat ratio that made it insensitive to concentration. As this method lead to practical

Table 1.1: Summary of thermal anemometry probes developed for concentration and velocity measurements

Authors	Upstream sensor: diameter and material	Downstream sensor: diameter and material	Upstream sensor: overheat ratio / wire temperature	Downstream sensor: overheat ratio / wire temperature	Diameter ratio	Separation distance	Angle between sensors
Way and Libby (1970)	2.5 μm platinum	25 μm platinum	100 °C AAT*	275 °C AAT*	10	50 μm	orthogonal
Way and Libby (1971)	2.5 μm platinum	25 μm quartz coated platinum	125 °C AAT*	300 °C AAT*	10	25 μm	orthogonal
Stanford and Libby (1974)	2.5 μm platinum	25 μm	85 °C	305 °C	10	25 μm	10°
Aihara *et al.* (1974)	1 μm tungsten	5 μm tungsten	Not given	Not given	5	0.3 mm	parallel
Sirivat and Warhaft (1982)	5 μm platinum-rhodium	3 μm tungsten	1.6	1.2	1.7	5 μm	10°
Panchapakesan and Lumely (1993)	9 μm tungsten	3 μm tungsten	1.8	1.6	3	5 μm	nearly parallel
Riva *et al.* (1994)	2.5 μm	70 μm	100 °C	250 °C	28	25 μm	orthogonal
Harion *et al.* (1996)	2.5 μm	70 μm	250 °C	100 °C	28	25 μm	orthogonal
Jonáš *et al.* (2003)	5 μm tungsten	70 μm nickel film plated quartz fiber	523 K	373 K	14	1 mm	Not given

*above ambient temperature

difficulty in selecting the appropriate overheat ratio, Sakai *et al.* (2001) proposed a simpler technique which made simultaneous use of two hot-wires at different overheat ratios, but equal diameters.

Although a variety of techniques for using thermal anemometry to make simultaneous concentration and velocity measurements have been presented, it should be noted that the majority of these are only concerned with the application of this measurement technique. It appears that only two studies, those of Way and Libby (1970) and Harion *et al.* (1996), have studied the design of these probes, the former demonstrating the effect of the separation distance, and the second, demonstrating the effect of overheat ratio choices. As will later be discussed in Chapter 3, a wide variety of other design characteristics exist, and may have an effect on the performance of these thermal-anemometry-based probes. It becomes evident that the existing literature on these probes is not sufficient for adequately documenting their design, motivating a more thorough investigation into the use of thermal anemometry for making turbulent concentration and velocity measurements.

1.3.4 Concentration and Velocity Measurements Using Methods Other than Thermal Anemometry

The previous three sections presented an overview of the principles and characteristics of thermal anemometry, as well as its use in measuring turbulent concentrations and velocities, as part of a general background for the work performed in this thesis. To further motivate the use of the thermal-anemometry-based interference probes, other techniques for measuring concentrations and velocities, as well as some of the advantages and disadvantages of these techniques, are briefly discussed here.

More recent concentration and velocity measurements in variable density flows have been made using methods other than thermal anemometry, citing the long calibration process (Al-Ammar *et al.* 1998; So *et al.* 1990), the limitations to flow velocity and admixture concentrations (Doroshko *et al.* 2008), and the intrusiveness of the probe in the flow (Koochesfahani *et al.* 2000) as drawbacks. There are additional limitations to hot-wire anemometry – specifically the types of flows in which hot-wire probes can be used. Firstly, the rotational symmetry of hot-wire probes makes them insensitive to flow reversals and not suitable for high-turbulence intensity flows. The delicate nature of hot-wire probes also makes them unsuitable for hostile environments, such as flows with chemical reactions or large solid particles. Finally, probe fouling and temperature contamination makes hot-wire probes unsuitable for liquid flows (Bruun 1995). In light of these limitations, a variety of other techniques for simultaneously measuring concentration and velocity have been proposed, including LDA (Laser Doppler Anemometry) combined with aspirating probes (So *et al.* 1990; Zhu *et al.* 1988), LDA combined with LIF (Laser Induced Fluorescence) or other laser scattering techniques (Lemoine *et al.* 1996), and PIV (Particle Image Velocimetry), DPIV (Digital Particle Image Velocimetry), or DPTV (Digital Particle Tracking Velocimetry) combined with PLIF (Planar Laser Induced Fluorescence) (Frank *et al.* 1996; Hu *et al.* 2004; Law and Wang 2000; Webster *et al.* 2001).[6] Each of these techniques measures concentration and velocity independently, using aspirating probes, LIF, PLIF, and other laser scattering techniques to measure

[6] Note that this list of techniques is not exhaustive, but represents a sampling of common experimental methods for making simultaneous concentration and velocity measurements.

concentration, and LDA, PIV, DPIV, and DPTV to measure velocity. Though it may be advantageous to measure concentration and velocity independently, so that concentration measurements are not dependent on velocity measurements, and vice versa, this is outweighed by the added complexity and cost of using two different experimental systems, especially considering that LDA, PIV, and other laser scattering techniques are known to be significantly more expensive than thermal anemometry techniques (Bruun 1995; Zhu *et al.* 1988).

The methods listed above are a reasonable alternative to flows in which thermal anemometry is not a choice (i.e. liquid flows, flows with high turbulent-intensities, and other hostile environments), where planar measurements, as opposed to point measurements, are required, and/or where spectral measurements are not desired. However, when it is possible to use hot-wire anemometry, it is the ideal instrument for studying turbulence, since the temporal and spatial resolution of velocity measurements made using hot-wire sensors operated in the constant-temperature mode are known to be superior (or in some cases, at the very least, comparable) to the temporal and spatial resolution obtained using LDA and PIV. (For example, the frequency response of a hot-wire probe reaches up to several hundreds of kilohertz, while measurements made by LDA are generally limited to less than 30 kHz, and PIV methods have low temporal resolution, due to the fact that they typically only sample the velocity field at frequencies below 10^2 Hz.) (Bruun 1995; Jensen 2004). Previous studies of interference probes, such as one conducted by Sirivat (1983),[7] had noted that the frequency response of both concentration and velocity measurements made

[7] A thesis containing a more detailed description of some of the work performed by Sirivat and Warhaft (1982)

by an interference probe are comparable to those made by a conventional single-normal hot-wire sensor. Based on this information, it is expected that the temporal resolution of an interference probe, at least in terms of velocity measurements should be superior to each of the non thermal-anemometry-based experimental techniques listed in the previous paragraph. It is for this reason, as well as the good spatial resolution that can be obtained with interference probes and the relatively low cost associated with this technique, that the use of hot-wire anemometry for making turbulent concentration and velocity measurements remains a valid and useful technique, and is used for the work conducted herein.

1.4 Organization of the Thesis

The remainder of the thesis is organized as follows. The experimental apparatus is presented in Chapter 2, and a description of the instrumentation is given in Chapter 3. Chapter 4 compares probes of differing designs so that the effects of overheat ratio, wire separation distance, wire diameter, and wire material can be studied and used to determine the optimal design of the interference probe. Chapter 5 presents results from the optimal probe to benchmark its accuracy and precision. Finally, Chapter 6 contains conclusions and suggestions for future work.

CHAPTER 2
Experimental Apparatus

The present chapter describes the experimental apparatus employed in this thesis. First, an overview of the experimental apparatus is given. Next, the helium and air mixing system is presented. Following that, a more thorough description of the mass flow meter and mass controller used in the mixing system is given. Afterwards, the automation of the helium and air mixing system is discussed. Finally, the calibration system is described.

2.1 Description of the Experimental Apparatus

The experimental apparatus, shown in figures 2.1 and 2.2, can be used to make measurements in flows of different concentrations, temperatures, or both. As the compressed air enters the system, it is passed through a filtering system to remove any dust and/or particles that could damage the mass flow meter or hot-wire probes. The shut-off valve enables quick shut-off of the airflow if necessary, and the pressure regulator is used to set the air supply to a pressure of roughly 25 psi, per the requirements of the calibration system. The experimental system is designed to contain two alternate pathways, labeled A and B in figure 2.2. The first pathway, A, can be used to make measurements in pure air and at higher velocities. The second pathway, B, is part of the helium/air mixing system and is used for all calibrations and experiments presented in this work. The maximum flow rate of air going though this pathway is limited to 100 slpm due to the specifications of the mass flow meter. Both tubing

Figure 2.1: Experimental apparatus

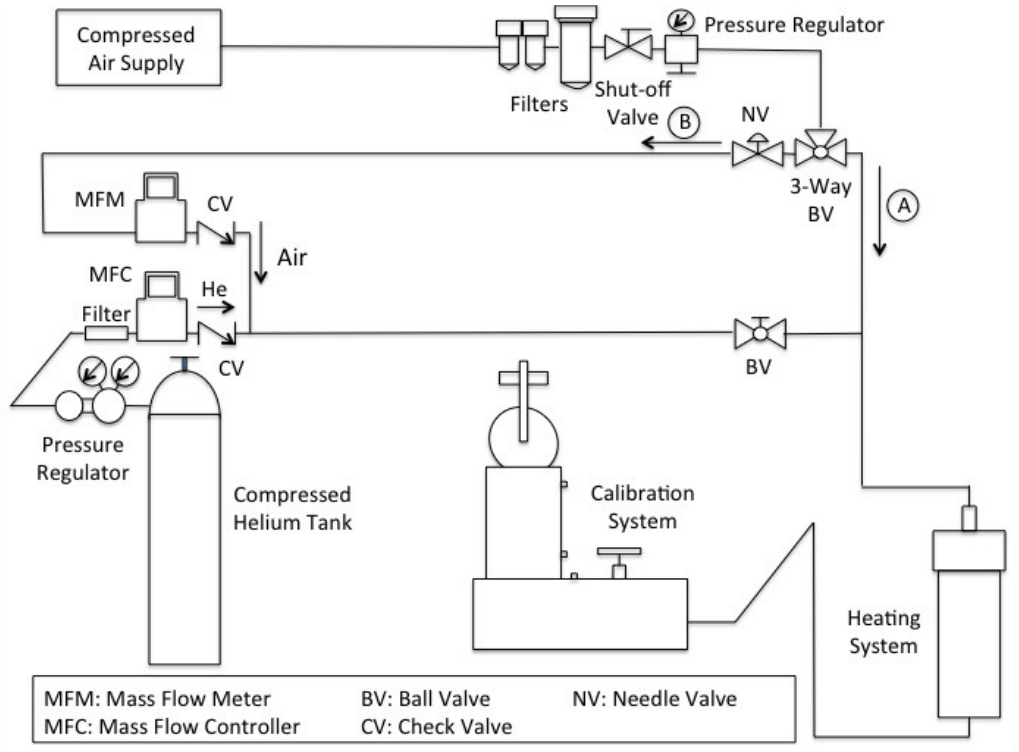

Figure 2.2: Schematic of the experimental apparatus

systems rejoin just before the heating system, which is composed of a long metal cylinder connected to a variable AC heater supply. The heating system can be used to perform calibrations or experiments at different temperatures, but as the focus of this thesis is on making measurements in heterogeneous, isothermal mixtures, it is not utilized. The fluid finally passes into the calibration system, which is used for calibrating the hot-wire probes and preliminary experiments.

Copper tubing and brass Swagelok fittings were used wherever possible to reduce the possibility of leaks around the fittings and effusion or diffusion through the tubing. The use of copper tubing had the additional benefit of equilibrating the temperature of the fluid due to the high thermal conductivity of copper. This reduced the effect of temperature drift or temperature fluctuations. Where it was not possible to use Swagelok fittings, a removable gas sealant was applied to prevent any possible leaks. After construction, every fitting in the system was checked for leaks by applying a soapy-water mixture to the fittings as pressurized gas passed through them (leaks can be identified by the presence of bubbles). The diameter (nominal size) of the tubing was 1/8 inch between the compressed cylinder tank and the mass flow-meter, 1/4 inch in the rest of pathway B, and 1/2 inch in all remaining sections. Tubing dimensions were chosen to maximize the length-to-diameter ratio in sections where the mixing of helium and air occurred, to minimize excessive velocities in the tubing, and for ease of construction.

2.2 The Helium/Air Mixing System

The helium/air mixing system is composed of a continuous stream of air joining with a continuous stream of helium at a T-junction. Mixing is achieved by the

naturally occurring turbulence in the piping system. Desired helium/air concentrations are maintained by using a mass flow controller (described in section 2.3) to adjust the flow rate of the helium relative to the measured flow rate of the air. A more detailed description of this process is given in section 2.4.

The air flow is controlled by a needle valve and measured downstream by a mass flow meter (described in section 2.3). A check valve following the mass flow meter prevents any reverse flow from potentially damaging the device or from affecting the accuracy of the measured flow rate.

Pure 99.995% compressed helium gas is stored in a tank containing 291 standard cubic feet of helium when full. The pressure in the tank is roughly 2600 psi when full and is regulated with a high purity dual stage pressure regulator. The delivery pressure is generally set between 25 and 45 psi, and small adjustments are made to it to ensure that the mass flow controller downstream runs smoothly. An in-line 20 micron filter located just upstream of the mass flow controller is installed to protect the mass flow controller from any particles that might have been introduced into the system (a possibility when an empty helium tank is replaced with a full one), and a check valve located just downstream of the mass flow controller prevents any back flow or contamination of the device with air from the tubing downstream. Additionally, a ball valve located just before pathway B rejoins with pathway A, is used to cut-off the flow to pathway B when pathway A is in use.

Following the T-junction where the air and helium join, a long straight length of tubing allows the helium and air to mix. Past studies have found that sufficient mixing is obtained anywhere from 2 diameters downstream to approximately 150 diameters (Forney and Lee 1982; Forney and Kwon 1979; Ger and Holley 1974). As these studies are only relevant for specific cases (specific fluids, diameters, and flow

rates), they cannot be used to predict the mixing length necessary in this work's specific application. Nevertheless, since the total length of tubing between the T-junction and the calibration jet exceeds 400 diameters and includes a number of 90° bends that create or enhance the turbulence, it can be assumed that sufficient mixing of the air and helium is achieved.

2.3 The Mass Flow Meter and Mass Flow Controller

A commercial mass flow meter (Alicat M-100SLPM-D) and mass flow controller (Alicat MC-20SLPM-D) were purchased and incorporated into the experimental system described previously. The mass flow meter is used to measure mass (and volume) flow rates, while the mass flow controller is additionally used to control the flow to a desired flow rate. Both the mass flow meter and the mass flow controller determine the volumetric flow rate Q from the Poiseuille equation below:

$$Q = \frac{\Delta P \pi r^4}{8 \mu L}, \tag{2.1}$$

by measuring the differential pressure drop ΔP across an internal restriction known as a Laminar Flow Element (LFE). This restriction is composed of hundreds of small-diameter tubes (of radius r and length L) designed specifically so that the fluid flowing through them is laminar.

The volume flow rate on the mass flow meter and the mass flow controller is reported in liters per minute at a standard temperature and pressure of 25°C and 14.696 psia respectively (a unit known as slpm). It has become standard practice to report the mass flow rate in standard liters per minute, but knowledge of the density at these conditions allows one to convert the volumetric flow rate to a true mass flow rate. Both devices compensate for the effects of temperature and absolute

pressure on the viscosity and density of the fluid, as well as compressibility effects. Additionally, the gas of the fluid being measured or controlled can be selected from a list of thirty or so common gases, including both helium and air.

The mass flow meter has an operating range of 0-100 slpm and is used for the air. The reported flow rate has an accuracy of 0.2% of full scale + 0.8% of flow rate (or a maximum of 0.1 slpm at the highest flow rate) and has a repeatability of 0.2% of full scale. It requires 7 to 30 VDC of power input, the typical response time is 10 ms, and the pressure drop across it is 2.5 psi or 17 kPa. Data, such as the mass flow rate, volumetric flow rate, pressure, and temperature, are displayed on a small LCD screen on the device. The value of the mass flow rate is also transmitted from the mass flow meter via a 0-5V analog signal to a computer running a LabVIEW program (described in section 2.4) that controls the helium/air mixing system.

The mass flow controller has an operating range of 0-20 slpm and is used for the helium. It also has an accuracy of 0.2% of full scale + 0.8% of flow rate and a repeatability of 0.2% of full scale. As the full scale of the mass flow controller is much lower than that of the mass flow meter, the mass flow controller is far more accurate than the mass flow meter. The mass controller requires 12 to 30 VDC, has response time of 100 ms, and has a pressure drop of 20 psi or 138 kPa. The mass flow rate, volumetric flow rate, pressure, and temperature are displayed on the screen on the mass flow controller device. The set point can be controlled either from the LCD screen on the device or from an analog input signal. It was decided to automate the functions of the mass flow controller to obtain continuous flows of the same concentrations. The set point was controlled from the LabVIEW program used to make the helium/air mixtures by transmitting a 0-5 V analog input signal from this program to the mass flow controller.

2.4 Automation of He/Air Mixing System

The mixing system, composed of the mass flow meter and the mass flow controller, was automated so that specified concentration levels would be maintained regardless of the flow rate. Communications between the mass flow meter and the mass flow controller are done through an 8 pin Mini-DIN connector located on the devices. Pins of interest control the output and ground signals. Single-ended 8 Pin Male Mini-DIN connector cables were supplied with the mass flow meter and mass flow controller. One end of the cables was connected to each device and the other was cut to expose the wires of interest. These were then soldered to a bulkhead BNC jack and connected to an oscilloscope and BNC 2110 board by BNC cables, as shown in figure 2.3. The analog signal coming from the mass flow meter is converted to a digital signal using a National Instrument PCI-MIO-16E-4 12-bit DAQ board. A LabVIEW program was written to acquire the data from the mass flow meter and determine the flow rate to which the mass flow controller should be set. Data from the mass flow meter is acquired as a 0-5 V signal (V_{MFM}) that can be linearly related to the measured airflow rate (Q_{air}). The voltage from the mass flow meter is known to be 5 V at full scale (100 slpm) and 0.01 V for zero flow, giving the following equation:

$$Q_{air} = \frac{(V_{MFM} - 0.01)}{4.99} 100. \tag{2.2}$$

This voltage signal is sampled at a rate of 500 Hz. 100 samples are taken and averaged to attenuate the effects of electronic noise. As the signal-to-noise ratio is very high, no further signal conditioning methods are used. The desired mass fraction of helium (X) is set in the program and converted to the desired volumetric fraction of helium

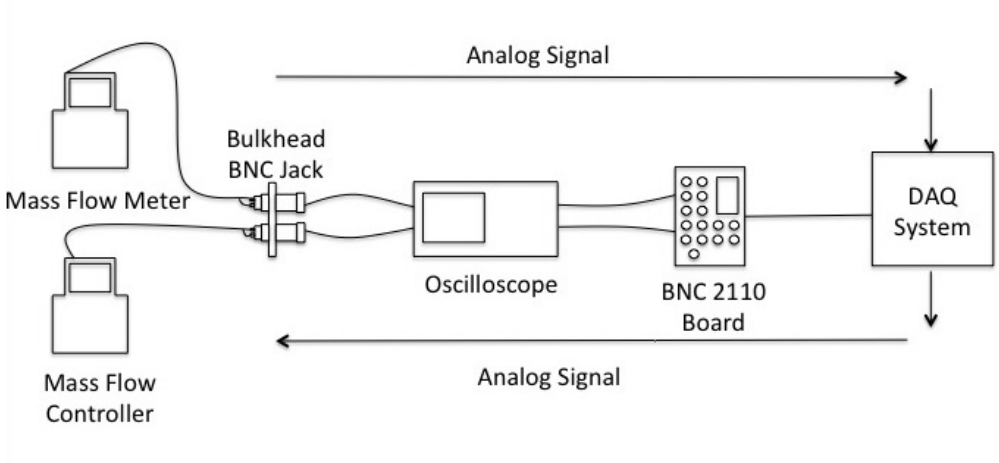

Figure 2.3: Data acquisition system for the helium/air mixing system

(Y) at standard conditions based on the following equation:

$$Y = \frac{X\rho_{air}}{(1-X)\rho_{He} + X\rho_{air}}. \tag{2.3}$$

The densities used in the following equation refer to the densities of air and helium at standard conditions, and are $\rho_{air} = 1.18402$ kg/m^3 and $\rho_{He} = 0.16353$ kg/m^3. The desired flow rate of helium (Q_{He}) can be calculated from the measured airflow rate (Q_{air}) and desired volumetric fraction of helium:

$$Q_{He} = \frac{Y}{1-Y} Q_{air}. \tag{2.4}$$

This volume flow rate is converted to a voltage signal (V_{MFC}), which is linearly related to the volume flow rate, and known to be 5V at full scale (20 slpm):

$$V_{MFC} = 5\left(\frac{Q_{He}}{20}\right). \tag{2.5}$$

The voltage V_{MFC} is then sent to the mass flow controller. The program is set to operate continuously, reading values from the mass flow meter and recalculating the desired flow for the mass flow controller based on those readings, until the user stops it. Fluctuations in the mass flow controller set point and reading are generally found to be within 0.01 slpm and deemed to have a negligible effect on the concentration of the helium-air mixtures.

2.5 The Calibration System

The calibration system is a commercially produced TSI Model 1128B Air Velocity Calibrator. It is a manually operated bench-top system designed to easily perform velocity calibrations for single, dual, and triple sensor hot-wire probes. The calibration system requires compressed air between 20 and 30 psi for operation, and

includes a settling chamber that generates an effectively laminar and uniform velocity profile at the exit nozzle. The system comes with two different exit nozzles: 10 mm and 14 mm diameter nozzles. The 10 mm nozzle is currently installed, although it can be switched for the 14 mm nozzle for cases in which lower velocity calibrations are desired. Typically the calibration system is operated using (i) fine and coarse adjustment valves, located on the calibration model itself, to adjust the flow, and (ii) a pressure transducer to determine the velocity. However, modifications have been made to the typical mode of operation to use this system for helium/air mixtures. The fine and coarse adjustment values are left open, and the flow rate is set using the needle valve located just upstream of the mass flow meter. The velocity at the nozzle exit (U_j) is determined from the total volume flow rate ($Q_{tot} = Q_{air} + Q_{He}$) and the area of the exit nozzle (of diameter D):

$$U_j = \frac{4Q_{tot}}{\pi D^2}. \tag{2.6}$$

Although the velocity profile at the nozzle exit is uniform and laminar, it becomes turbulent farther downstream. Initial measurements within a turbulent jet, validating the design of the interference probe, are also performed using this calibration system. These measurements are taken at a distance of $x/D = 10$ from jet exit, at concentrations that do not exceed a helium mass fraction of 0.04. Following work done by Chen and Rodi (1980),[1] this region of the jet can be characterized as non-buoyant, and the scalar, concentration in this case, can be said to be passive.

[1] See Appendix B

CHAPTER 3
Instrumentation

The instrumentation used in the present work consists of two different hot-wire probes: (i) a single-normal hot-wire probe used to make velocity measurements, and (ii) an interference probe used to make simultaneous concentration and velocity measurements.

3.1 Single-Normal Hot-Wire Probe

The single-normal hot-wire probe consists of a fine platinum-rhodium wire, 2.5 μm in diameter, mounted on a TS1 1210 single-wire probe. It forms one arm of a Wheatstone bridge circuit and is maintained at a constant resistance by an IFA300 Constant Temperature Anemometer. To maintain the wire at a constant resistance, the IFA300 must adjust the power supplied to balance the energy lost by convection. As described earlier in Chapter 1, a semi-theoretical relationship known as King's Law (equation 1.8) can be derived relating the anemometer voltage to the flow velocity. As the single-normal wire has been extensively studied, details regarding its design, construction, and calibration will not be extensively discussed.

3.2 Interference Probe

The focus of this work is the design of an interference probe to measure concentration and velocity at high spatial and temporal resolutions in turbulent flow (a turbulent jet in the case of the present work). The goal is to create a probe capable of measuring turbulent concentrations, ranging from a helium mass fraction of 0 to

0.06, and velocities, ranging from 0 to 13 m/s, with the same accuracy, precision, and resolution as conventional hot-wire sensors – that is with an accuracy of $< 1\%$, and sufficient precision and resolution that the measured PDFs in a laminar jet approximate delta functions and the concentration noise spectrum (which should merely be an electronic noise spectrum) is several decades below any concentration spectra measured by the interference probe. The interference probe should also have sufficient spatial resolution for measuring the finest scales of turbulence (about 0.1 mm), and wire length and separation distances should be minimized as much as possible in order to so. Furthermore, the frequency response of this probe should be comparable to that a single-normal-hot-wire probe, and it should be possible to make measurements at high frequencies (well beyond 1 kHz). Finally, the interference probe to be designed should be reliable enough, that when probes are calibrated directly before experiments, any voltage drift during the experiments is negligible, so that the equations governing the probe's response are accurate during both calibrations and experiments.

As the construction of an interference probe is a difficult task, and the design goals are numerous and difficult to achieve (as will be seen in Chapter 4), the objective will be to create an interference probe that fulfills as many of the design goals as possible, and to identify which of an interference probe's design parameters can be used to achieve these goals. To do so, six different probes, of differing materials and diameters, were constructed. The particular details of their design, construction, and calibration are presented in the following sections.

3.2.1 Design

Previous works developing hot-wire probes to simultaneously measure concentration and velocity have shown it was possible to do so with two wires of differing velocity-to-concentration sensitivity ratios. This could be achieved by using wires (or films) with different diameters (Harion *et al.* 1996), by allowing the wires (or films) to thermally interfere with each other (Panchapakesan and Lumley 1993; Sirivat and Warhaft 1982; Way and Libby 1970), or by using wires with different overheat ratios and materials (Sakai *et al.* 2001). From these works, six different design considerations are identified: the use of a hot-wire or hot-film, the material of the wire or film, the overheat ratio (OH) (defined as the wire operating resistance, R_w, divided by the resistance of the wire at the ambient temperature, R_a) of the wire or film, the diameter of the wire or film, the separation distance between the wires or films, and the angle between wires or films.

One of the first design characteristics to consider is whether to use a hot-wire or hot-film. A number of the interference probes[1] listed above involved the combination of a hot-film and a hot-wire. The primary advantage of using such a probe is a large diameter ratio, which increases the difference between the velocity-to-concentration sensitivity ratios of the wire and film. This makes it easier to accurately and precisely determine the concentration and velocity from the two voltage readings. Therefore, these hot-film and hot-wire probes may not need to have wires which thermally interfere with each other, and can be constructed with separation distances on the order of 25-1000 μm. Additionally, hot-films are more robust than hot-wires, have

[1] In this thesis, this term is used for all probes used to make concentration and velocity measurements, including those that do not make use of an interference effect.

greater long-term calibration sensitivity, and can be used in dirty flows (Bruun 1995). Despite all these advantages, hot-films have a much lower frequency response than hot-wires (Bruun 1995). Many investigations of turbulence mixing require accurate measurement of the finest scales of turbulence, which occur at high frequencies (generally above 10^3 Hz), and for this reason the use of a hot-film is not recommended. The design of the interference probe is therefore based on the designs of Sirivat and Warhaft (1982) and Panchapakesan and Lumley (1993), which do not use a hot-film.

The choice of wire material, another design criterion, affects the strength, resistance, and temperature of the wire due to the varying material properties of common hot-wire materials described in Table 2.1. Typically tungsten, platinum, and platinum alloys are used to make hot-wire probes. Tungsten has the advantage of strength, which is important during the construction process of the interference probe, but it has a low oxidation point and cannot be operated at high temperatures. Platinum is often the other material of choice. Although it has a relatively low tensile strength compared to tungsten, it suffers no oxidation problems and is available in the form of a Wollaston wire.[2] As the tensile strength of platinum is rather low, platinum-rhodium and platinum-iridium alloys are often used to increase the tensile strength of the wire while retaining the advantages of a platinum wire.

Although the choice in hot-wire material was mainly based on availability and ease of handling, the effect of material properties on the operation of a hot-wire

[2] A Wollaston wire is a platinum, or platinum alloy wire, (generally) covered in a thick sheath of silver. It is drawn through a die to give a small outer diameter (reducing the diameter of the fine inner platinum wire). The silver coating can later be etched away to expose the platinum wire. Through this process, wires with diameters as small as 0.25 μm are available.

probe should not be neglected. The temperature coefficient of resistivity α_a (defined to be at ambient temperature and $\approx \alpha_{20}$) is related to the operating temperature difference of the wire (derived from equation 1.4) as follows:

$$T_w - T_a = \frac{1}{\alpha_a}(OH - 1). \tag{3.1}$$

It can be seen from the equation above, as well as table 3.1, that when operated at the same overheat ratio, materials with smaller coefficients of resistivity, such as platinum-rhodium, will have higher wire temperatures than materials like tungsten or platinum, which have large coefficients of resistivity. The wire temperature, in turn, has an effect of the velocity (S_u) and temperature (S_θ) sensitivities of the wire as evidenced below:

$$S_u = \frac{\partial E}{\partial U} = \frac{nBU^{n-1}(T_w - T_a)^{0.5}}{2(A + BU^n)^{0.5}}, \tag{3.2a}$$

$$S_\theta = \frac{\partial E}{\partial \theta} = \frac{(A + BU^n)^{0.5}}{2(T_w - T_a)^{0.5}}. \tag{3.2b}$$

An increase in wire temperature leads to an increase in the probe's sensitivity to velocity and a decrease in the sensitivity to temperature. As the wire temperature is dependent on both the temperature coefficient of resistivity and the overheat ratio, the sensitivity of the probe to either velocity or temperature can be controlled by these two factors.

The wire material additionally has an effect on the resistivity of the wire (χ), which is related to the resistance of the wire as follows:

$$R = \frac{4\chi l}{\pi d^2}. \tag{3.3}$$

Table 3.1: Physical properties of common hot-wire materials from Bruun (1995)

Material	Ultimate tensile strength (N cm^{-2})	Temperature coefficient of resistivity α_{20} ($^{\circ}C^{-1}$)	Resistivity χ_{20} ($\mu\Omega$ cm)	Available as a Wollaston wire	Thermal conductivity (W $cm^{-1}{}^{\circ}C^{-1}$)
Tungsten	250000	0.0036	5.5	no	1.9
Platinum	35000	0.0038	9.8	yes	0.7
Platinum-Rhodium	70000	0.0016	19	yes	0.4
Platinum-Iridium	140000	0.008	32	yes	0.17

Care should therefore be taken when selecting the wire material, length (l) and diameter (d), to ensure compatibility with the instrumentation used. The IFA300 Constant Temperature Anemometer used in these experiments can only measure resistances up to 80 Ω and cannot be used to operate very fine platinum, platinum-rhodium, and platinum-iridium wires at high overheat ratios.

In addition to the resistance, the geometry also affects the spatial resolution of the wire and heat conduction to the prongs. To achieve ideal spatial resolution, the hot-wire probe should have a length (l) that is smaller than all the eddy sizes which occur in a turbulent flow. Therefore l should be smaller than η, the smallest length scale in a turbulent flow, called the Kolmogorov length scale. This value varies from flow to flow but is generally on the order of 0.1 mm. In order to minimize heat conduction to the prongs relative to heat loss to the air by forced convection, which may degrade the frequency response, the wire should be as long as possible. It has been found that a wire length-to-diameter ratio which is greater than 200 minimizes heat conduction effects Bruun (1995). Therefore hot-wires should be designed to have small diameters so that they can have small lengths but large length-to-diameter ratios.

The final design criteria are the wire separation distance and angle between wires. Decreasing the separation distance and/or angle has the effect of increasing the thermal interference effect between the wires. Way and Libby (1970) found that when their wire and film were too far apart, and did not thermally interfere with each other, it was impossible to distinguish low-concentration high-velocity voltage pairs from high-concentration low-velocity voltage pairs. Allowing the wires to thermally interfere with each other increases the sensitivity of the interference probe to concentration because the upstream wire and downstream wire behave differently. For example, if the wires are positioned so that one wire is in the the thermal field of

a second wire (but not vice versa), then the response of the first wire will be governed by the concentration and velocity field, as well as the thickness of the thermal boundary layer of the second wire. However, the second wire will only be governed by the concentration and velocity field, and will continue to follow King's Law. So if the concentration of helium suddenly increases, the voltage of the second wire will increase to compensate for the increased heat loss due to the higher thermal conductivity of helium, as expected. The thermal boundary layer of this wire will expand as a result, and expose the first wire to higher temperatures. If the first wire is operated at a low overheat ratio, it will be sensitive to the change in temperature. Under certain conditions (dependent on the velocity, concentration, and design of the probe), this increase in temperature will outweigh the effects of higher concentrations, and the voltage of this second wire will decrease. Under these conditions, the responses of the two wires are sufficiently different that it is then possible to extract accurate and precise concentration and velocity data from the voltage readings.

Based on the design considerations outlined above, the interference probes used in this work consisted of two hot-wires of differing characteristics (overheat ratio, diameter, wire material) which are placed on a modified X-wire probe, close enough to have one of the wires thermally interfere with the other. The various interference probes designed in this work are listed in table 3.2. They are abbreviated with the wire material (W for tungsten, Pt for platinum, Pt/R for platinum rhodium) and the approximate spacing between the wires in micrometers. This distance was measured by using the 100-tick scale on a microscope, which was compared with known distances on the order of mm's. The rough nature of this process means that the wire spacing distances are accurate to ± 5 μm.

Table 3.2: Summary of interference probes developed in this thesis

Thermal Anemometry Probe	Upstream sensor: diameter and material	Downstream sensor: diameter and material	Diameter ratio	Separation distance	Angle between sensors	Construction Method
W-Pt-35	3 μm Tungsten	1.2 μm Platinum	2.5	35 μm	25°	1
W-W-55	3 μm Tungsten	3 μm Tungsten	1	55 μm	25°	1
W-W-25	3 μm Tungsten	3 μm Tungsten	1	25 μm	25°	1
W-W-20	2.5 μm Tungsten	2.5 μm Tungsten	1	20 μm	25°	3
W-W-10	2.5 μm Tungsten	2.5 μm Tungsten	1	10 μm	25°	3
W-Pt/R-10	2.5 μm Tungsten	2.5 μm Platinum-Rhodium	2	10 μm	25°	2

The wires on each of these probes cross each other at an angle of roughly 25° (also accurate to about ±5°), so that the effect of thermal interference is increased. When the probes contain wires of differing diameters (W-Pt-35, W-Pt/R-10), the large-diameter wire is placed in the upstream position, and the small-diameter is placed in the downstream position. This is partly a result of the construction process, and partly an attempt to increase the thermal interference effect of the upstream wire on the downstream wire (the thermal wake of a larger wire being larger). This is in contrast to many previous designs in literature; however this was due to the fact that many of these designs made use of a hot-film, and hot-films are prone to vortex shredding. To avoid these effects on the wire, the hot-film would have to have been placed in the downstream position. The lengths of the wires are limited by the construction process, and ideally would be shorter to maximize the spatial resolution of the interference probe.

The various designs of the interference probes listed in table 3.2 were chosen in an attempt to (i) improve the accuracy and precision of measurements by an interference probe, and meet as many design goals as possible, and (ii) study the effects of various design characteristics on the responses of these probes. For example, as the W-W-55, W-W-25, W-W-20, and W-W-10 probes differ only in the separation distance between the two wires, it is then possible to study what effect this has on their response. It should also be noted, that the availability of wire materials, and the difficulty of the construction process, limited the choices in design. Specific details regarding the construction process are given in the following subsection.

3.2.2 Construction

The interference probes developed in this work were constructed using three different methods. Method 1 involved the use of two coated wires (copper-coated tungsten wires or silver-coated Wollaston platinum and platinum-rhodium wires). Method 2 used one coated wire and one bare wire, and Method 3 required two bare wires. The processes to secure the different types of wires is fairly complex and will first be described. The materials necessary for construction are listed below, with distinctions between those required when coated wires are used and those required when bare wires are used.

Required for all construction methods (1,2, and 3):

- Stereo microscope and flexible LED lamp
- Soldering iron with pointy tip
- Multimeter
- Solder (Leaded is perferred)
- Acid flux (Decapant 817)
- Isopropanol 99%
- TS1-1240 X-wire probe
- Sharp cutting blade (razor blades)
- Wood skewers and Q-tips
- Sandpaper

Required for methods involving coated wires (1 and 2):

- Traversing mechanism with small metal hook
- Acid paste flux (Kester SP-30)
- Nitric acid (68-70%)

- Fine coated wires (2.5 μm silver coated platinum-rhodium, 3 μm copper coated tungsten, 1.2 μm silver coated platinum)
- Metal pointer (or other instrument to manipulate wires)
- Capillary tubes (about 1 mm inner diameter)
- Sheet of paper

Required for methods involving bare wires (2 and 3):

- Fine bare wires on spool (2.5 μm tungsten, 5 μm tungsten)
- Wire transfer block
- Micromanipulator
- Glue gun

3.2.2.1 Process to Solder Coated Wires to a Hot-Wire Probe

The steps to solder coated wires to a hot-wire probe are described below. Single-wire probes, as depicted in figure 3.1 are constructed using this process, but it can easily be extended to the interference probe, as will described in section 3.2.2.3.

Step 1: Remove old solder from the prongs of the hot-wire probe using the heated soldering iron. Clean the prongs of any remaining solder and particles using a Q-tip soaked in the isopropanol. Dip the wooden skewer in the acid flux and place a drop of the acid flux on the prong tips.

Step 2: Make little shavings of solder using the razor blade. Select appropriately sized shavings and place them on the prongs using a metal pointer. Place the soldering iron tip near the prong tips and wait until the solder shaving melts and forms a bubble. The diameter of the bubble should not exceed that of the prong tips, as it must not become an aerodynamic obstacle to the flow.

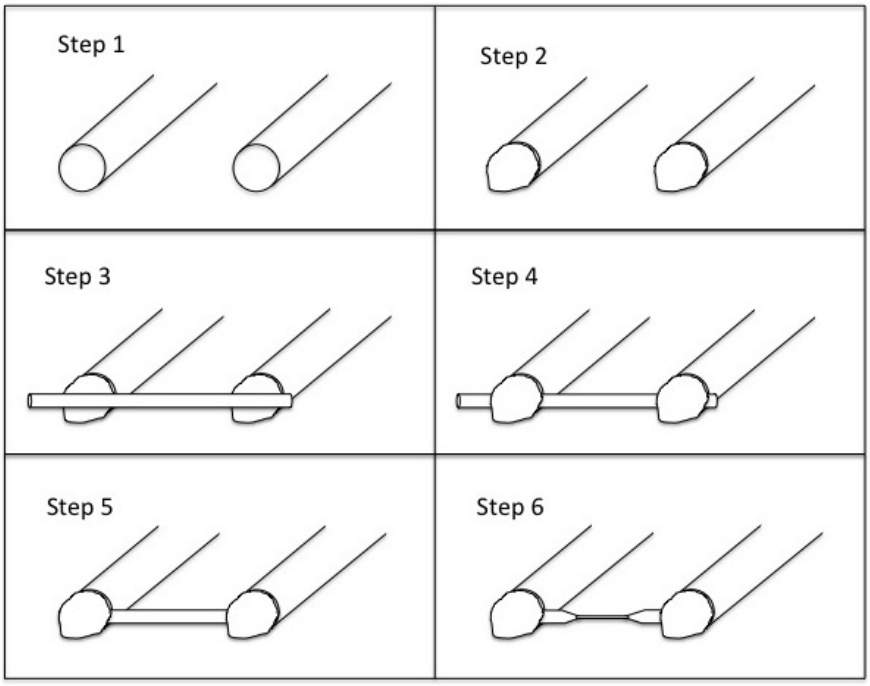

Figure 3.1: Steps for construction of a single-wire probe

Step 3: Take the metal pointer and dip the tip in the acid paste flux and place a very small amount on the solder bubbles. This is to hold the wire in place before it is soldered. Use the razor blade to the cut the hot-wire. Ideally it should be cut to a length as close as possible to the distance between the prong tips, however if it is too long it can be cut to length afterwards. Using the metal pointer, place the wire on the prongs and position it.

Step 4: Take the soldering iron and place it close to the solder bubbles and wait until the wire is sucked into the bubble of melted solder by the action of surface tension. Additional acid flux may be applied if necessary to help bring the wire inside the solder bubble.

Step 5: Check that wire is well soldered to the prongs using the multimeter. The resistance it reads should typically be around 0.4-0.7 Ω. Cut any ends that extend past the solder bubbles using the razor blade. To make the cut as clean as possible use a new razor blade each time and shear off the excess wire by applying force on the razor blade parallel to the prongs of the probe.

Step 6: Dip a capillary tube in the nitric acid. Place a small bubble on a hook of fine wire attached to the traversing mechanism. Bring the bubble up to the center portion of the wire using the traversing mechanism and make sure the wire is entirely submerged in the bubble. Monitor the resistance on the multimeter. Continue applying bubbles of nitric acid until the wire has reached its desired resistance. For the 2.5 μm platinum-rhodium wires and 3 μm tungsten wires used, this corresponds to resistances of approximately 20 Ω and 5 Ω respectively. Inspect the wire to ensure there are no leftover impurities. Clean it with a drop of isopropanol on the wire hook of traversing mechanism.

3.2.2.2 Process to Solder Bare Wires to a Hot-Wire Probe

As the bare wires are only a few micrometers in diameter, they are incredibly fragile and difficult to see with the naked eye. Special equipment, such as the wire transfer block (see figure 3.2) and micromanipulator (see figure 3.3), has been developed by Afara (2011) to manipulate these wires. The wire transfer block was designed and constructed to transfer fine wires located on a spool[3] to a wire holder. The primary wire holder was used to transfer the wire from the wire transfer block to a micromanipulator. A secondary wire holder was required so that the wire could always be kept connected to something. So long as the wire remained connected to one of the wire holders the process ran smoothly; on the rare occasions it came loose it was very difficult to reattach and often resulted in the loss of some (expensive) wire. The specific steps to remove the primary wire holder are illustrated in figure 3.4 and described below:

Step 1: The primary wire holder was rotated counterclockwise about 45° so that the secondary wire holder could be installed without damaging the wire.

Step 2: The secondary wire holder was installed in the slot on the wire transfer block and positioned close to the primary wire holder. The screw above was tightened to keep the secondary wire holder in place.

Step 3: The primary wire holder was rotated clockwise so that its pins were horizontal. The secondary wire holder was rotated counterclockwise so the top (left) pin came into contact with the hot-wire. The spool was rotated clockwise to keep the wire taut. A small amount of glue from a glue gun was applied to secure the wire to

[3] The commercially purchased wires used in this work came on a spool.

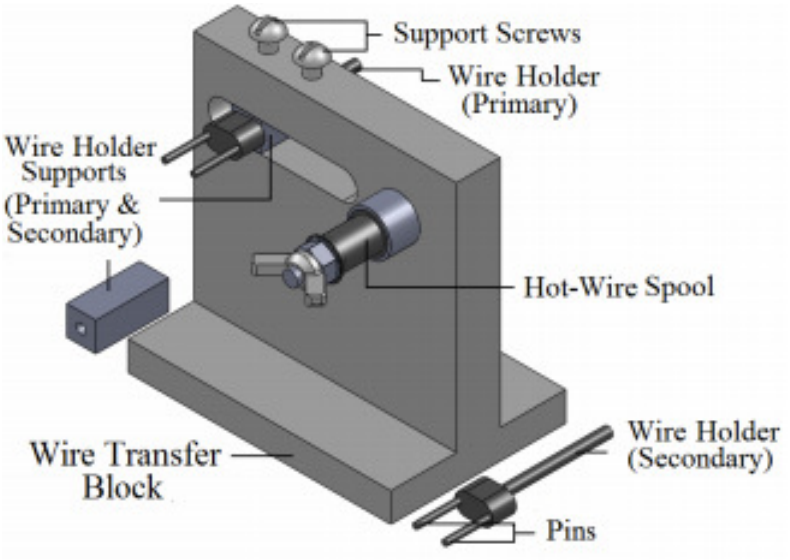

Figure 3.2: Wire transfer block - from Afara (2011)

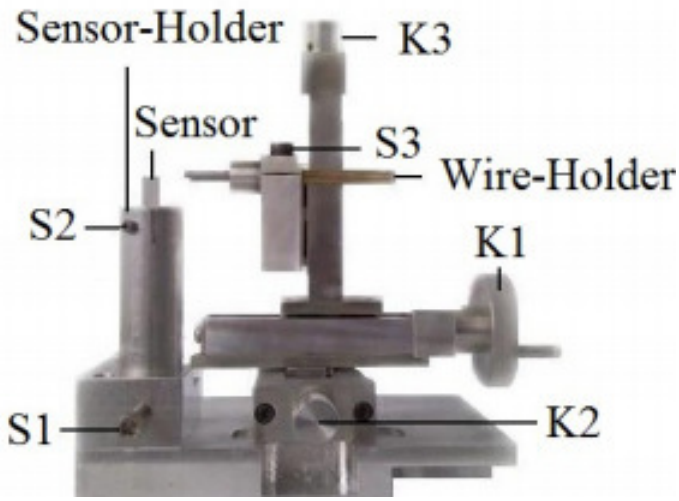

Figure 3.3: Micromanipulator - from Afara (2011)

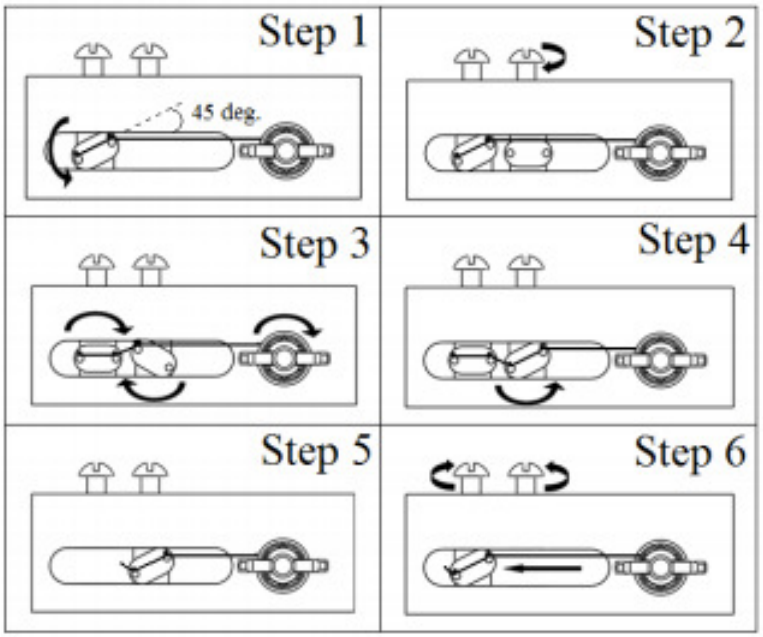

Figure 3.4: Steps to remove primary wire holder - from Afara (2011)

the top pin.

Step 4: Once the glue had dried, the secondary wire holder was rotated clockwise so that the other pin (right) came into contact with the wire. The spool was rotated clockwise to keep the wire taut, and a small amount of glue from the glue gun was applied to secure the wire to this pin.

Step 5: Once the wire was well secured to the secondary wire holder, a razor blade was used to the cut the wire between the primary and secondary wire holder. The primary wire holder was removed and transferred to the micromanipulator.

Step 6: The screw above the secondary wire holder was loosened and the spool was rotated counterclockwise a small amount, so that the secondary wire holder could carefully be shifted over to the primary wire holder's location. Once the secondary wire holder, now the primary wire holder, was in position the screw above it was tightened and the spool was rotated clockwise until the wire was taut. This returned the wire transfer block to its state in step 1, and the entire process could be repeated again if desired.

The micromanipulator was developed to bring the wire holder close to the hot-wire probe so that the wire could be soldered to its prong. The sensor and sensor-holder depicted in the figure 3.3 are not utilized in the present work (they were required to construct the wall shear sensors used by Afara (2011)).

3.2.2.3 Methods 1, 2 and 3 for Construction of Interference Probes

The interference probes developed (with each method of construction) were mounted on a modified TS1-1240 X-wire probe. The TS1-1240 X-wire probe is designed so that the two wires on the probe are at 90° to each other, as shown in figure 3.5.

The prongs of the modified probe used herein are ground using sandpaper so that all prongs are now of equal length. These prongs are then bent to bring the ends closer together. The goal is to have the wires cross at an angle as small as possible while still leaving sufficient distance between opposite prong ends to prevent a short circuit. As a compromise between these two design considerations, the distance between the prongs is about 0.5 mm, resulting in wires that cross at an angle of roughly 25°.

Method 1: Interference probe with two coated wires

Step 1: Little shavings of solder are placed on each of the prong ends and heated to create small solder bubbles. The exact details of this process are given in steps 1-2 of section 3.2.2.1. The size of these solder bubbles should be carefully chosen so that the wires can be positioned within a few micrometers of each other, but are not touching.

Step 2: The downstream wire is placed on the interference probe in the manner depicted in the figure 3.5, with the wire placed diagonally across the probe. The steps for soldering the wire to the probe and etching it are described in steps 3-6 in section 3.2.2.1.

Step 3: The upstream wire is thinned in a solution of nitric acid so that it can be placed as close as possible to the downstream wire. This is necessary, since coated wires have diameters on the order of 100 μm, thus limiting the separation distance between the two wires. This is done by using a capillary tube to place a small drop of nitric acid on a flat surface. The wire is then placed in the drop of solution using a metal point until it has reached its desired size (either fully or nearly etched). The best results are obtained when the wire is placed so that only the center portion of the wire comes into contact with the acid; the ends of the wire therefore remain visible and easy to manipulate.

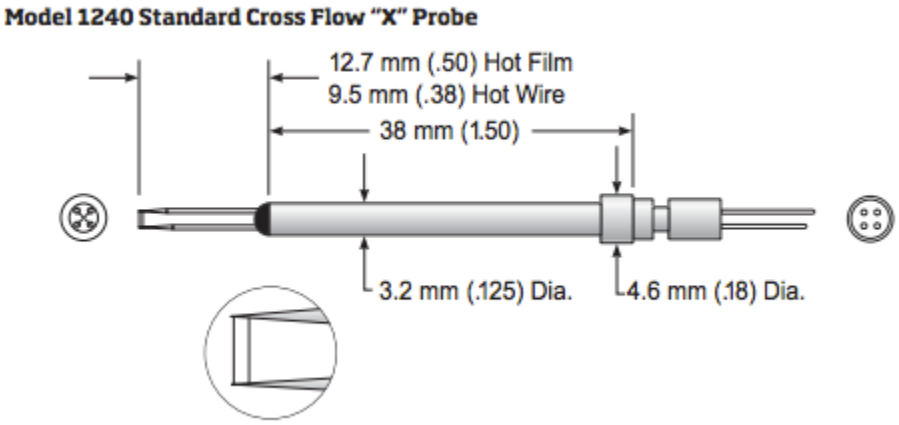

Figure 3.5: TS1-1240 X-Wire probe - from TSI catalogue of Thermal Anemometry Probes (2013)

Step 4: After thinning the wire in nitric acid it should be cleaned. It is set on a piece of paper and a capillary tube is used to place a small drop of isopropanol on top of it. Once the isopropanol has evaporated, the wire is ready to use.

Step 5: The upstream wire is soldered to the probe following steps 3-5 in section 3.2.2.1. Care should be taken in positioning the upstream wire so that the separation distance is on the order of 5 μm (or as small as possible if this proves difficult).

Step 6: Once both wires have been soldered in place, the traversing mechanism, with a fine wire hook, should be used to place a drop of nitric acid in the center of the probe to ensure that both wires have been completely etched. The wires should be checked for any remaining impurities or possible short circuits. Once the probe is deemed acceptable, it can be cleaned by placing a drop of isopropanol on the traversing mechanism hook.

An example of a probe constructed using Method 1 (W-Pt-35 probe) is shown in figure 3.6. The advantage of this method is that by using coated wires with an etched central portion, the spatial resolution of the probe may be increased (the active portion of bare wires is about 2-3 times longer). However as all wire placements are done using a metal pointer, it is difficult to place the wires close enough without breaking them. Additionally, the process of thinning the wire until the central portion is bare, makes the wire extremely fragile; this is not a problem when using tungsten wires, but may be a concern when attempting to use platinum or platinum alloy wires because of their low tensile strength. In light of the difficulties associated with this method of construction, alternative methods were developed.

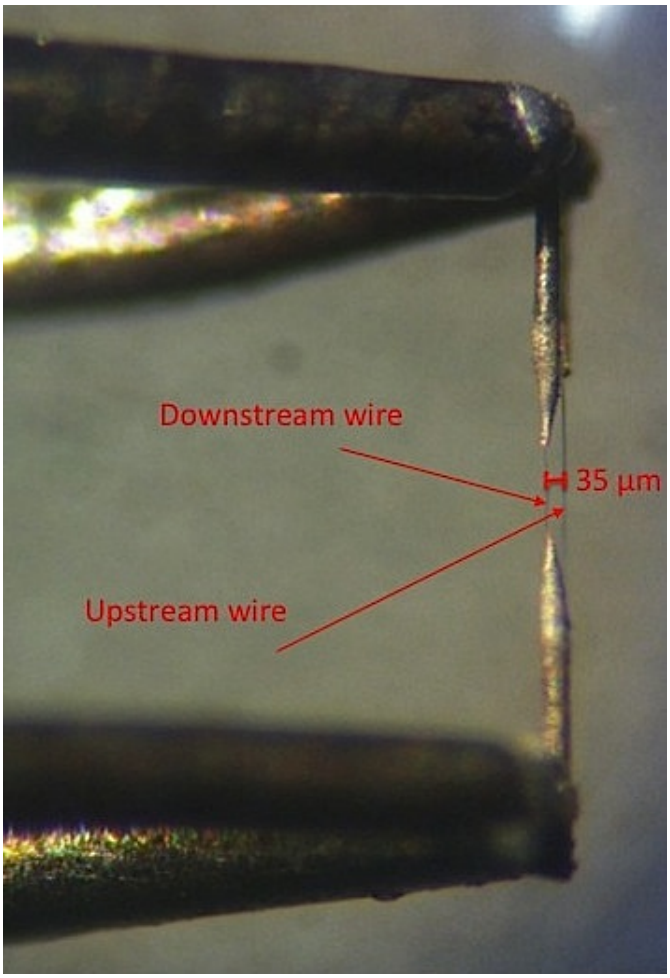

Figure 3.6: W-Pt-35 probe constructed using Method 1

Method 2: Interference probe with one coated wire and one bare wire

Step 1: Little shavings of solder are placed on two of the prongs, diagonally opposite from each other, and the coated wire is soldered to these prongs, as in steps 1 and 2 of Method 1.

Step 2: A commercially produced bare wire, initially located on a spool, is transferred to the micromanipulator following the steps given in section 3.2.2.2. The bare wire can then be positioned so that is flush with the prong ends using the K1, K2, and K3 controllers on the micromanipulator (see figure 3.3). The angle of the wire can be changed by twisting the wire holder in place. Once the wire is in place, the K1 axis controller should be turned slightly so that the wire is pulled tightly across the prong ends.

Step 3: A small bubble of leaded solder is applied to the tip of the soldering iron and placed over one of the prongs for a very short period of time (< 1 s). If this is not sufficient to solder the wire to the prongs, a very small shaving of solder can be applied over the bare wire. The soldering iron is then placed on the prongs, a small distance away, until the shaving of solder melts. Once one end of the wire has been soldered, the wire is tightened again slightly by turning the K1 controller, and the other end of the wire is soldered to the other prong using the same procedure. An oscilloscope should be connected to the interference probe to check if the wire has been well soldered (the final resistance will vary with wire material and diameter, but can be estimated with knowledge of the wire properties).

Step 4: A sharp razor blade is used to cut the ends of the wire beyond the prongs and detach the probe from the wire holder. It is suggested that a fresh razor blade be used each time to make the cut as clean as possible.

Method 3: Two bare wires

The procedure for this method is nearly identical to the one described in Method 2. In this case, both wires are bare wires and both are positioned using the micromanipulator. Since the micromanipulator allows for finer control of the wire, it is possible to make the separation distance between the wires much smaller using Methods 2 and 3. The probes created using Method 1 had separation distances ranging from about 25-55 μm, but the probes created using Methods 2 and 3 had separation distances ranging from about 10-20 μm. These two methods are therefore preferable to the first. Since no significant advantages or disadvantages were noticed between Methods 2 and 3, these can be used interchangeably depending the availability of certain sorts of wire.

3.2.3 Calibration

Once a new probe has been built, its wires should be "burned in" at their anticipated operating resistances for at least 24 hours before being used to allow the material properties to reach a steady-state. The calibration system described in Section 2.5 is used to relate the known velocity and concentration data to the squared voltages across the wire. First, the resistance of each wire is determined using the IFA300. The operating resistance is set by multiplying the desired overheat ratio with the resistance. Before the start of the calibration, the ambient temperature and pressure are recorded so that the mass flow rate (in reality a volume flow rate) measured by the mass flow meter can be corrected to find the volume flow rate at the jet exit. During the calibration process, voltages are recorded from a LabVIEW program developed to find the mean voltages coming from the hot-wire probe. The details of the data acquisition process are given in the section 2.4.

3.2.3.1 Calibration and Data Reduction for the single-normal Probe

The singe normal wires used in these experiments were calibrated in flows of pure air at twenty different speeds ranging from about 1.5 m/s to 13 m/s. The majority of these speeds were chosen to occur in the lower part of the velocity range, where the voltage is more sensitive to velocity changes. Once the voltages and velocities had been satisfactorily recorded, a power fit was applied to the data to find the constants A, B, and n for the King's Law equation (figure 3.7). Based on these results, the velocity of the hot-wire probe in subsequent experiments could be determined from the following equation:

$$U = \left(\frac{E^2 - A}{B} \right)^{1/n}. \tag{3.4}$$

3.2.3.2 Calibration and Data Reduction for the Interference Probe

The interference probe was calibrated in flows of 4 different concentrations, ranging from pure air to a helium mass fraction of 0.06, and 20 different velocities, ranging from about 1.5 m/s to 13 m/s and distributed in the same manner as those used for the single-normal probe. A number of different data reduction schemes were compared, and the following scheme was ultimately employed to determine concentration and velocity from the voltages of the two wires in the interference probe:

$$\begin{aligned} C = {} & a_1 E_u^3 E_d^3 + a_2 E_u^2 E_d^3 + a_3 E_u E_d^3 + a_4 E_d^3 + a_5 E_u^3 E_d^2 + \\ & a_6 E_u^2 E_d^2 + a_7 E_u E_d^2 + a_8 E_d^2 + a_9 E_u^3 E_d + a_{10} E_u^2 E_d + \\ & a_{11} E_u E_d + a_{12} E_d + a_{13} E_u^3 + a_{14} E_u^2 + a_{15} E_u + a_{16}, \end{aligned} \tag{3.5a}$$

$$U = \left(\frac{E^2 - A(C)}{B(C)} \right)^{1/n_{av}}, \tag{3.5b}$$

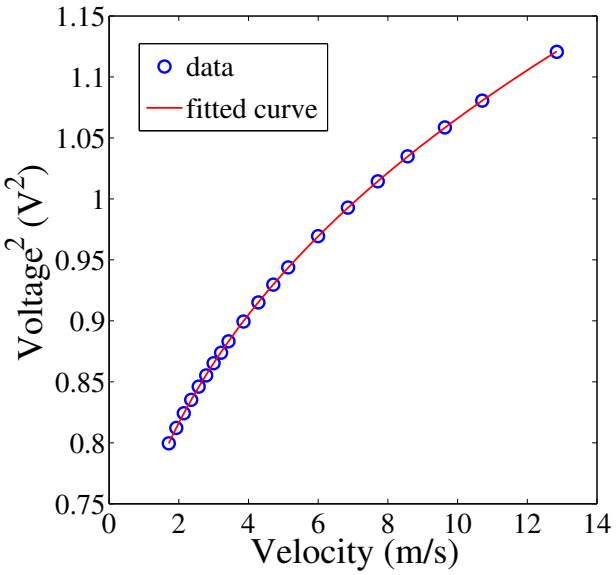

Figure 3.7: King' Law calibration for a platinum-rhodium single-normal hot-wire: $E^2 = A + BU^n$, with A=0.5288, B=0.2196, and n=0.3885.

where the concentration (C) was determined from a mixed, third-order polynomial function[4] of the downstream wire voltage (E_d) and the upstream wire voltage (E_u). Although other methods for determining the concentration were considered, such as the approach used by Way and Libby (1970, 1971), the polynomial method proved to be the most accurate and easy to implement. Using higher-order polynomials did not improve the accuracy of the calibration, and so the voltages used in the data reduction scheme were limited to the third-order.

To find the velocity, a King's Law fit was applied to the upstream wire[5] for each concentration, as shown in figure 3.8. The value of the exponent n for each concentration was averaged to give a mean value of n_{av}. The King's Law fit was performed again, but this time using the fixed value of n_{av} for each concentration. A second order polynomial was applied to the constants A and B to find the functions $A(C)$ and $B(C)$ (see figure 3.9). With $A(C)$, $B(C)$, n_{av} and c known, U could be calculated from the equation 3.5b.

To determine the accuracy of the data reduction scheme, the original voltages gathered during the calibration process were inputted into the above scheme, and the calculated values of concentration and velocity were compared to their calibrated values. The maximum percent errors between the calculated and calibrated values

[4] For certain experiments a mixed second-order polynomial function was used to improve the accuracy of the measurements for voltages beyond the ranges recorded during calibration.

[5] Analysis had shown that using the downstream wire to determine the velocity was usually far less accurate

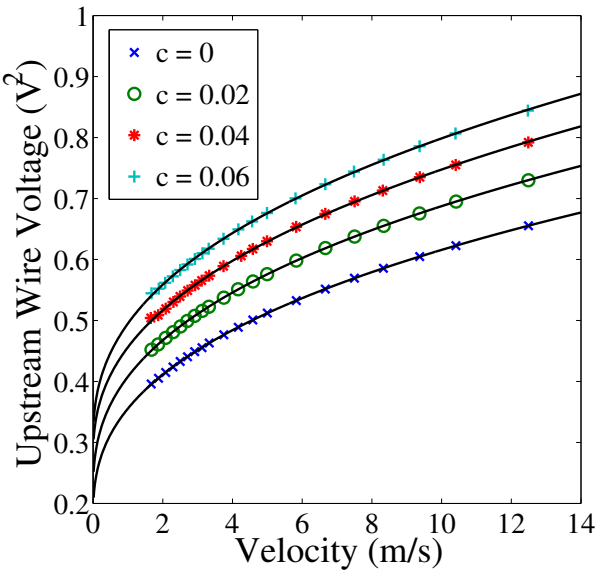

Figure 3.8: King's Law calibration for the upstream wire of the interference probe in flows of different concentrations: $E^2 = A(C) + B(C)U^n$. Concentrations range from 0 to 0.06, and are given in terms of the helium mass fraction.

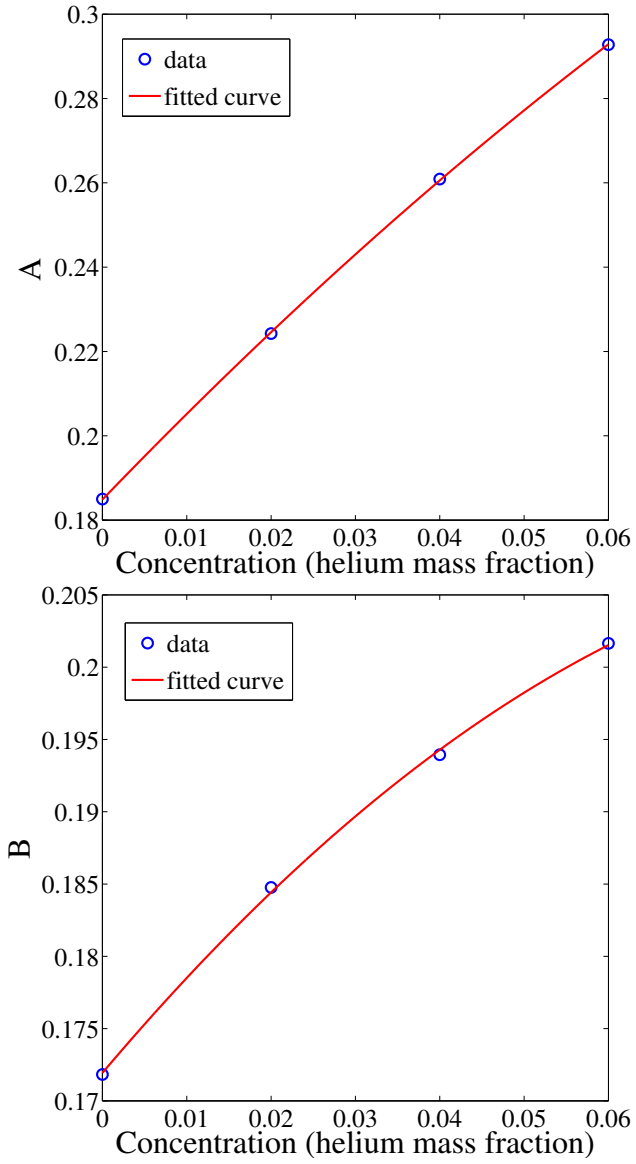

Figure 3.9: Variation of coefficients A and B from King's Law with concentration. Second order polynomials are used to fit the curves.

were generally less than 3%, for both concentration and velocity, and the average percent errors over the entire data range of the calibration were less than 1%. Unfortunately, outside the data range in the calibration process, the accuracy of the results quickly degraded and sometimes became clearly unrealistic. Since small amounts of voltage drift could lead to large errors, calibrations were performed before each set of experiments.

3.2.4 Data Acquisition

The output signal of the hot-wire anemometer probe was connected to the IFA300 constant temperature anemometer, and for measurements in turbulent flows, it was band-pass filtered using a 4-channel Krohn-Hite 3384 filter. For each wire, one channel of data was low-pass filtered to remove high frequency electronic noise and used to determine the mean voltages from the probe. The low-pass frequency was set to the maximum frequency of the flow, and estimated by using a real-time spectrum analyzer developed in LabVIEW. The spectrum of $f^2F_{11}(f)$ was plotted; the maximum frequency occured approximately at the minimum in the spectrum beyond its peak if the signal-to-noise ratio of the flow was good. The second channel was both high and low-pass filtered to remove the DC component of the signal. The remaining filtered signal was amplified by 20 dB to minimize discretization errors. Both signals were connected to an oscilloscope used to monitor the output. These analog signals were then digitized with a 16-bit National Instrument PCI-6143 DAQ board controlled by LabVIEW. To obtain the time series of the turbulent signals and determine the power spectra, data had to be sampled at twice the low-pass frequency (known as the Nyquist Criterion). Spectral data was recorded as sets of 200 blocks containing 4096 samples each, for a total of 819200 samples taken over a period of a few minutes (the

exact value depending on the low-pass filter and therefore the sampling frequency). To determine statistical moments and PDFs, it is best if each sample is independent from the next. Therefore sampling should be done at frequencies on the order of the integral frequency ($\approx u/l$) (Tennekes and Lumley 1972). In the following experiments, the sampling frequency used to determine the large-scale statistics was set to 200 Hz, and data was sampled for 50 blocks containing 4096 samples each, for a total of 204800 samples taken over roughly 17 minutes. The voltage samples from both wires of the probe were assumed to taken simultaneously, although in reality the DAQ has in inter-channel delay of 5 μs.

CHAPTER 4
Effects of Design Characteristics on the Performance of an Interference Probe

The six interference probes constructed for this thesis (see table 3.2) are compared to identify the essential characteristics in the design of such a probe. In the previous chapter, the design of the interference probe was discussed, and several different design criteria were identified. These include the overheat ratio, wire separation distance, wire diameter, and wire material. The effects of these design characteristics on the probe's performance are studied in the present chapter and used to identify the optimal design for an interference probe. First, a description of the response of an ideal probe is given in section 4.1. In the following section, experiments are performed on the first three probes (W-Pt-35, W-W-55, and W-W-25) to study the effects of the overheat ratio on the probe's performance. Next, in section 4.3, experiments on the W-W-55, W-W-25, W-W-20, and W-W-10 probes are used to infer the effects of the separation distance. Following that, the W-W-10 and W-Pt/R-10 probes are compared to investigate the effect of wire diameter on the interference probe. A brief description of the effects of wire material is presented in section 4.5, and the design of the optimal probe is finally discussed in section 4.6.

4.1 Characteristics of an Ideal Interference Probe

To sensibly discuss the effects of the various design criteria on the interference probe and determine the optimal probe design, a brief description of the response of an ideal interference probe must first be given. Such an ideal interference probe

should be capable of accurately measuring the (i) mean concentrations and velocities, and (ii) fluctuating components of concentration and velocity in turbulent flows. The first step involves successfully distinguishing mean concentration and velocity data in both laminar and turbulent flows. Since increases in helium concentration and increases in velocity both cause the voltage of a single wire to increase, the probe must be designed so that low-concentration, high-velocity voltage pairs can be distinguished from high-concentration, low-velocity voltage pairs. Next, it should also be possible to distinguish fluctuating concentrations and velocities with a reasonable degree of accuracy. (This does not not necessarily follow from successful measurements of the mean components of concentration and velocity, as will be shown in section 4.2.) Using an ideal interference probe, the measured concentration spectrum in a (laminar or turbulent) flow of pure air would exhibit minimal spurious concentration fluctuations, and tend to a spectrum of electronic noise, similar to the velocity spectrum measured by a hot-wire probe in a laminar flow of pure air, or a temperature spectrum measured by a cold-wire thermometer in a (laminar or turbulent) isothermal flow. In reality, this will not be the case, but the measured concentration spectrum in a flow of pure air should be substantially lower than spectra measured in flows with concentration fluctuations, resulting in a large signal-to-noise ratio. Furthermore, the PDF (probability density function) of concentration in a flow of pure air should be a delta function about zero concentration. In reality, however, there will be a small range of apparent concentrations measured.

Having identified the characteristics of an ideal interference probe, attention can now be given to discussing the effects of the various design criteria (overheat ratio, wire separation distance, wire diameter, and wire material) on the performance of such probes. The effect of the overheat ratio will be discussed first.

4.2 Effect of the Overheat Ratio

The various overheat ratio combinations used in previous interference probes (see table 1.1) suggest that the optimal overheat ratio of an interference probe is dependent on other design characteristics, such as the diameter ratio or the wire configuration, and therefore unique to each probe. To (i) gain a better understanding of the effects of the overheat ratio on an interference probe, and (ii) determine the optimal overheat ratios of the interference probes developed in this work, several experiments were carried out on the W-Pt-35, W-W-55 and W-W-25 probes.

The first of these experiments, the results of which are shown in figure 4.1, involved studying the effect of the overheat ratio on the calibration map. (The term "calibration map" is used herein to refer to a plot of the downstream wire voltage as function of upstream wire voltage, as measured during a calibration for the various concentration-velocity pairs.) The W-Pt-35 probe, which is composed of a 3 μm tungsten wire in the upstream position, and a 1.2 μm platinum wire in the downstream position, was calibrated with (i) both wires at a low overheat ratio (OH=1.2), (ii) the upstream wire at a high overheat ratio (OH=1.8) and the downstream wire at a low overheat ratio (OH=1.2), (iii) the upstream wire at a low overheat ratio (OH=1.2) and the downstream wire at a high overheat ratio (OH=1.8), and (iv) both wires at a high overheat ratio (OH=1.8). As can be seen in figure 4.1, unless the (larger) upstream wire is operated at a high overheat ratio, and the (smaller) downstream wire is operated at a low overheat ratio, as is the case in figure 4.1b, it is difficult to unambiguously distinguish low-concentration, high-velocity voltage pairs from high-concentration, low-velocity voltage pairs. In figures 4.1a, 4.1c, and

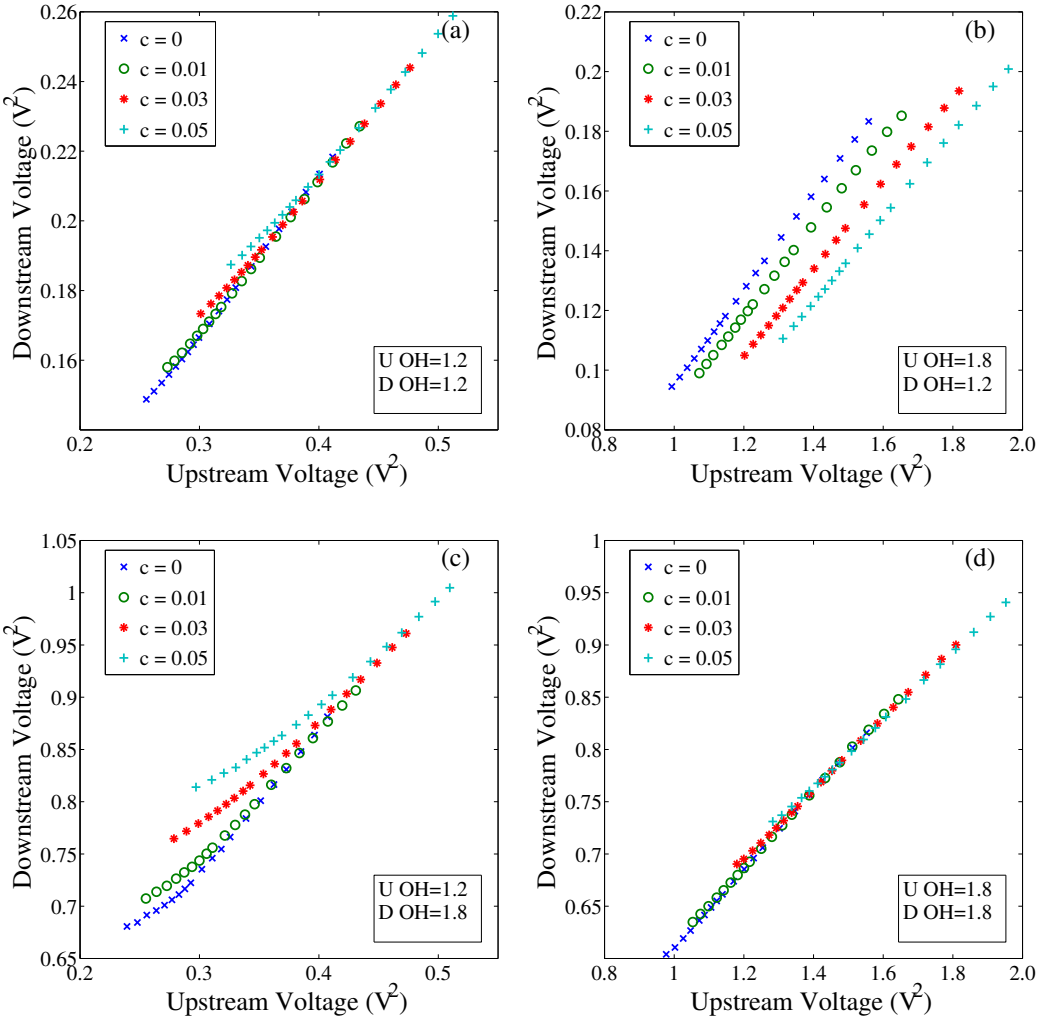

Figure 4.1: Comparison of the effects of the overheat ratio on the calibration map of the W-Pt-35 Probe. (a) Upstream wire OH=1.2 and Downstream wire OH=1.2. (b) Upstream wire OH=1.8 and Downstream wire OH=1.2. (c) Upstream wire OH=1.2 and Downstream wire OH=1.8. (d) Upstream wire OH=1.8 and Downstream wire OH=1.8.

4.1d, the interference effect[1] of the larger wire on the smaller wire is not sufficient to accurately extract velocity and concentration data. Such results mirror those of Way and Libby (1970), who used separation distance to study the interference effect and concluded that, in the range of flows they studied, sufficient sensitivity to concentration could not be achieved in non-interfering sensors. It should not be concluded, however, that interference effects are necessary to make concentration and velocity measurements. Harion *et al.* (1996) obtained satisfactory results even when minimizing these effects. Rather, the data of figure 4.1 should be taken as a piece of evidence in the following hypothesis: successful velocity and concentration measurements are dependent on the diameter ratio of the probe, and when this ratio is not large enough, interference effects should be used to increase the probe's sensitivity to concentration, whether it be by changing the separation distance, overheat ratio, or even wire material.

From the results of figure 4.1, it was concluded that the interference probes of this work should be operated with the upstream wire at a high overheat ratio and the downstream wire at a low overheat ratio. To further explore the values of the optimal overheat ratio combination, the W-Pt-35, W-W-55, and W-W-25 probes were operated with (i) an upstream wire overheat ratio of 1.8 and a downstream wire

[1] The interference effects can be said to increase the more one wire's (A) response is dictated by the thermal field of the other (B). A combination of a low and a high overheat ratio makes wire A more sensitive to the thermal field of wire B. The position of the wire at a low overheat ratio (A) also matters – advection expands the thermal field in the downstream direction, meaning that interference effects are greater when the wire at the low overheat ratio (A) is placed in the downstream position.

overheat ratio of 1.05, (ii) an upstream wire overheat ratio of 1.8 and a downstream wire overheat ratio of 1.2, (iii) an upstream wire overheat ratio of 1.8 and a downstream wire overheat ratio of 1.4, and (iv) an upstream wire overheat ratio of 1.6 and a downstream overheat ratio of 1.2. PDFs and statistical moments were measured at a distance of $x/D = 10$ from the calibration jet exit (within the turbulent region of the jet) in flows of (i) pure air, and (ii) a helium/air mixture (with a helium mass fraction at the jet exit, C_j, of 0.04). The jet exit velocity (U_j) was approximately 6.8 m/s, and kept nominally constant between different experiments. For each experiment, the overheat ratio was varied while keeping all other flow conditions (i.e. concentration and velocity) constant, to determine its effect on the probes' performance in turbulent flows, and identify the optimal overheat ratio combination from those listed above.

When the results from the experiments are studied, it can be seen that the W-Pt-35 probe is much more sensitive to the overheat ratio combination than the W-W-55 and W-W-25 probes. The concentration PDFs measured by the W-Pt-35 probe, and depicted in figure 4.2, are distinct for each overheat ratio combination, exhibiting greater spread when the difference between the overheat ratios of the two wires is small. Likewise, c_{rms}, the standard deviation of concentration (in both air and the helium/air mixture) is nearly doubled when going from an overheat ratio combination of 1.8 (upstream wire) and 1.05 (downstream wire) to an overheat ratio combination of 1.6 (upstream wire) and 1.2 (downstream wire), as depicted in table 4.1. In contrast, much smaller differences are observed in the statistics when the W-W-55 and W-W-25 probes are operated at different overheat ratios, with the PDFs measured by these probes nearly collapsing at each overheat combination. Although increasing

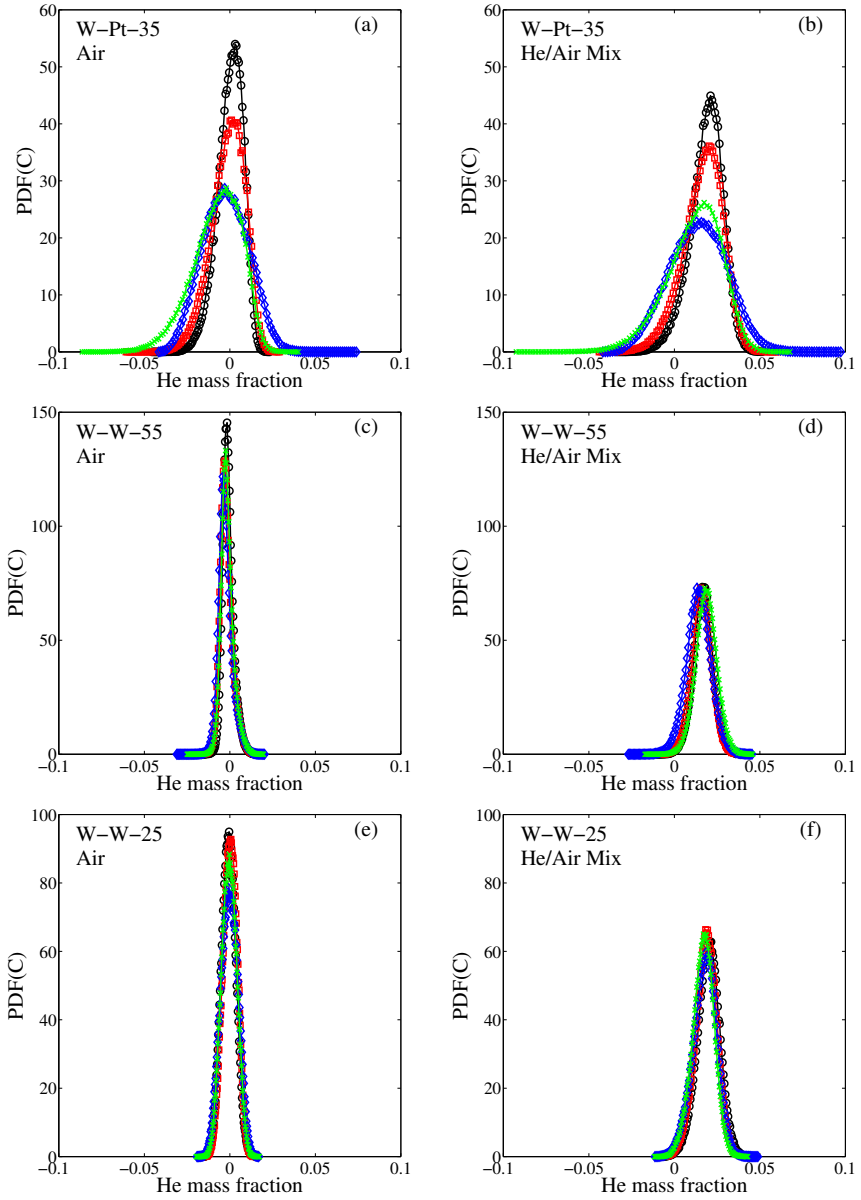

Figure 4.2: Comparison of the effects of the overheat ratio on the PDFs of concentration at $x/D = 10$ in air ($C_j = 0$) and a He/Air mixture ($C_j = 0.04$). The jet exit velocity is 6.8 m/s and $Re_D \approx 4000$. (a) W-Pt-35 probe in air. (b) W-Pt-35 probe in a He/air mixture. (c) W-W-55 probe in air. (d) W-W-55 probe in a He/air mixture. (e) W-W-25 probe in air. (f) W-W-25 probe in a He/air mixture. Symbols denote the different overheat ratio combinations: ○: Upstream OH=1.8 and Downstream OH=1.05, □: Upstream OH=1.8 and Downstream OH=1.2, ◇: Upstream OH=1.8 and Downstream OH=1.4, +: Upstream OH=1.6 and Downstream OH=1.2.

Table 4.1: Concentration statistics, including the mean concentration ($\bar{C}$), standard deviation (c_{rms}), skewness (S_c), kurtosis (K_c), and turbulent intensity of the concentration fluctuations ($c_{rms}/\bar{C}$), for experiments performed on the W-Pt-35, W-W-55, and W-W-25 probes. Experiments are performed in air ($C_j = 0$), and a helium/air mixture ($C_j = 0.04$) at a distance of $x/D = 10$ from the calibration jet exit. The jet exit velocity is 6.8 m/s and $Re_D \approx 4000$. Units of concentration (for $\bar{C}$ and c_{rms}) are in terms of the helium mass fraction.

		Air ($C_j = 0$)				He/Air Mixture ($C_j = 0.04$)				
Probe	Overheat Ratios	$\bar{C}$	c_{rms}	S_c	K_c	$\bar{C}$	c_{rms}	S_c	K_c	$c_{rms}/\bar{C}$
W-Pt-35	U OH=1.8, D OH=1.05	0.000 216	0.007 56	−0.539	3.21	0.0186	0.009 67	−0.509	3.39	50.2%
	U OH=1.8, D OH=1.2	−0.001 16	0.009 87	−0.5406	3.16	0.0166	0.0117	−0.509	3.31	70.5%
	U OH=1.8, D OH=1.4	−0.002 39	0.0133	0.0543	2.61	0.0137	0.0168	−0.0255	2.76	123 %
	U OH=1.6, D OH=1.2	−0.007 61	0.0142	−0.577	3.25	0.0113	0.0163	−0.591	3.45	144 %
W-W-55	U OH=1.8, D OH=1.05	0.001 09	0.003 23	0.602	3.99	0.0168	0.005 66	−0.0510	3.25	33.7%
	U OH=1.8, D OH=1.2	−0.002 06	0.003 73	0.628	3.96	0.0160	0.005 78	−0.0503	3.31	36.1%
	U OH=1.8, D OH=1.4	−0.002 64	0.004 06	0.619	4.14	0.0150	0.006 27	0.0161	3.38	41.8%
	U OH=1.6, D OH=1.2	−0.001 51	0.003 70	−0.635	4.13	0.0135	0.005 78	0.0303	3.34	42.3%
W-W-25	U OH=1.8, D OH=1.05	−0.000 621	0.004 17	0.0644	2.85	0.0198	0.006 55	−0.160	3.15	33.1%
	U OH=1.8, D OH=1.2	−0.000 103	0.004 11	−0.0849	2.70	0.0184	0.006 36	−0.202	3.13	34.6%
	U OH=1.8, D OH=1.4	−0.000 245	0.004 89	−0.0426	2.66	0.0177	0.006 97	−0.237	3.08	39.4%
	U OH=1.6, D OH=1.2	−0.000 397	0.004 40	−0.001 76	2.70	0.0169	0.006 34	−0.180	3.06	37.5%

the difference between the overheat ratios of the wires, significantly improves concentration measurements for the W-Pt-35 probe, and slightly improves them for the W-W-55 and W-W-25 probes, it should be noted, that all of these concentration measurements are unambiguously poor, especially in the case of the W-Pt-35 probe. All three probes measure spurious concentration fluctuations in air, that are nearly as large as those in the helium/air mixture, as well as negative and/or excessively large concentrations that are clearly incorrect. It therefore appears that the W-Pt-35, W-W-55, and W-W-25 probes erroneously measure velocity fluctuations as concentration fluctuations.

The velocity field results are not significantly more promising, and exhibit similar trends as those observed for the concentration measurements. It can be seen in the velocity PDFs of figure 4.3, as well as in the statistics of table 4.2, that the overheat ratio has a greater effect on measurements made by the W-Pt-35 probe than those made by the W-W-55 and W-W-25 probes. In the case of the W-Pt-35 probe, more extreme (and clearly incorrect) velocities and greater values of u_{rms}, the standard deviation of the velocity, are observed when the difference in the wire overheat ratios is small. However, PDFs measured by the W-W-55 and W-W-35 approximately collapse for each overheat ratio combination, just as was observed for the concentration measurements.

It is unclear why the W-Pt-35 probe is more sensitive to the overheat ratio combination than the W-W-55 and W-W-25 probes. One possible explanation, may be that due to the higher temperature coefficient of resistivity of platinum, the downstream wire of the W-Pt-35 probe is more sensitive to temperature, making it more sensitive to changes in the overheat ratio. However given that the difference in the

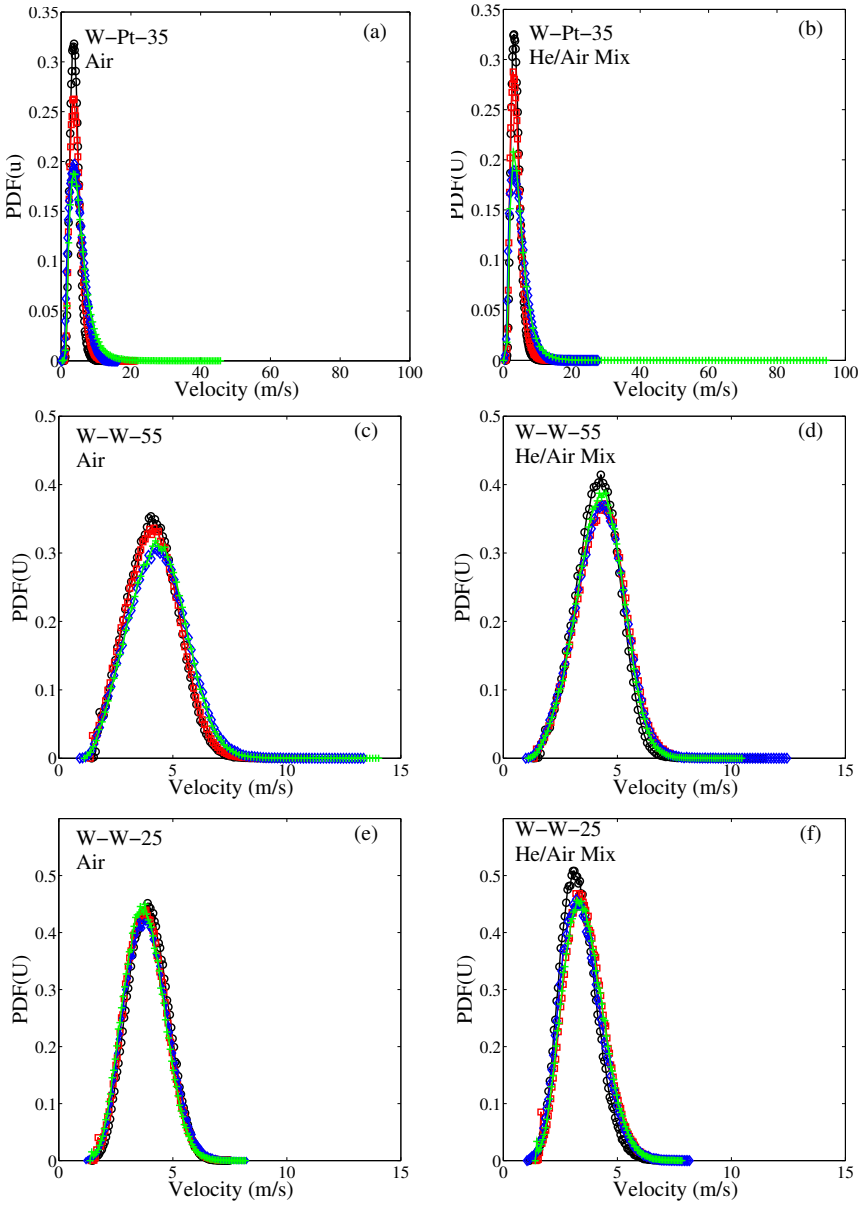

Figure 4.3: Comparison of the effects of the overheat ratio on the PDFs of velocity at $x/D = 10$ in air ($C_j = 0$) and a He/Air mixture ($C_j = 0.04$). The jet exit velocity is 6.8 m/s and $Re_D \approx 4000$. (a) W-Pt-35 probe in air. (b) W-Pt-35 probe in a He/air mixture. (c) W-W-55 probe in air. (d) W-W-55 probe in a He/air mixture. (e) W-W-25 probe in air. (f) W-W-25 probe in a He/air mixture. Symbols denote the different overheat ratio combinations: ○: Upstream OH=1.8 and Downstream OH=1.05, □: Upstream OH=1.8 and Downstream OH=1.2, ◇: Upstream OH=1.8 and Downstream OH=1.4, +: Upstream OH=1.6 and Downstream OH=1.2.

Table 4.2: Velocity statistics, including the mean velocity ($\bar{U}$), standard deviation (u_{rms}), skewness (S_u), kurtosis (K_u) and turbulent intensity ($u_{rms}/\bar{U}$), for experiments performed on the W-Pt-35, W-W-55, and W-W-25 probes. Experiments are performed in air ($C_j = 0$), and a helium/air mixture ($C_j = 0.04$) at a distance of $x/D = 10$ from the calibration jet exit. The jet exit velocity is 6.8 m/s and $Re_D \approx 4000$. Units of velocity (for $\bar{U}$ and u_{rms}) are in m/s.

		Air ($C_j = 0$)					He/Air Mixture ($C_j = 0.04$)				
Probe	Overheat Ratios	$\bar{U}$	u_{rms}	S_u	K_u	$u_{rms}/\bar{U}$	$\bar{U}$	u_{rms}	S_u	K_u	$u_{rms}/\bar{U}$
W-Pt-35	U OH=1.8, D OH=1.05	3.98	1.31	0.800	4.33	32.9%	3.81	1.30	0.919	4.69	34.1%
	U OH=1.8, D OH=1.2	4.34	1.73	1.22	6.03	39.9%	3.89	1.58	1.26	6.20	40.6%
	U OH=1.8, D OH=1.4	4.64	2.17	0.851	3.74	46.8%	4.55	2.36	1.18	5.17	51.9%
	U OH=1.6, D OH=1.2	5.56	3.37	2.88	23.04	60.6%	4.91	3.05	5.48	171.2	62.2%
W-W-55	U OH=1.8, D OH=1.05	4.13	0.955	0.0221	3.18	23.1%	4.18	1.10	0.154	2.79	26.3%
	U OH=1.8, D OH=1.2	4.28	1.07	0.0377	2.92	25.0%	4.18	1.15	0.159	2.80	27.5%
	U OH=1.8, D OH=1.4	4.25	1.07	0.0603	3.10	25.2%	4.40	1.27	0.230	2.97	28.9%
	U OH=1.6, D OH=1.2	4.22	1.02	−0.0102	2.90	24.2%	4.39	1.24	0.215	3.05	28.2%
W-W-25	U OH=1.8, D OH=1.05	3.90	0.852	0.112	2.69	21.8%	3.42	0.815	0.394	3.11	23.8%
	U OH=1.8, D OH=1.2	3.82	0.880	0.206	2.84	23.0%	3.65	0.884	0.340	3.00	24.2%
	U OH=1.8, D OH=1.4	3.86	0.921	0.256	2.89	23.9%	3.52	0.896	0.413	3.13	25.5%
	U OH=1.6, D OH=1.2	3.75	0.873	0.206	2.87	23.3%	3.60	0.88	0.362	3.06	24.4%

the temperature coefficient of resistivity between platinum and tungsten is small, 0.0038 versus 0.0036, respectively, this is unlikely to explain the significant differences between the results of the W-Pt-35 probe and those of the W-W-55 and W-W-25 probes. An alternate explanation may be that these differences in results are related to the strength of the interference effect in each probe, but it is unclear exactly why this would cause the W-Pt-35 probe to be more sensitive to the choice of overheat ratio than the W-W-55 and W-W-25 probes. In figure 4.4, which displays select calibration maps for each of the probes, the strength of the interference effect can be seen to vary from to probe to probe, as well as with the overheat ratio combination. Stronger interference effects are identified by a decrease in the voltage of the downstream wire as helium concentration increases,[2] and weaker interference effects result in iso-concentrations that tend to collapse onto a single line. Though interference effects are observed to be weaker for the W-Pt-35 probe, than for the W-W-55 and W-W-25 probes, greater differences are observed between different overheat ratio combinations than between different probes.

Interference effects may not be sufficient to explain why the choice in overheat ratio only has a significant effect on the W-Pt-35 probe, but they can explain some of the extreme and erroneous values displayed by this probe when the difference between the overheat ratios of the two wires is small. Though the probes studied in this section were capable of distinguishing mean concentrations and velocities within a reasonable amount of accuracy (results from tables 4.1 and 4.3 are used to verify this), as discussed previously, they failed to do so for the fluctuating components.

[2] Without interference effects, the added presence of helium causes the voltage of a hot-wire to increase due to its higher thermal conductivity.

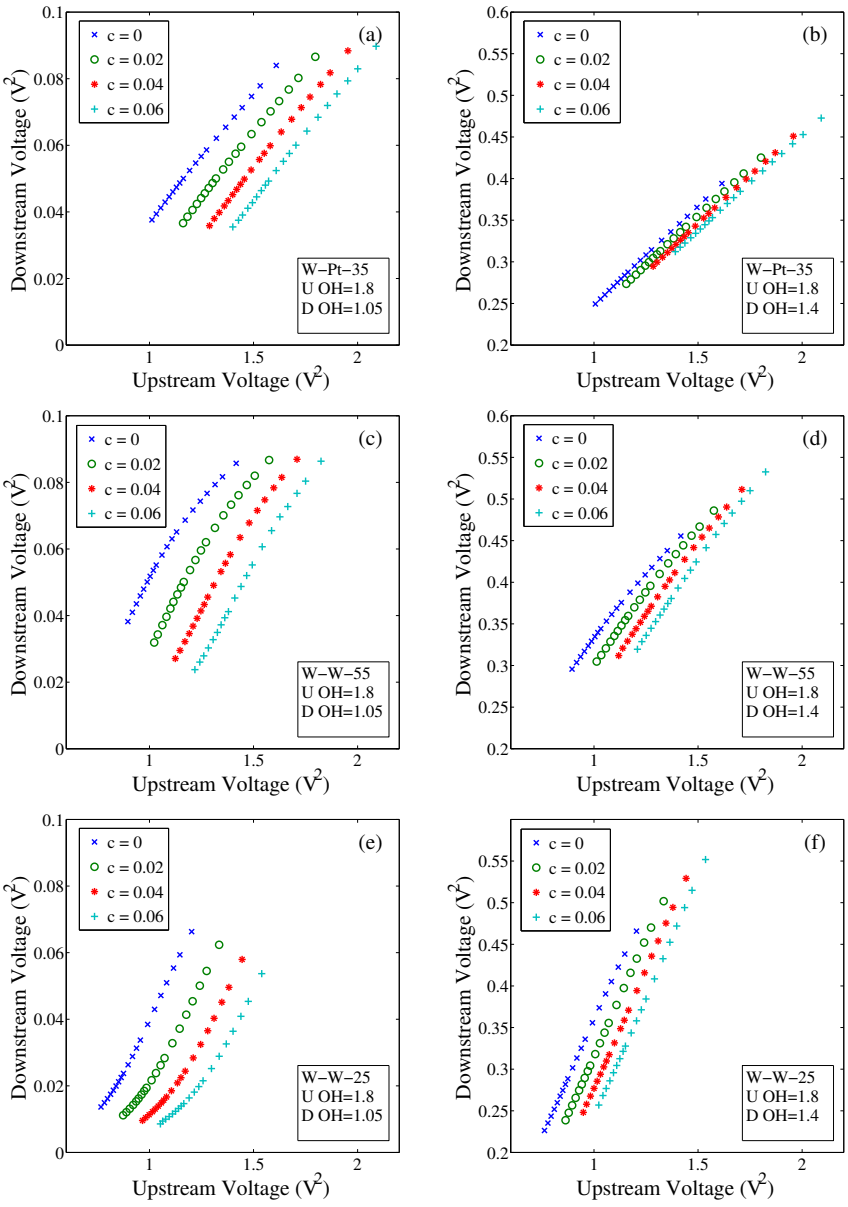

Figure 4.4: Comparison of the effects of the overheat ratios on the calibration map for the W-Pt-35, W-W-55, and W-W-25 probes. (a) W-Pt-35 probe, Upstream wire OH=1.8 and Downstream wire OH=1.05. (b) W-Pt-35 probe, Upstream wire OH=1.8 and Downstream wire OH=1.4. (c) W-W-55 probe, Upstream wire OH=1.8 and Downstream wire OH=1.05. (d) W-W-55 probe, Upstream wire OH=1.8 and Downstream wire OH=1.4. (e) W-W-25 probe, Upstream wire OH=1.8 and Downstream wire OH=1.05. (f) W-W-25 probe, Upstream wire OH=1.8 and Downstream wire OH=1.4.

Large concentration fluctuations, sometimes exceeding the ranges of the calibration map, were recorded when the interference probe inaccurately responded to velocity fluctuations as if they were concentration fluctuations. The voltage pairs corresponding to these concentration measurements were therefore known to deviate from the calibration map. If the interference effects were weak, resulting in a poor sensitivity to concentration, these deviations from the calibration map had a more significant effect on the recorded concentration and velocity data, exacerbating already unsatisfactory results, and leading to the extreme values (helium mass fractions of -0.1 and velocities of 100 m/s) observed for this probe.

In summary, initial tests on the W-Pt-35 probe concluded that that the overheat ratio can be used to increase or decrease an interference probe's sensitivity to concentration, and that the interference probes developed in this work should ideally be operated with the upstream wire at a high overheat ratio and the downstream wire at low overheat ratio. Subsequent tests on the W-Pt-35, W-W-55, and W-W-25 probes in turbulent flow were somewhat inconclusive, and revealed that the overheat ratio had a significant effect on the W-Pt-35 probe's performance, but not on the W-W-55 and W-W-25 probes. Given the probes' differing responses to overheat ratio, it was difficult to identify a precise optimal overheat ratio combination. Furthermore, since the results gathered from the W-Pt-35, W-W-55, and W-W-25 probes were not satisfactory, additional probes were constructed with smaller separation distances to try and improve the results. These probes are used to study the effects of separation distance on the probe's performance.

Table 4.3: Accuracy of the mean concentration ($\bar{C}$) and velocity ($\bar{U}$) values measured by the W-W-55 and W-W-25 probes in a laminar jet. Experiments are performed at $x/D = 0$, and $Re_D \approx 4000$. Units of concentration are in terms of the helium mass fraction and units of velocity in m/s.

Probe	Overheat Ratios	$\bar{C}$ – Air ($C_j = 0$) Measured	Expected	Percent Error	$\bar{C}$ – He/Air Mixture ($C_j = 0.02$) Measured	Expected	Percent Error
W-W-55	U OH=1.8, D OH=1.05	0.000 234	0	–	0.0164	0.02	18 %
	U OH=1.8, D OH=1.2	−0.000 915	0	–	0.0162	0.02	19 %
	U OH=1.8, D OH=1.4	−0.001 96	0	–	0.0161	0.02	20 %
	U OH=1.6, D OH=1.2	−0.001 21	0	–	0.0164	0.02	18 %
W-W-25	U OH=1.8, D OH=1.05	−0.001 64	0	–	0.0174	0.02	13 %
	U OH=1.8, D OH=1.2	−0.001 14	0	–	0.0189	0.02	5.5%
	U OH=1.8, D OH=1.4	−0.002 13	0	–	0.0211	0.02	5.5%
	U OH=1.6, D OH=1.2	−0.001 22	0	–	0.0186	0.02	7.0%

Probe	Overheat Ratios	$\bar{U}$ – Air ($C_j = 0$) Measured	Expected	Percent Error	$\bar{U}$ – He/Air Mixture ($C_j = 0.02$) Measured	Expected	Percent Error
W-W-55	U OH=1.8, D OH=1.05	6.59	6.79	3.0 %	7.25	6.80	6.6 %
	U OH=1.8, D OH=1.2	6.79	6.79	0.0 %	7.26	6.80	6.8 %
	U OH=1.8, D OH=1.4	6.95	6.79	2.4 %	7.25	6.80	6.6 %
	U OH=1.6, D OH=1.2	6.82	6.79	0.44%	7.17	6.80	5.4 %
W-W-25	U OH=1.8, D OH=1.05	6.71	6.79	1.2 %	6.85	6.80	0.74%
	U OH=1.8, D OH=1.2	6.60	6.79	2.8 %	6.66	6.80	2.1 %
	U OH=1.8, D OH=1.4	6.68	6.79	1.6 %	6.44	6.80	5.3 %
	U OH=1.6, D OH=1.2	6.52	6.79	4.0 %	6.58	6.80	3.2 %

4.3 Effect of the Wire Separation Distance

Experiments on the first three (W-Pt-35, W-W-55, and W-W-25) probes, revealed that it was not possible to accurately distinguish concentration fluctuations from velocity fluctuations, as evidenced by the fact that these probes measured overly large concentration fluctuations in turbulent flows of pure air. To some extent, this is not entirely unexpected. Similar results can be obtained by cold-wire thermometers (a well established tool in turbulence research) in turbulent isothermal flows, where velocity fluctuations are erroneously recorded as temperature ones, when the current passing though the cold-wire is too large. As these effects cannot be avoided, the objective is thus to increase the signal-to-noise ratio, so that, as stated in section 4.1, measured concentration spectra in flows of pure air are substantially lower than those measured in flows with concentration fluctuations. It may be possible to increase the signal-to-noise ratio by decreasing the separation distance between the wires. The spectra of the W-W-55, W-W-25, W-W-20, and W-W-10 probes are therefore compared to investigate this hypothesis.

Concentration and velocity spectra were measured in the calibration jet at a distance of $x/D = 10$ from the jet exit. Conditions for each experiment were nominally constant: the jet exit velocity was roughly 6.8 m/s, and the probes had an overheat ratio combination of 1.8 (upstream wire) and 1.2 (downstream wire). The one exception was the W-W-20 probe, which was operated at a slightly higher velocity of 8.8 m/s and an overheat ratio combination of 1.8 (upstream wire) and 1.1 (downstream wire). The concentration and velocity spectra (figures 4.5 and 4.6), taken under these conditions, show little improvement when the separation distance is decreased. In fact, decreasing the separation distance has an adverse effect on the signal-to-noise ratio of the concentration spectra, as shown in figure 4.5. While the concentration

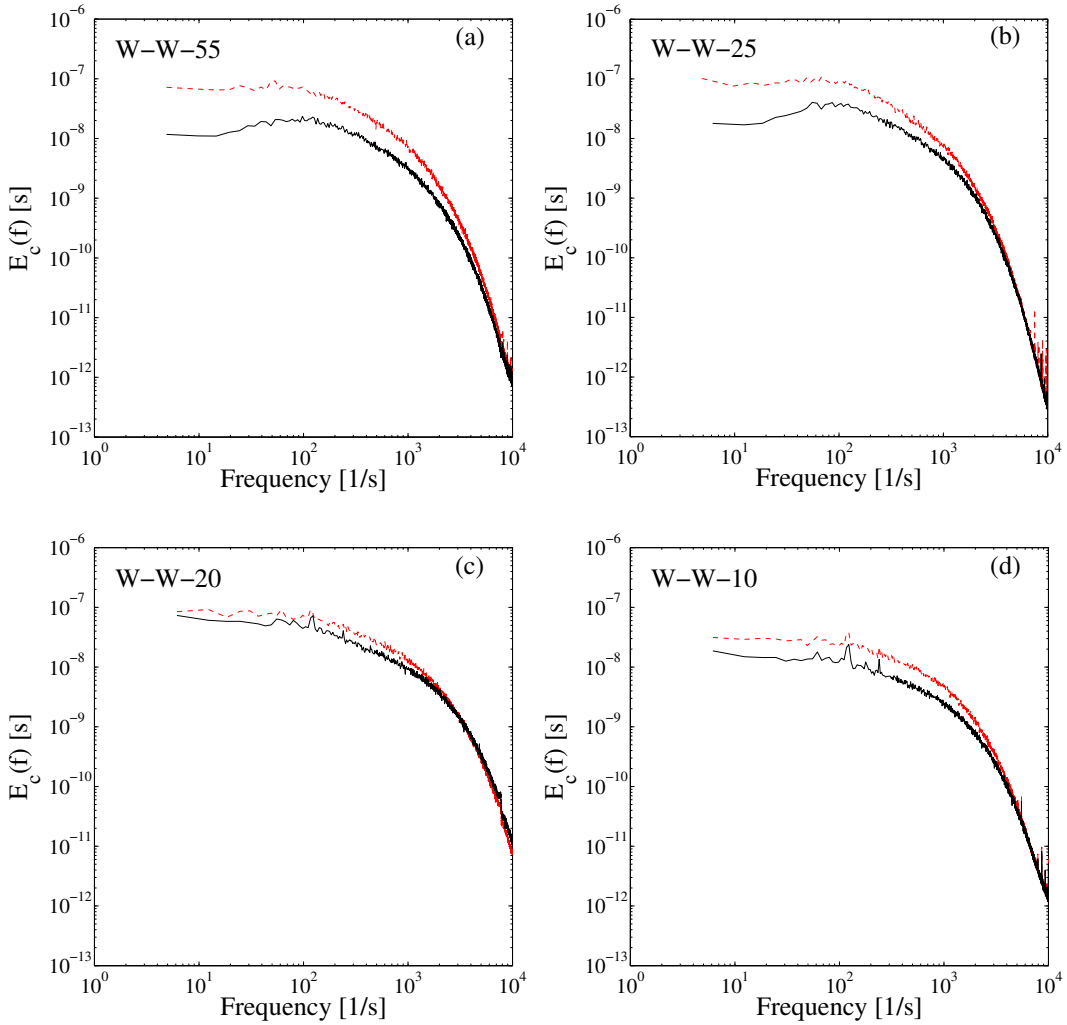

Figure 4.5: Comparison of the effect of separation distance on the concentration spectra measured by the W-W-55, W-W-25, W-W-20, and W-W-10 probes at $x/D = 10$. (a) W-W-55 probe.(b) W-W-25 probe. (c) W-W-20 probe. (d) W-W-10 probe. Dashed red line: He/air mixture (C_j=0.04). Solid black line: air (C_j=0). The jet exit velocity is 6.8 m/s for (a), (b), and (d), and 8.8 m/s for (c). $Re_D \approx 4000$ for (a), (b), and (d), and $Re_D \approx 6000$ for (c).

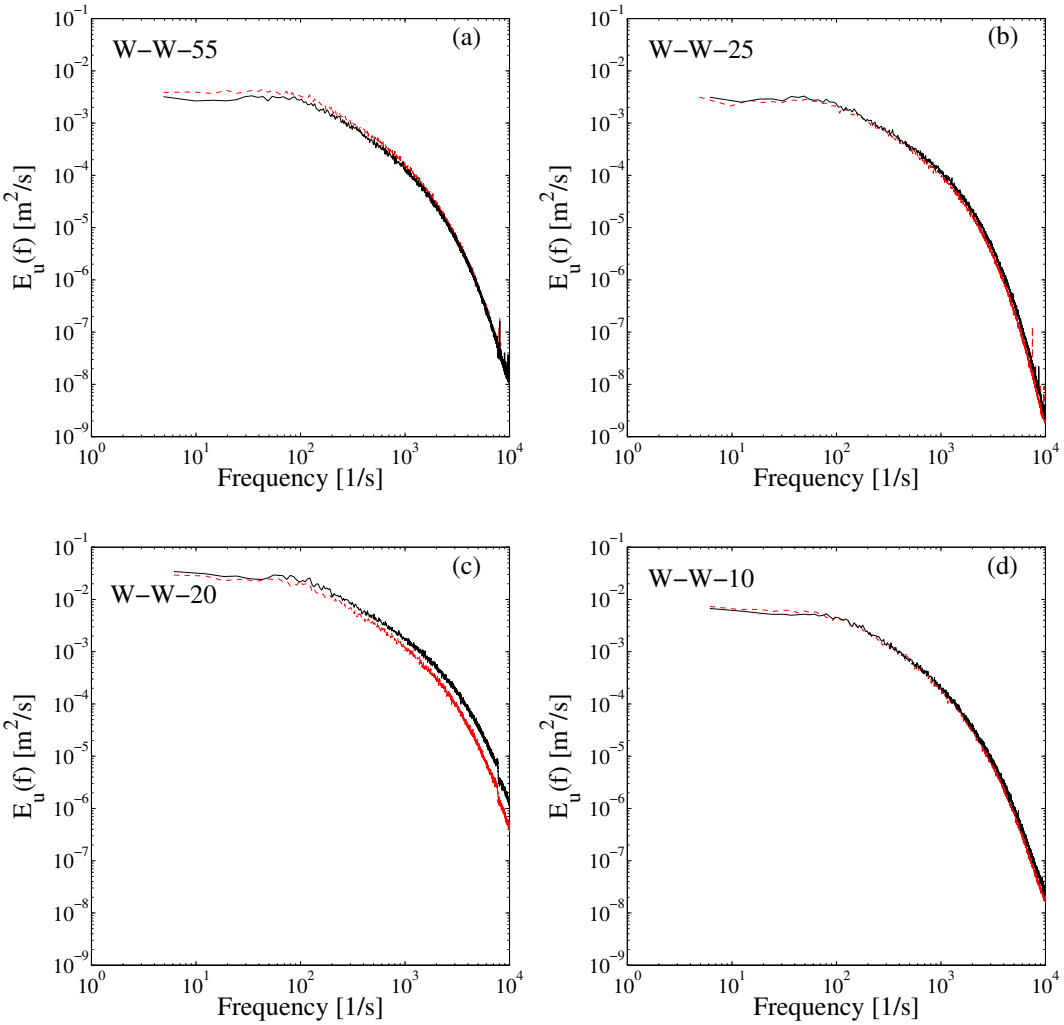

Figure 4.6: Comparison of the effect of separation distance on the velocity spectra measured by the W-W-55, W-W-25, W-W-20, and W-W-10 probes at x/D=10. (a) W-W-55 probe. (b) W-W-25 probe. (c) W-W-20 probe. (d) W-W-10 probe. Dashed red line: He/air mixture (C_j=0.04). Solid black line: air (C_j=0). The jet exit velocity is 6.8 m/s for (a), (b), and (d), and 8.8 m/s for (c). $Re_D \approx 4000$ for (a), (b), and (d), and $Re_D \approx 6000$ for (c).

spectra measured by the W-W-55 probe appear to have a signal-to-noise ratio of roughly one decade (at frequencies below approximately 100 Hz, which are those that contribute to the majority of the fluctuations), the spectra using the W-W-20 probe are nearly indistinguishable, and those of the W-W-10 probe differ by merely a factor of two at low frequencies. The velocity spectra are slightly more promising. With the exception of the W-W-20 probe, the velocity spectra taken in air are nearly indistinguishable from those taken in helium/air mixtures, which is to be expected when the scalar (i.e. helium concentration) is passive.[3] In the case of the W-W-20 probe, somewhat unusual results are reported, with the velocity spectra agreeing well at small frequencies, but not at large frequencies. As the opposite behavior is normally observed, it is possible that the W-W-20 probe may have suffered from some sort of frequency response problem, making its results suspect. Neglecting these results, it appears that the separation distance has little to no effect on measurements of the velocity field.

From the results described above, it appears that at the very least, decreasing the separation distance, has little added benefit, even having a negative impact on the signal-to-noise ratio of the concentration spectra. However, it should be noted that these results are not entirely consistent. Greater differences are observed between those of the W-W-25 and W-W-20 probes (which one would expect to be quire similar) than between those of the W-W-55 and W-W-25 probes or the W-W-20 and W-W-10 probes. Interestingly, the W-W-55 and W-W-25 probes, which have similar responses, were constructed using Method 1 (see section 3.2.2.3), and the W-W-20

[3] As mentioned in section 2.5, the helium concentration is expected to be a passive scalar within the flows in which experiments were performed.

and W-W-10 probes were constructed using Method 3. It may be that different construction methods and construction materials also play an important role in the performance of an interference probe.

Given that the interference probes investigated so far were unable to make precise concentration measurements, even when the separation distance was as small as possible and interference effects were assumed to be greatest, it was concluded that interference effects alone may not be sufficient to make these measurements. Corrsin's early theoretical work had suggested that differences in wire diameter could play a role in making simultaneous velocity and concentration measurements, so the effect of wire diameter is investigated next.

4.4 Effect of the Wire Diameter

To compare the effects of wire diameter, a final interference probe, the W-Pt/R-10 probe, was constructed and compared with the W-W-10 probe. Both interference probes have a similar separation distance – roughly 10 μm between the wires. The W-Pt/R-10 probe consists of a 5 μm tungsten wire upstream of a 2.5 μm platinum-rhodium wire, and the the W-W-10 probe is made up of two 2.5 μm tungsten wires. Velocity and concentration spectra for the W-Pt/R-10 probe were measured in the calibration jet under the same conditions as those for the W-W-10 probe (described earlier in section 4.3). The results of both probes are compared in figure 4.7. It can clearly be seen in this figure, that the signal-to-noise ratio of the concentration spectra is drastically improved for the W-Pt/R-10 probe. The W-W-10 probe has a signal-to-noise ratio of no more than two, while the signal-to-noise ratio of the the W-Pt/R-10 probes is nearly two decades – a value large enough to make precise concentration

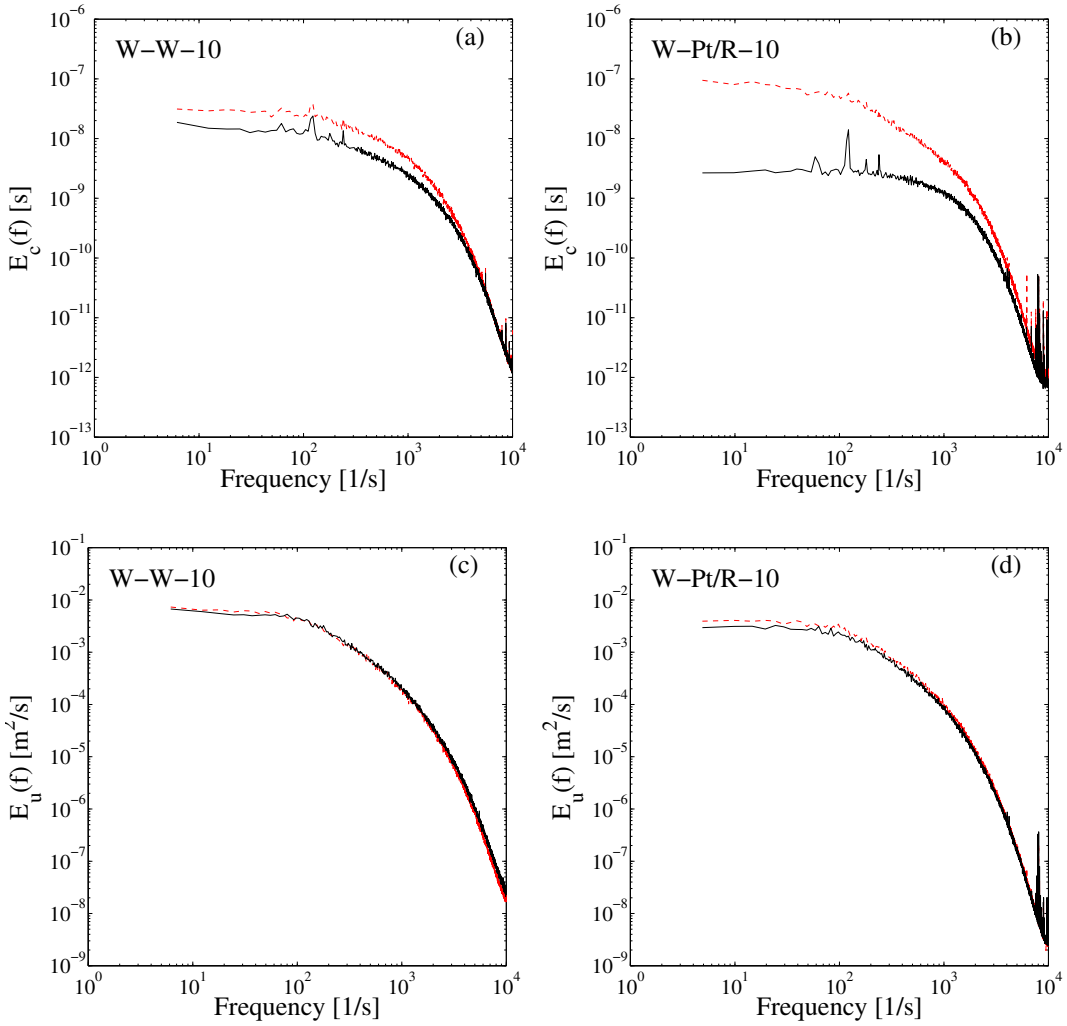

Figure 4.7: Comparison of the effect of diameter ratio on the spectra measured by the W-W-10 and W-Pt/R-10 probes at x/D=10. The jet exit velocity is 6.8 m/s and $Re_D \approx 4000$. (a) Concentration spectra of the W-W-10 probe. (b) Concentration spectra of the W-Pt-R-10 probe. (c) Velocity spectra of the W-W-10 probe. (d) Velocity spectra of the W-Pt-R-10 probe. Dashed red line: He/air Mixture (C_j = 0.04). Solid black line: air ($C_j = 0$).

measurements feasible.[4] With respect to the velocity spectra, those measured with the W-W-10 probe in air and helium/air mixtures are indistinguishable from each other, whereas very slight differences between the velocity spectra measured using the W-Pt/R-10 can be observed at lower frequencies. This is hopefully attributable to small differences from one experiment to the next. Nevertheless, this relatively small difference in the velocity spectra is deemed acceptable given the drastic increase in the signal-to-noise ratio achieved using the W-Pt/R-10 probe.

Although these results may indicate that diameter differences (between the upstream and downstream wires) are essential for making concentration and velocity measurements, this cannot be definitively concluded from the results above, since the probes differ in more than just their diameter ratios. For example, different construction methods were used to build the probes, different materials were used for the downstream wires of the probes, and different diameters were used for the upstream wires of the probes. Nevertheless, it is thought that these differences do not significantly contribute to the improvement in results observed between the W-Pt/R-10 probe and the W-W-10 probe. Ideally, the construction method would have no effect on the results, and the use of platinum-rhodium in the W-Pt/R-10 probe, as opposed to tungsten in the W-W-10 probe, should have an adverse effect on the results, given that platinum-rhodium (used for the downstream wire) is less sensitive to temperature fluctuations, which would decrease the interference effect in the wires. Moreover, the size of the upstream wire, which is larger in the W-Pt/R-10 probe than the W-W-10 probe, only serves to increase the interference effect, which

[4] Note that these signal-to-noise ratios are quoted at lower frequencies, which contributed to the majority of the fluctuations, as previously noted.

as discussed in section 4.3, is not sufficient for making precise concentration measurements. It seems reasonable to conclude, that it is the difference in diameter ratio (upstream wire diameter / downstream wire diameter) between the W-W-10 probe and the W-Pt/R-10 probe that is the essential factor in improving the results. This supports Corrsin's (1949) hypothesis regarding the use of diameter differences for making concentration and velocity measurements, and claims about the role of these diameter differences made by Harion *et al.* (1996).

Though it was concluded above that diameter differences (between the upstream and downstream wires) were, at least partly, responsible for the comparatively excellent results of the W-Pt/R-10 probe, this cannot be the only design characteristic required to make an interference probe. The results of the W-Pt-35 probe are unambiguously poor, as evidenced in figures 4.1 and 4.2, but like the W-Pt/R-10 probe, wires of different diameters were used to construct the W-Pt-35 probe. In the case of the W-Pt-35 probe, it is thought that the interference effect between the wires is not strong enough to make accurate or precise measurements. Perhaps if the separation distance between the wires had been decreased, satisfactory measurements could have been obtained. This has lead to following hypothesis, already mentioned in section 4.1: successful velocity and concentration measurements require: (i) wires of different diameters, and (ii) an interference effect if these diameter differences are not large enough. The strength of the interference effect can be controlled by choosing the wire material, diameter, overheat ratio, as well as the separation distance between wires.

4.5 Effect of the Wire Material

The six interference probes designed, and the experiments performed on them, did not lend themselves to making a rigorous study of the effect of the wire material. No two probes, differing only in material, were designed. Given that other factors, such as diameter ratio and separation distance affect the results, it is difficult to conclusively determine the effect of wire material. It was expected that sensitivity to concentration could be increased by increasing interference effects, and that these interference effects, in turn, could be increased by using materials with larger temperature coefficients of resistivity, such as platinum or tungsten. But the results of the W-W-55, and W-W-25 probes are superior to those of the W-Pt-35 probe, even though the temperature coefficient of resistivity of platinum is larger than that of tungsten, and the results of the W-Pt/R-10 probe are superior to those of the W-W-10 probe, even though the temperature coefficient of resistivity of tungsten is more than two times larger than the temperature coefficient of resistivity of platinum-rhodium. Though other factors, such as the diameter ratio and separation distance are presumably also responsible for the differences in results, it is interesting to note that the expected trends were not followed. At the very least, it seems that these other factors (wire separation distance and diameter ratio) have a greater effect on the results than the wire material.

4.6 Optimal Probe Design

In sections 4.2 through 4.5, the effects of overheat ratio, wire separation distance, wire diameter, and wire material on the performance of an interference probe were studied to find the optimal design for such of a probe. It was determined that the most important design criterion was a difference between the upstream wire diameter

and the downstream wire diameter, without which, large spurious concentrations in flows of pure air are measured. The overheat ratio was also to seen to have some effect, such that it was concluded that the interference probes in this work should be operated with the upstream wire at a high overheat ratio and the downstream wire at a low overheat ratio to unambiguously determine low-concentration, high-velocity voltage pairs from high-concentration, low-velocity voltage pairs. However, the exact degree to which each wire was heated did not necessarily have an effect on the probe's performance. The effects of wire separation distance and wire material were somewhat more inconclusive. In the case of wire separation distance, it was seen to have little effect on the performance of interference probes containing two wires of the same diameter, but when interference probes designed with different wire diameters (W-Pt-35 and W-Pt/R-10) are compared, the performance of the interference probe is greatly increased by decreasing the wire separation distance.

Given the results discussed in the previous sections, the W-Pt/R-10 probe is identified as that having the optimal design out of the six interference probes studied in this thesis. Compared to the other probes investigated in this work, it does a better job of meeting one of the design goals discussed in chapter 3 - good precision in measurements. While the other probes had signal-to-noise ratios of one decade or less in their concentration spectra, the W-Pt/R-10 probe had a signal-to-noise ratio of two decades (at low frequencies). The results for the velocity field are furthermore good – with only small differences observed between the velocity spectra measured in air and the velocity spectra measured in a helium/air mixture. To further quantify the performance, accuracy, and precision of this probe, and the extent to which design goals from section 3.2 were achieved, results for the W-Pt/R-10 probe are presented in greater detail in the following chapter.

CHAPTER 5
Validation of the Interference Probe of Optimal Design

Results for the W-Pt/R-10 interference probe, identified as having the "optimal design" of probes studied in this work, are presented and used to benchmark the accuracy, precision, and performance of the probe in the present chapter. These results are compared against known flow conditions, previous studies involving interference probes, and measurements made with a single-normal hot-wire probe, for which the accuracy and precision are well established. In the first section, results obtained in a laminar jet are discussed. In the subsequent section, concentration and velocity measurements in a turbulent jet are presented. Finally, a summary assessing the accuracy and precision of the W-Pt/R-10 probe, as well as the extent to which the design goals of section 3.2 were achieved, is given in the last section.

5.1 Results in a Laminar Jet

Experiments using the W-Pt/R-10 probe were performed at the calibration jet exit ($x/D = 0$), where the velocity profile is laminar and uniform, to investigate the accuracy and precision of the probe with respect to known flow conditions. As the flow conditions are known at this point, they can be compared with the measured values obtained with the interference probe. These results are presented in table 5.1, as well as figure 5.1, and reveal that the mean values measured by the the W-Pt/R-10 differ from the known flow conditions by at most 12%, with somewhat greater accuracy being reported for the velocity data. When the voltages corresponding to these mean values are compared with the calibration data, these errors are revealed

Table 5.1: Comparison of measurements using the W-Pt/R-10 probe in a laminar jet with known flow conditions. Experiments are performed in air ($C_j = 0$) and helium/air mixtures ($C_j = 0.04$) at $x/D = 0$. The jet exit velocity is about 6.4 m/s and $Re_D \approx 4000$. Units of velocity are given in m/s and units of concentration are in terms of the helium mass fraction.

Experiment	Data	Measured	Expected	Percent Error
Exp 1: $x/D = 0$, $C_j = 0$	$\bar{U}$	6.78	6.37	6.4%
	u_{rms}	0.006 35	0	–
	$u_{rms}/\bar{U}$	0.0937%	0%	–
	$\bar{C}$	−0.003 44	0	–
	c_{rms}	0.000 200	0	–
Exp 2: $x/D = 0$, $C_j = 0.04$	$\bar{U}$	6.54	6.35	3.0%
	u_{rms}	0.0158	0	–
	$u_{rms}/\bar{U}$	0.249%	0%	–
	$\bar{C}$	0.0358	0.04	11.7%
	c_{rms}	0.000 742	0%	–
	$c_{rms}/\bar{C}$	2.07%	0%	–

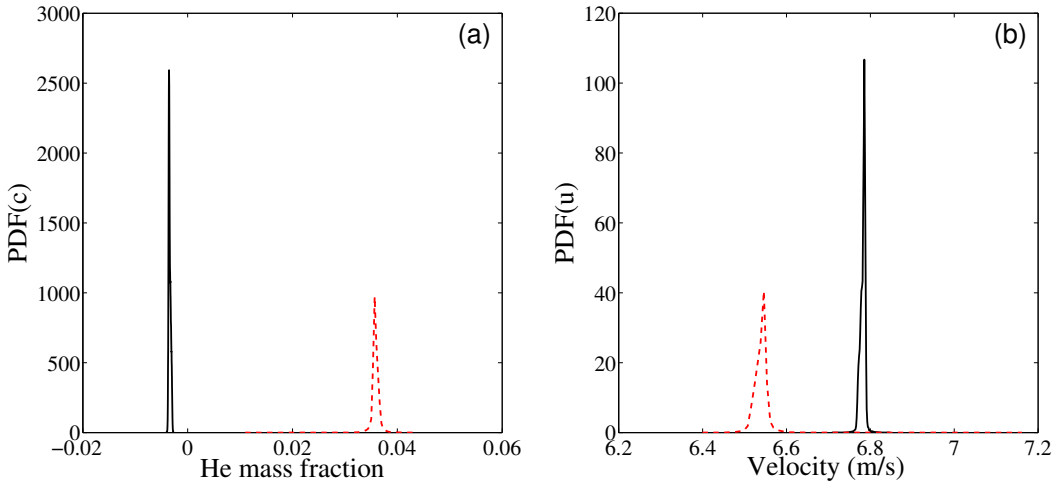

Figure 5.1: Concentration and velocity PDFs measured by the W-Pt/R-10 probe at $x/D = 0$. The jet exit velocity is about 6.4 m/s and $Re_D \approx 4000$. (a) Concentration. (b) Velocity. Solid black line: Air ($C_j = 0$). Dashed red line: He/air mixture ($C_j = 0.04$).

to be mainly due to voltage drift. In figure 5.2, the mean voltages gathered from these experiments are plotted on the calibration map to visually depict the resulting voltage drift that occurred between calibration and experiments. It can clearly be seen that the symbols representing the mean voltages are shifted left from their respective calibration curves, resulting in an overestimate or underestimate of the concentration and/or velocity.

Previous experiments studied herein, had also exhibited signs of voltage drift, though certain probes, such as the W-W-55 and W-W-25 probes, appeared to be less susceptible to voltage drift. Because more significant voltage drift was observed in the W-Pt-35 and W-Pt/R-10 probes, there is anecdotal evidence to suggest that voltage drift may be related to the choice in wire material, but this was not rigorously confirmed in this work. Experiments on the W-Pt-35 probe, in which the effects of voltage drift were first observed, revealed that the voltage drift was mostly confined to the downstream wire, and all but disappeared when the upstream wire was not operated, implying that voltage drift is somehow related to the interference effects. It may be that minute deformations (due to thermal expansion) occur when the wires are heated, which changes the separation distance between the wires, and in turn affects the response of the downstream wire. Encouragingly, voltage drift in the W-Pt-35 probe was reduced after it had been operated for several days, suggesting that voltage drift could be minimized by "burning in" the interference probes for longer periods of time.[1]

[1] Experiments on the six interference probes were performed directly after calibrations to minimize the effects of voltage drift. For most of the probes studied in this work, this method was sufficient to reduce voltage drift to acceptable levels, and

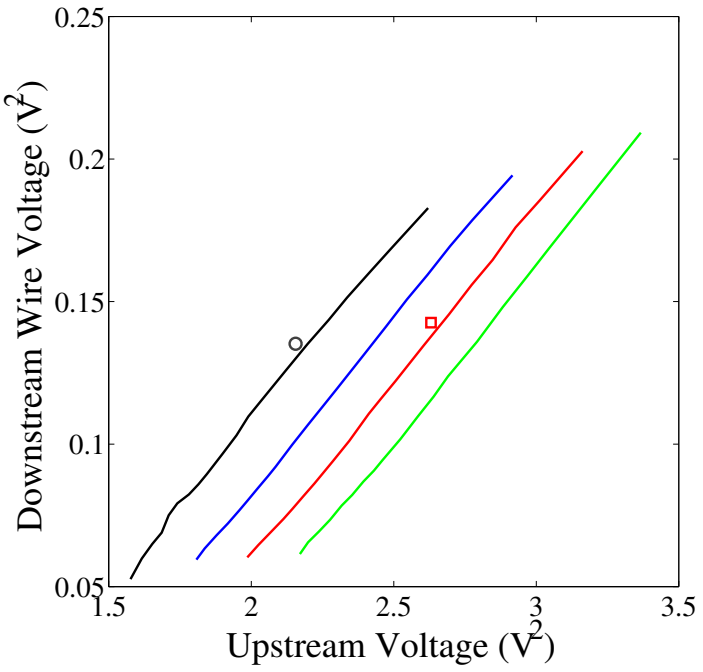

Figure 5.2: Calibration map of the interference probe with mean values from experiments at $x/D = 0$. Solid lines are used for the calibration map. Black: C = 0. Blue: C = 0.02. Red: C = 0.04. Green: C = 0.06. Symbols are used for the mean values from experiments. ∘: $C_j = 0$ (air). □: $C_j = 0.04$ (He/air mixture).

Despite errors relating to the voltage drift (which can hopefully be reduced by increased "burning in" of the probe), the results taken in the laminar jet are acceptable. The concentration and velocity statistics measured at $x/D = 0$, along with their respective PDFs, show only minimal concentration and velocity fluctuations, as expected in laminar flow, and are an indication of very precise measurements. The small fluctuations that are present, are mainly a result of electrical noise produced during the data collection process, and can be seen to have a relatively small impact on the results. The recorded standard deviations of velocity (u_{rms}) represent 0.09% and 0.24% of the recorded mean velocity ($\bar{U}$) in air and the helium/air mixture respectively. Moreover the recorded standard deviations of concentration (c_{rms}) are on the order of 10^{-4} (in terms of the helium mass fraction). Although somewhat greater noise is observed in the helium/air mixture measurements, this should not be taken as evidence that the helium/air mixtures are not adequately mixed. Firstly, the RMS of the concentration fluctuations in the helium/air mixture are small (2% of the mean concentration). Secondly, the concentration and velocity fluctuations measured at the jet exit by other interference probes studied herein (such as the W-W-55 and W-W-25 probes), are not significantly larger in the helium/air mixture than they are in pure air. This phenomenon has only been observed in the W-Pt/R-10 probe, making it possible that the increased noise measured by the W-Pt/R-10 probe in the helium/air mixture, is not related to quality of the mixing system.

---

no further steps were taken. The connection between the wire material and voltage drift was not initially made, and significant voltage drift was not expected in the W-Pt/R-10 probe, otherwise it would have "burned in" for a longer period of time.

Having characterized the accuracy and precision of the W-Pt/R-10 probe with respect to known flow conditions in a laminar jet, attention can now be turned to experiments performed in the turbulent region of the jet.

5.2 Results in a turbulent jet

Experiments are performed at a distance of $x/D = 10$ from the jet exit in turbulent flows of pure air ($C_j = 0$) and a helium/air mixture ($C_j = 0.04$) to continue gauging the accuracy and precision of the W-Pt/R-10 probe. Concentration results are presented first in the following subsection.

5.2.1 Concentration Results

The accuracy and precision of concentration measurements can be assessed against flows of known composition, such as pure air, and also compared with results in similar flows from the existing scientific literature. As shown in table 5.2, the experiment in air reveals that the W-Pt/R-10 probe records a mean concentration ($\bar{C}$) in air of -0.00481, with a standard deviation (c_{rms}) of 0.00137. In comparison, interference probes developed by Sirivat (1983),[2] Stanford and Libby (1974), and Way and Libby (1971) measured concentrations in air that were accurate to a helium mass fraction on the order of almost 10^{-3}, with standard deviations on the order of 10^{-4}. The reduced accuracy of the mean concentration of the W-Pt/R-10 probe can be explained by the effects of voltage drift, which were discussed in the previous section. Figure 5.3 shows that the recorded mean voltage for the experiment in air deviates from the

[2] This is the same probe as the one described in Sirivat and Warhaft (1982). Additional information available in Sirivat (1983) is used for the purpose of comparison with the W-Pt/R-10 probe.

Table 5.2: Concentration statistics measured by interference probes in turbulent flows of pure air

Interference Probe	$\bar{C}$	c_{rms}
W-Pt/R-10	-0.00481	0.00137
Sirivat(1983)	0.00063	0.000155
Stanford and Libby (1974)	0.00091	0.00013
Way and Libby (1971)	-0.0008	Not given

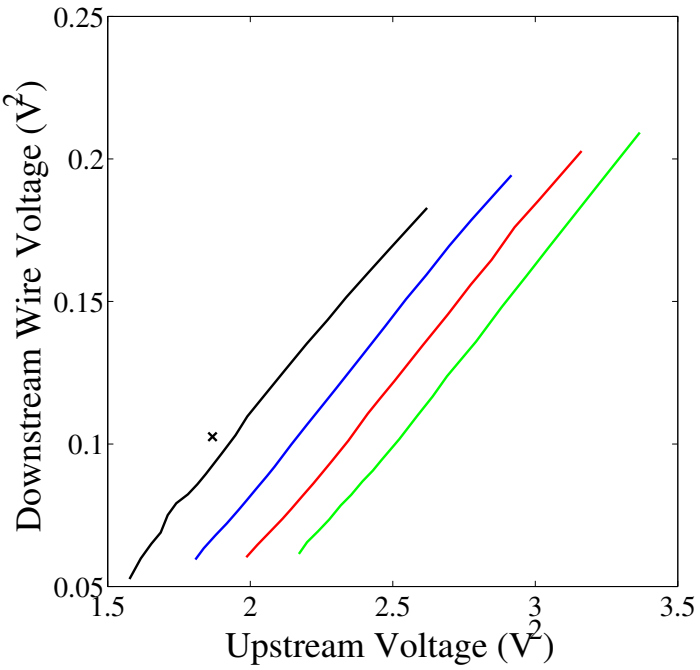

Figure 5.3: Calibration map for the W-Pt/R-10 probe with the mean value from experiment in air at $x/D = 10$. Solid lines are used for the calibration map. Black: C = 0. Blue: C = 0.02. Red: C = 0.04. Green: C = 0.06. Symbol $\times$ is used to denote the mean value from the experiment in air ($C_j = 0$).

corresponding calibration curve in air, resulting in a concentration that is clearly incorrect. If the effects of voltage drift can be minimized, then the only major sources of error remaining, with regards to mean values, are those associated with the data reduction scheme, which have been shown to be minimal (see section 3.2.3.2). In this scenario, the accuracy of the W-Pt/R-10 probe should be comparable to the accuracy of the interference probes developed by Sirivat (1983), Stanford and Libby (1974), and Way and Libby (1971).

Although the standard deviations of concentration measured by Sirivat (1983) and Stanford and Libby (1974) are roughly ten times smaller than those measured by the W-Pt/R-10 probe, this should not be taken to mean that these probes are 10 times more precise. The various results in table 5.2 were taken under distinctly different conditions: in a turbulent jet for the W-Pt/R-10 probe, in grid turbulence in the work of Sirivat (1983), and in turbulent pipe flow for the experiments of Stanford and Libby (1974). Though not all experimental conditions are specified, the mean velocities, Reynolds number and turbulent intensities of these flows can all be assumed to be different, which may explain some of the variability in the results. In Chapter 4, it was noted that an interference probe will measure spurious concentration fluctuations in turbulent flows of pure air because it responds to some velocity fluctuations as if they were concentration fluctuations. It therefore follows that a turbulent flow of air, exhibiting a larger turbulence intensity, would also exhibit larger spurious "concentration" fluctuations. Sirivat (1983) lists the mean velocity and its standard deviation from his experiment as 4.62 m/s and 0.130 m/s, respectively (resulting in a turbulence intensity of 2.8%). By comparison, the mean velocity and its standard deviation measured by the W-Pt/R-10 probe are 4.14 m/s and 0.871 m/s, respectively (giving a turbulence intensity of 21%). The velocity

fluctuations for the experiment performed by the W-Pt/R-10 probe are seven times larger than those measured by Sirivat (1983), which is presumably the cause of the larger spurious concentration fluctuations recorded by the W-Pt/R-10 probe.

Moreover, the signal-to-noise ratio of these two probes are revealed to be comparable, despite differences in the scale of measured c_{rms} values. In figure 5.4, at frequencies in the energy-containing range (below 100 Hz), the concentration spectra in air measured by the W-Pt/R-10 probe and the interference probe developed by Sirivat and Warhaft (1982) (also Sirivat 1983), are both observed to be nearly two decades lower than the concentration spectra measured in helium/air mixtures. Such a signal-to-noise ratio was deemed sufficient for studying the energy-containing range by Sirivat and Warhaft (1982), and it reasonable to draw the same conclusion with respect to the W-Pt/R-10 probe. The signal-to-noise ratio of the two probes remains similar beyond frequencies of 100 Hz, and up to frequencies of 2 kHz. The behavior of the two probes only deviates at the highest frequencies, with Sirivat and Warhaft (1982) measuring concentration fluctuations for frequencies up to 4 kHz, and the W-Pt/R-10 probe measuring for frequencies up to 10 kHz.

Although, results from the W-Pt/R-10 probe have been shown to be comparable with those of Sirivat and Warhaft (1982) (also Sirivat 1983), and differences in the results of table 5.2 have been mostly explained, it should be noted that the authors listed in table 5.2 report very precise concentration measurements in the flows in which they were used. Ideally, it is desired to make measurements with this level of precision. (Though it may not be possible to do so in the experiments conducted herein, due to the higher turbulence intensities reported.) The concentration PDFs measured by the W-Pt/R-10 probe, which are depicted in figure 5.5, reveal that

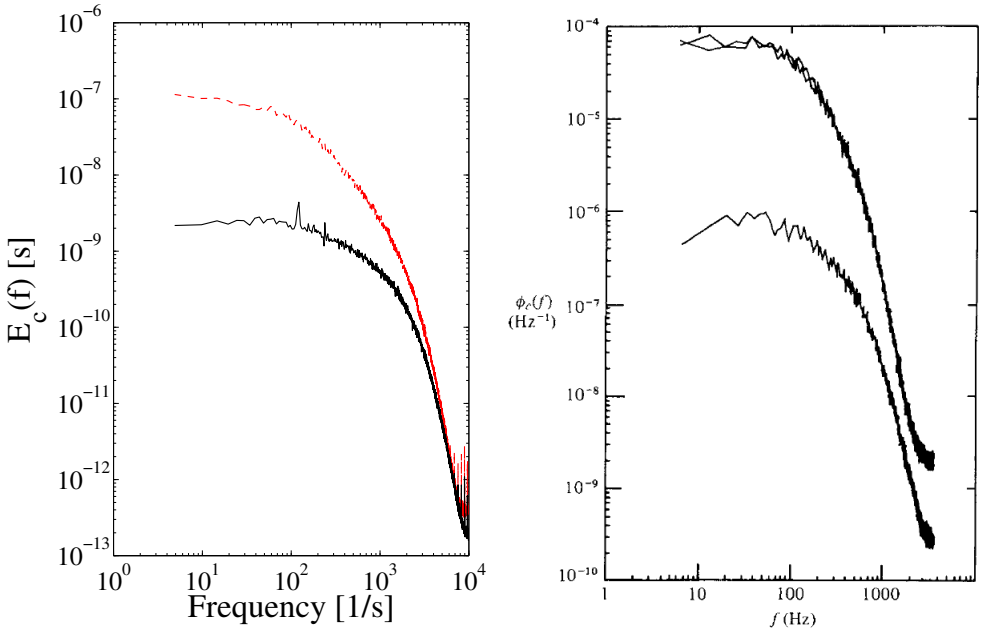

Figure 5.4: Comparison of the concentration spectra measured by the W-Pt/R-10 probe (left) with the concentration spectra measured by Sirivat and Warhaft (1982) (right). In the left figure, experiments are performed in a turbulent jet at $x/D = 10$. The jet exit velocity is about 6.4 m/s, $Re_D \approx 4000$, and $Re_\lambda \approx 280$. The dashed red line represents the experiment performed in a helium/air mixture (C_j =0.04), and the solid black line, the experiment performed in air (C_j=0). In the figure to the right, experiments are performed in turbulent grid flow at a distance of $x/M = 34$. The mean velocity is about 4.7 m/s, $Re_M \approx 3600$, and $Re_\lambda \approx 26$. The two upper curves are with helium in the flow and with helium and temperature fluctuations in the flow. The lower curve is the helium noise spectrum. Note that measurements for the W-Pt/R-10 probe are made in terms of the helium mass fraction, while those of Sirivat and Warhaft (1982) have multiplied this fraction by 100, to make measurements in terms of the helium mass percentage

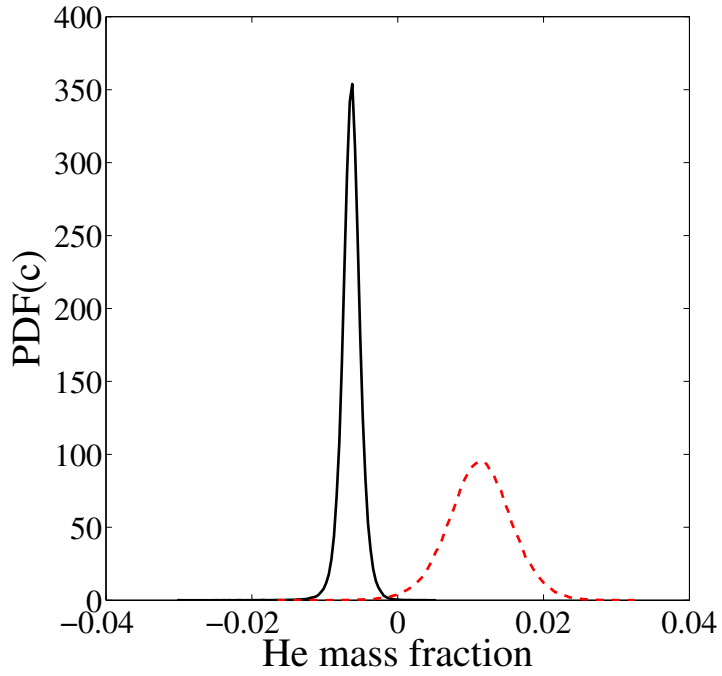

Figure 5.5: Concentration PDFs measured by the W-Pt/R-10 probe at $x/D = 10$. The jet exit velocity is about 6.4 m/s and $Re_D \approx 4000$. Solid black line: Air ($C_j = 0$). Dashed red line: He/air Mixture ($C_j = 0.04$).

although the precision of this probe is adequate, there is nevertheless room for improvement. While the shape of the PDF of concentration measured in air is notably different from the shape of the PDF measured in the helium/air mixture (in contrast to the PDFs measured by the W-Pt-35, W-W-55 and W-W-25 probes), and tends to shape of the concentration PDFs measured at the jet exit (see figure 5.1a), a somewhat larger than desired variance in the reported concentration in air can still be observed. These concentrations span a helium mass fraction range of roughly 0.01, just a third of the concentration range spanned in the helium/air mixture. Though "concentration" fluctuations in air cannot be entirely eliminated, further reductions may still be possible.

5.2.2 Velocity Measurements in a Turbulent Jet

In the previous subsection, experiments performed in the turbulent region of the jet ($x/D = 10$) were used to discuss the accuracy and precision of the concentration measurements made with the W-Pt/R-10 probe. In the present section, these experiments are used to gauge the accuracy and precision of the corresponding velocity measurements. This was done by comparing the velocity spectrum, PDF, and statistics in a turbulent jet of air measured by the W-Pt/R-10 probe with those measured by a single-normal hot-wire probe. As can be observed in figures 5.6 and 5.7, as well as table 5.3, the measurements of the velocity field by the W-Pt/R-10 probe are comparable to those made by the single-normal hot-wire probe. Most importantly, as shown in figure 5.6, the frequency response of the W-Pt/R-10 probe is comparable to that of the single-normal hot-wire probe.

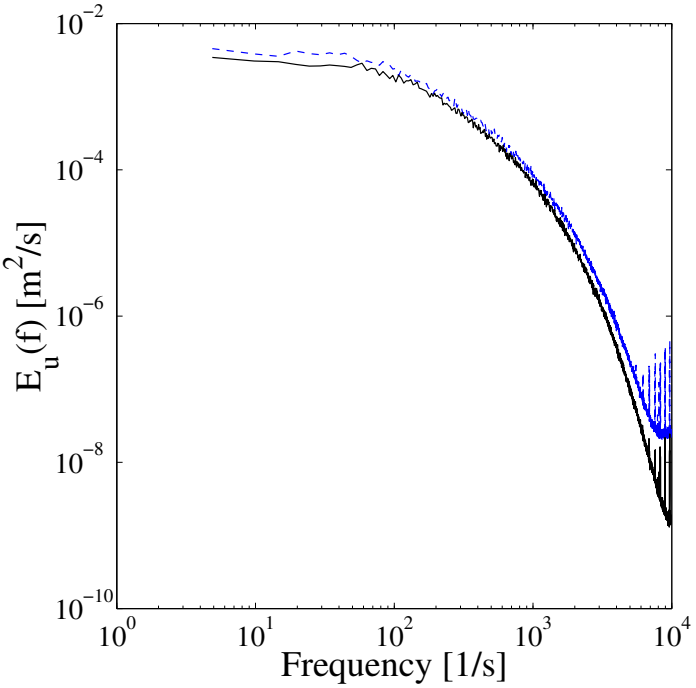

Figure 5.6: Comparison of the velocity spectrum measured by the W-Pt/R-10 probe with the velocity spectrum measured by a single-normal hot-wire probe at $x/D = 10$ and in pure air ($C_j = 0$). The jet exit velocity is about 6.4 m/s and $Re_D \approx 4000$. Solid black line: W-Pt/R-10 probe. Dashed blue line: single wire probe.

Though the results of the W-Pt/R-10 probe show good agreement with those of the single-normal probe, some slight differences can be seen between the responses of the two probes. These differences can be observed at the lowest and highest frequencies of the spectra, as well in the PDFs of figure 5.7 and statistics of table 5.3. They reveal that although the mean velocities recorded by these probes are nearly identical, there are some differences in the standard deviations (u_{rms}) and the skewness (S_u), with larger values of u_{rms} being measured by the single-normal hot-wire probe, and larger values of S_u being measured by the W-Pt/R-10 probe. The relatively small differences in skewness are explained by the fact that no velocities below 2 m/s are recorded by the W-Pt/R-10 probe, while velocities recorded by the single-normal hot-wire probe approach zero. Given that the interference probe is known to respond to some velocity fluctuations as if they were concentration fluctuations, these missing low velocities may be responsible for the spurious concentrations measured by the interference probe in air.

5.3 Assessment of the Accuracy and Precision of the W-Pt/R-10 Probe and Realization of Design Goals

The results of the previous three sections were used to benchmark the accuracy, precision, and performance of the W-Pt/R-10 probe in a variety ways. Though certain design goals were not met, most notably, it was not always possible to obtain an accuracy of $< 1\%$ due to errors resulting from voltage drift, and erroneous concentrations were still measured in flows of pure air, the response of the W-Pt/R-10 probe was, on an overall basis, satisfactory. The spurious concentration measurements in air cannot be entirely eliminated, as discussed in Chapter 4, merely minimized, and the results show high signal-to-noise ratios for the helium concentration over a broad

Table 5.3: Velocity statistics measured by the W-Pt/R-10 probe and a single-normal hot-wire probe in a turbulent flow of pure air ($C_j = 0$) at x/D=10. The jet exit velocity is about 6.4 m/s and $Re_D \approx 4000$. Units of velocity (for $\bar{U}$ and u_{rms}) are given in m/s.

Data	W-Pt/R-10 Probe	Single-Normal Hot-Wire Probe	Percent Difference
$\bar{U}$	4.14	4.16	0.48%
u_{rms}	0.871	0.962	9.5 %
S_u	0.161	0.0848	90 %
K_u	2.84	2.97	4.4 %

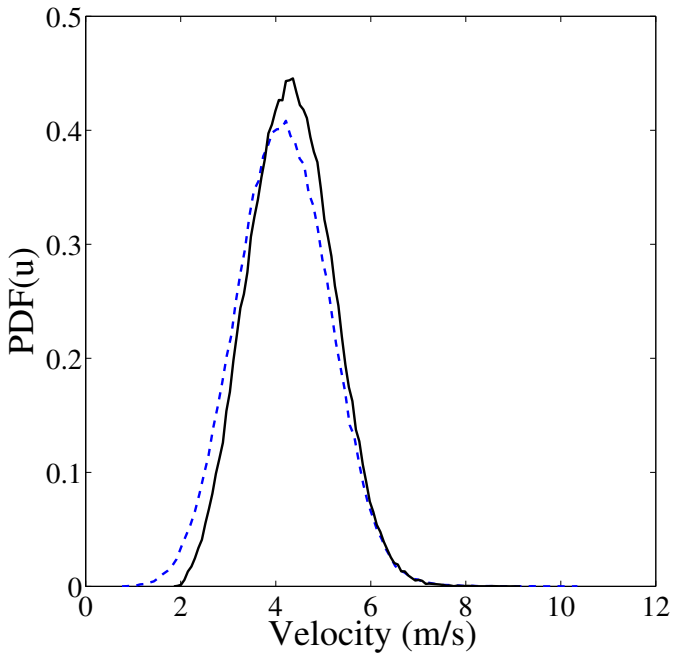

Figure 5.7: Comparison of the velocity PDF measured by the W-Pt/R-10 probe with the velocity PDF measured by a single-normal hot-wire probe at $x/D = 10$ and in pure air ($C_j = 0$). The jet exit velocity is about 6.4 m/s and $Re_D \approx 4000$. Solid black line: W-Pt/R-10 probe. Dashed blue line: single wire probe.

range of frequencies. Most notably, the helium noise spectrum is two decades below the concentration spectrum in a helium/air mixture, as per one of the design goals from section 3.2. Additionally, comparison of results with those a single-normal hot-wire probe shows good accuracy with respect to velocity measurements and a comparable frequency response. There is no doubt that some improvements to the W-Pt/R-10 probe could be made, or that the design of this probe could be tweaked somewhat to more fully meet the the design goals from section 3.2, and this will be further discussed in section 6.2. However, at the present the W-Pt/R-10 probe meets many of design goals for an interference probe (see section 3.2), and can be used to make simultaneous concentration and velocity measurements in a turbulent flow with a reasonable degree of accuracy and precision.

CHAPTER 6
Conclusion

The final chapter of this thesis is divided into two sections. The first presents a review of the work reported in this thesis, and the second contains recommendations for extensions of this work.

6.1 Review of the Thesis

The objectives of this work were to discuss the development of a thermal anemometry based probe to simultaneously measure concentration and velocity within turbulent flows and identify the essential design characteristics of such a probe. Though such probes, more commonly known as interference probes, have been previously constructed and successfully used, the documentation on their design is scarce, making it difficult to recreate these modified hot-wire probes.

A thorough review of the pertinent published literature revealed that simultaneous concentration and velocity measurements could be achieved with the use of two hot-wires, or a hot-wire and hot-film, placed close enough together that their thermal fields would interfere. Six design considerations were identified: the use of a hot-wire or hot-film, the materials of the wires or films, the overheat ratios of the wires or films, the separation distance between the wires or films, and the angles between the wires or films. Given that it was desired to make concentration and velocity measurements with high temporal and high spatial resolutions, and that the frequency response of a hot-film is much lower than the frequency response of a hot-wire, the use of a hot-film was excluded for the interference probes constructed in this work.

A total of six interference probes of varying characteristics were created to study the effects of some of the remaining design criteria, specifically, the overheat ratio, the separation distance, the wire diameter, and the wire material, and determine the optimal probe design.

Experiments were performed within the non-buoyant region of a turbulent helium-air jet to study these design characteristics. The experiments revealed that in order to make successful concentration and velocity measurements, the interference probes should be designed with (i) wires of different diameters to distinguish concentration fluctuations from velocity fluctuations with greater accuracy and (ii) small separation distances, of about 10 μm, to increase interference effects. Additionally, the upstream wire should be operated a high overheat ratio and the downstream wire should be operated at a low overheat ratio. Based on results gathered from the six interference probes developed herein, the W-Pt/R-10 probe, consisting of a 5 μm tungsten wire roughly 10 μm upstream of a 2.5 μm platinum-rhodium wire, was identified as the probe having the optimal design.

Although the other probes studied in this thesis measured large spurious concentration fluctuations in turbulent flows of pure air, these effects were minimized in the W-Pt/R-10 probe, which reported a signal-to-noise ratio of nearly two decades over wide range of frequencies in the concentration spectra – a value large enough to make precise concentration and velocity measurements feasible. Furthermore, velocity measurements in air with this probe compare favorably with those made by a single-normal hot-wire probe. Finally, it should be noted that the W-Pt/R-10 probe comes close to achieving many of the design goals for an interference probe listed in section 3.2 (save for issues related to voltage drift that affect its accuracy). Though some improvements in the performance of the W-Pt/R-10 probe remain to be made,

results obtained with this probe are on an overall basis quite satisfactory, especially considering (i) the exceptionally delicate nature of such probes in which two wires with diameters on the order of micrometers must be place alongside each other, separated by a distance on the order of tens of micrometers, and (ii) the difficulty of making simultaneous measurements of turbulent concentrations and velocities at sub-millimeter spatial resolutions and frequencies well above 1 kHz. It was concluded that the W-Pt/R-10 probe could be used to make simultaneous concentration and velocity measurements in turbulent flows.

6.2 Extensions of the Present Work

The first objective of any future work, is to develop an interference probe with greater accuracy and precision than the W-Pt/R-10 probe. After comparing results from this probe with those of interference probes developed in previous literature studies, it is believed that errors resulting from erroneous concentration measurements in turbulent flows of pure air can still be minimized. It was shown that diameter differences between the wires of the interference probe were essential for precisely distinguishing concentration fluctuations from velocity fluctuations. Therefore, an interference designed with larger diameter differences, for example with an upstream wire of 7 μm or 9 μm, and a downstream wire of 2.5 μm, might make more precise measurements. Another design idea would be to substitute the downstream platinum-rhodium wire in the W-Pt/R-10 probe with a tungsten wire. Though it was shown that the wire material has relatively little effect compared to diameter differences between wires or wire separation distance, in theory, a tungsten wire should be more sensitive to temperature, increasing the interference effect in such a probe, and increasing the sensitivity to concentration. Furthermore, the use of tungsten, as

opposed to platinum-rhodium could potentially reduce errors resulting from voltage drift and increase accuracy. These new probes, once constructed, could be used to continue studying the effects of various design characteristics (i.e. wire separation distances, wire diameter and wire material) in an effort to further define the optimal and/or essential characteristics of an interference probe.

Following that, a second objective, is to construct a three-wire probe to simultaneously measure concentration, velocity, and temperature in turbulent flows. This could be achieved by combining an interference probe with a third wire to measure temperature. Such a probe could be used to study the mixing of multiple scalars within turbulent flows, one of the main motivations behind the work conducted in this thesis.

REFERENCES

Adler, D (1972). "A hot wire technique for continuous measurement in unsteady concentration fields of binary gaseous mixtures". *Journal of Physics E: Scientific Instruments* 5.2, pp. 163–169.

Afara, S. (2011). "Development and testing of a wall-shear-stress sensor for measurements within notebook computers". M Eng thesis. McGill University.

Ahmed, S. and So, R. (1986). "Concentration distributions in a model combustor". *Exp Fluids* 4.2, pp. 107–113.

Aihara, Y, Kassoy, D., and Libby, P. A. (1967). "Heat transfer from circular cylinders at low Reynolds numbers. II. Experimental results and comparison with theory". *Physics of Fluids (1958-1988)* 10.5, pp. 947–952.

Aihara, Y., Koyama, H., and Morishita, E. (1974). "Effects of an air stream on turbulent diffusion of a helium jet from a small nozzle". *Physics of Fluids (1958-1988)* 17.4, pp. 665–673.

Al-Ammar, K. *et al.* (1998). "Application of rainbow schlieren deflectometry for concentration measurements in an axisymmetric helium jet". *Exp Fluids* 25.2, pp. 89–95.

Andrews, G., Bradley, D, and Hundy, G. (1972). "Hot wire anemometer calibration for measurements of small gas velocities". *Int J Heat Mass Tran* 15.10, pp. 1765–1786.

Baccaglini, G, Kassoy, D., and Libby, P. A. (1969). "Heat Transfer to Cylinders in Nitrogen-Helium and Nitrogen-Neon Mixtures". *Physics of Fluids (1958-1988)* 12.7, pp. 1378–1381.

Banerjee, A. and Andrews, M. (2007). "A Convection Heat Transfer Correlation for a Binary Air-Helium Mixture at Low Reynolds Number". *J Heat Transf* 129.11, p. 1494.

Birch, A. *et al.* (1986). "Aspects of design and calibration of hot-film aspirating probes used for the measurement of gas concentration". *Journal of Physics E: Scientific Instruments* 19.1, pp. 59–63.

Blackshear, P. L. and Fingerson, L. M. (1962). "Rapid-response heat flux probe for high temperature gases". *ARS Journal* 32.11, pp. 1709–1715.

Brown, G. and Rebollo, M. (1972). "A small, fast-response probe to measure composition of a binary gas mixture". *AIAA Journal* 10.5, pp. 649–652.

Bruun, H. (1995). *Hot-wire Anemometry: Principles and Signal Analysis*. Oxford University Press.

Cabannes, M, Ferchichi, M, and Tavoularis, S (2004). "Temperature variation correction for aspirating probes in heliumair mixtures". *Measurement Science and Technology* 15.6, p. 1211.

Chassaing, P (1979). "Mélange turbulent de gaz inertes dans un jet de tube libre. Thèse Doc". *Sciences* 42.

Chen, C. J. and Rodi, W. (1980). "Vertical turbulent buoyant jets: a review of experimental data". *NASA STI/Recon Technical Report A* 80.

Collis, D and Williams, M (1959). "Two-dimensional convection from heated wires at low Reynolds numbers". *J Fluid Mech* 6.03, p. 357.

Comte-Bellot, G (1976). "Hot-Wire Anemometry". *Annual Review of Fluid Mechanics* 8.1, pp. 209–231.

Corrsin, S (1949). *Extended application of the hot-wire anemometer NACA Tech.* Tech. rep. Note 1864.

Corrsin, S (1963). "Turbulence: experimental methods". *Handbuch der Physik* 8.2, pp. 524–533.

Doroshko, M. *et al.* (2008). "Measurements of admixture concentration fluctuations in a turbulent shear flow using an averaged Talbot image". *Exp Fluids* 44.3, pp. 461–468.

D'Souza, G., Montealegre, A., and Weinstein, H. (1968). *Measurement of turbulent correlations in a coaxial flow of dissimar fluids.* NASA CR-960.

Forney, L. and Lee, H. (1982). "Optimum dimensions for pipeline mixing at a Tjunction". *Aiche J* 28.6, pp. 980–987.

Forney, L. and Kwon, T. (1979). "Efficient single-jet mixing in turbulent tube flow". *AIChE Journal* 25.4, pp. 623–630.

Frank, J., Lyons, K., and Long, M. (1996). "Simultaneous scaler/velocity field measurements in turbulent gas-phase flows". *Combust Flame* 107.1-2, pp. 1–12.

Ger, A. M. and Holley, E. R. (1974). "Turbulent Jets in Crossing Pipe Flow". *Hydraulic Engineering Series, no. 30.*

Guibert, P. and Dicocco, E. (2002). "Development of a local continuous sampling probe for the equivalence air-fuel ratio measurement. Application to spark ignition engine". *Exp Fluids* 32.4, pp. 494–505.

Harion, J.-L., Favre-Marinet, M, and Camano, B (1996). "An improved method for measuring velocity and concentration by thermo-anemometry in turbulent helium-air mixtures". *Exp Fluids* 22.2, pp. 174–182.

Harion, J.-L., Favre-Marinet, M., and Binder, G. (1997). "Density and velocity measurements in turbulent He-air boundary layers". *Exp Therm Fluid Sci* 14.1, pp. 92–100.

Hinze, J. (1959). *Turbulence: An Introduction to Its Mechanism and Theory.* McGraw-Hill.

Hinze, J. (1975). *Turbulence:* 2nd ed. McGraw-Hill.

Hu, H *et al.* (2004). "Analysis of a turbulent jet mixing flow by using a PIV-PLIF combined system". *J Visual-japan* 7.1, pp. 33–42.

Jensen, K. (2004). "Flow measurements". *J Braz Soc Mech Sci* 26.4, pp. 400–419.

Jonáš, P. *et al.* (2003). "Contribution to the simultaneous measurements of the gas-mixture velocity and concentration". *Pamm* 3.1, pp. 356–357.

Kassoy, D. (1967). "Heat Transfer from Circular Cylinders at Low Reynolds Numbers. I. Theory for Variable Property Flow". *Phys Fluids* 10.5, p. 938.

Koochesfahani, M., Cohn, R., and MacKinnon, C. (2000). "Simultaneous whole-field measurements of velocity and concentration fields using a combination of MTV and LIF". *Measurement Science and Technology* 11.9, p. 1289.

Kramers, H (1946). "Heat transfer from spheres to flowing media". *Physica* 12.2-3, pp. 61–80.

LaRue, J. and Libby, P. (1977). "Measurements in the turbulent boundary layer with slot injection of helium". *Phys Fluids* 20.2, p. 192.

LaRue, J. and Libby, P. (1980). "Further results related to the turbulent boundary layer with slot injection of helium". *Phys Fluids* 23.6, p. 1111.

Lavertu, T, Mydlarski, L, and Gaskin, S (2008). "Differential diffusion of high-Schmidt-number passive scalars in a turbulent jet". *J Fluid Mech* 612.

Law, A. W.-K. and Wang, H. (2000). "Measurement of mixing processes with combined digital particle image velocimetry and planar laser induced fluorescence". *Experimental Thermal and Fluid Science* 22.3, pp. 213–229.

Lemoine, F., Wolff, M., and Lebouche, M. (1996). "Simultaneous concentration and velocity measurements using combined laser-induced fluorescence and laser Doppler velocimetry: Application to turbulent transport". *Exp Fluids* 20.5.

McQuaid, J and Wright, W (1973). "The response of a hot-wire anemometer in flows of gas mixtures". *International Journal of Heat and Mass Transfer* 16.4, pp. 819–828.

McQuaid, J and Wright, W (1974). "Turbulence measurements with hot-wire anemometry in non-homogeneous jets". *International journal of heat and mass transfer* 17.2, pp. 341–349.

Ng, W. and Epstein, A. (1983). "High-frequency temperature and pressure probe for unsteady compressible flows". *Review of Scientific Instruments* 54.12, pp. 1678–1683.

Ninnemann, T. and Ng, W. (1992). "A concentration probe for the study of mixing in supersonic shear flows". *Exp Fluids* 13.2-3, pp. 98–104.

Panchapakesan, N and Lumley, J (1993). "Turbulence measurements in axisymmetric jets of air and helium. Part 2. Helium jet". *J Fluid Mech* 246.-1, p. 225.

Perry, A. (1977). "The time response of an aspirating probe in gas sampling". *Journal of Physics E: Scientific Instruments* 10.9, pp. 898–902.

Perry, A. (1982). *Hot-wire anemometry*. Clarendon Press.

Pitts, W. M. and McCaffrey, B. J. (1986). "Response behaviour of hot wires and films to flows of different gases". *Journal of Fluid Mechanics* 169, pp. 465–512.

Pope, S. (2000). *Turbulent Flows*. Cambridge University Press.

Riva, R. *et al.* (1994). "Development of turbulent boundary layer with large density gradients". *Exp Therm Fluid Sci* 9.2, pp. 165–173.

Sakai, Y. *et al.* (2001). "Simultaneous measurements of concentration and velocity in a CO2 jet issuing into a grid turbulence by two-sensor hot-wire probe". *Int J Heat Fluid Fl* 22.3, pp. 227–236.

Simpson, R. and Wyatt, W. (1973). "The behaviour of hot-film anemometers in gas mixtures". *Journal of Physics E: Scientific Instruments* 6.10, p. 981.

Sirivat, A and Warhaft, Z (1982). "The mixing of passive helium and temperature fluctuations in grid turbulence". *J Fluid Mech* 120.-1, p. 475.

Sirivat, A. (1983). "Experimental Studies of Homogeneous Passive Scalars in Grid-generated Turbulence". PhD thesis. Cornell University.

So, R. *et al.* (1990). "Some measurements in a binary gas jet". *Experiments in Fluids* 9.5, pp. 273–284.

Soudani, A. and Bessaïh, R. (2006). "Conditional analysis in a turbulent boundary layer with strong density differences". *Acta Mech* 181.3-4, pp. 207–229.

Stanford, R. A. and Libby, P. (1974). "Further applications of hot-wire anemometry to turbulence measurements in helium-air mixtures". *Phys Fluids* 17.7, p. 1353.

Tennekes, H. and Lumley, J. (1972). *A First Course in Turbulence*. MIT Press.

Wasan, D. and Baid, K. (1971). "Measurement of velocity in gas mixtures: Hotwire and hotfilm anemometry". *Aiche J* 17.3, pp. 729–731.

Wasan, D., Davis, R., and Wilke, C. (1968). "Measurement of the velocity of gases with variable fluid properties". *Aiche J* 14.2, pp. 227–234.

Way, J and Libby, P. (1970). "Hot-wire probes for measuring velocity and concentration in helium-air mixtures". *AIAA Journal* 8.5, pp. 976–978.

Way, J and Libby, P. (1971). "Application of hot-wire anemometry and digital techniques to measurements in a turbulent helium jet". *AIAA Journal* 9.8, pp. 1567–1573.

Webster, D., Roberts, P., and Ra'ad, L. (2001). "Simultaneous DPTV/PLIF measurements of a turbulent jet". *Exp Fluids* 30.1, pp. 65–72.

White, B. (1987). "Wind tunnel wake measurements of heavier-than-air gas dispersion near a two-dimensional obstacle". *Boundary-Layer Meteorology* 38.1-2, pp. 105–124.

Wilke, C (1950). "A Viscosity Equation for Gas Mixtures". *J Chem Phys* 18.4, p. 517.

Wilson, D. and Netterville, D. (1981). "A fast-response, heated-element concentration detector for wind-tunnel applications". *Journal of Wind Engineering and Industrial Aerodynamics* 7.1, pp. 55–64.

Wu, P. and Libby, P. (1971). "Heat transfer to cylinders in helium and helium-air mixtures". *Int J Heat Mass Tran* 14.8, pp. 1071–1077.

Zhu, J., So, R., and Otugen, M. (1988). "Turbulent mass flux measurements using a laser/hot-wire technique". *Int J Heat Mass Tran* 31.4, pp. 819–829.

Appendix A - Calculations of Fluid Properties in Helium/Air Mixtures

To find the mixture fluid properties it is necessary to know the mole fractions of air (x_{air}) and helium (x_{He}) in the mixtures. If the mass fraction of helium, denoted as w_{He}, is known, then the mole fractions can be calculated from the following expressions:

$$x_{He} = \frac{w_{He} M_{air}}{M_{He}(1 - w_{He}) + M_{air}}, \tag{A.1a}$$

$$x_{air} = 1 - x_{He}, \tag{A.1b}$$

where M_{air} is the molecular weight of air and defined to be 28.994 kg/kmol and M_{He} is the molecular weight of helium and defined to be 4.002602 kg/kmol. According to Banerjee and Andrews (2007), the density of a helium/air mixture (ρ_{mix}) is found to be a linear function of the densities and mole fractions of the pure components:

$$\rho_{mix} = \rho_{air} x_{air} + \rho_{He} x_{He}. \tag{A.2}$$

The viscosity of the mixture (μ_{mix}) is found using the expression below derived by Wilke (1950):

$$\mu_{mix} = \frac{\mu_{air}}{1 + \frac{x_{He}}{x_{air}} \left[1 + (\frac{\mu_{air}}{\mu_{He}})^{1/2} (\frac{M_{He}}{M_{air}})^{1/4}\right]^2 \left[8(1 + \frac{M_{air}}{M_{He}})\right]^{-1/2}} + \frac{\mu_{He}}{1 + \frac{x_{air}}{x_{He}} \left[1 + (\frac{\mu_{He}}{\mu_{air}})^{1/2} (\frac{M_{air}}{M_{He}})^{1/4}\right]^2 \left[8(1 + \frac{M_{He}}{M_{air}})\right]^{-1/2}}, \tag{A.3}$$

where μ_{air} and μ_{He} refer to the viscosity of air and helium respectively.

Appendix B - Characterization of the Buoyancy Effects in the Jet

The relative importance of the inertial to buoyant forces can be characterized by the densimetric Froude number (F) (Chen and Rodi 1980; Panchapakesan and Lumley 1993), defined below:

$$F = U_j^2 \rho_j / (\rho_a - \rho_j) g D. \tag{B.1}$$

It is a function of velocity at the jet exit (U_j), the density at the jet exit (ρ_j), the density of the surroundings (ρ_a), the diameter at the jet exit (D), and the gravitational constant (g). Low Froude numbers are indicative of greater buoyancy effects, with $F = 0$ representing a pure plume, and higher Froude numbers are indicative of greater interial effects, with $F = \infty$ representing a pure jet. A buoyant jet, whose Froude number falls somewhere between 0 and infinity, behaves first like a pure jet, but its behavior eventually transitions to that of a pure plume. The flow field of this jet can therefore be split into three regions: the non-buoyant jet region, the intermediate region, and the buoyant plume region (Panchapakesan and Lumley 1993). A non-dimensional length scale, x_1, developed by Chen and Rodi (1980), is used to delineate the different regions of jet:

$$x_1 = F^{-1/2} (\rho_a / \rho_j)^{1/4} (x/D), \tag{B.2}$$

with x representing the distance from the jet exit. Chen and Rodi (1980) found that $x_1 = 0.5$ marked the boundary beyond the non-buoyant jet region and the intermediate region and $x_1 = 5$ marked the boundary between the intermediate region and the buoyant plume region. The table below summarizes the Froude numbers and

values of x_1 in different flow conditions. The flow conditions listed are those used in the various experiments conducted on the interference probes and are defined at the jet exit. For each of the experimental conditions, the Froude number is large, and the value of $x_1 \ll 0.5$ – the experiments are conducted firmly in the non-buoyant region of the jet and the concentration can therefore be deemed to be a passive scalar.

Table B.1: Characterization of buoyancy effects in various flow conditions

Flow Condtions	Froude Number	x_1	Region of the flow
0% He (Air) $U_j \approx 7$ m/s	∞	0	non-buoyant
4% He $U_j \approx 7$ m/s	14990	0.08	non-buoyant
0% He (Air) $U_j \approx 9$ m/s	∞	0	non-buoyant
4% He $U_j \approx 9$ m/s	25365	0.06	non-buoyant